Active layer thermal regime in subarctic wetlands at the southern edge of continuous permafrost in Canada

A Thesis Submitted to the Committee of Graduate Studies in Partial Fulfillment of the

Requirements for the Degree of Master of Science in the Faculty of Arts and Science

TRENT UNIVERSITY

Peterborough, Ontario, Canada

Environmental and Life Sciences M.Sc. Graduate Program

May 2022

Abstract

Active layer thermal regime in subarctic wetlands at the southern edge of continuous permafrost in Canada

Gillian Muir

The fine-scale controls of active layer dynamics in the subarctic at the southern edge of continuous permafrost are currently poorly understood. The goal of this thesis was to understand how environmental conditions associated with upland tundra heath, open graminoid fen, and palsas/peat plateaus affected active layer thermal regime in a subarctic peatland in northern Canada. Indices of active layer thermal regime were derived from in-situ measurements of ground temperature and related to local measurements of air temperature, snow depth, and surface soil moisture. Active layer thaw patterns differed among landforms, with palsas and tundra heath having the least and greatest amount of thaw, respectively. Tundra heath thaw patterns were influenced by the presence of gravel and sandy soils, which had higher thermal conductivity than the mineral and organic soils of fens and palsas. Vegetation also influenced thaw patterns; the lichen cover of palsas better protected the landform from incoming solar radiation than the moss, lichen, and low-lying shrub cover of upland tundra heath, thus allowing for cooler ground temperatures. Air temperature was the most significant predictor of active layer thermal regime. Surface soil moisture varied among landforms and greater surface soil moisture reduced the amount of active layer thaw. These findings improved understanding of how landform and climate can interact to affect the active layer.

Keywords: active layer thermal regime, permafrost, active layer thickness, peatland, subarctic, climate change, Hudson Bay Lowlands

Acknowledgments

I would like to start by thanking my supervisor, Dr. Glen Brown, for giving me an opportunity to pursue a master's degree and research such an interesting topic. I am very grateful for your patience, guidance, and support throughout the thesis process. I appreciate the opportunity to go to such an amazing field site and for all the opportunities you have given me. I would also like to thank my committee, Dr. Erica Nol, Dr. Robert Metcalfe, and Dr. Baoxin Hu, for their advice, support, and assistance in completing my thesis. I would also like to extend my deepest gratitude to Rod Brooke and Kim Bennett, who make the field season possible every year.

This project would not have been possible without the support of my friends and family. Thank you for the continuous encouragement and the many discussions about permafrost and my struggles with R. The biggest thank you to Hayden for your unwavering support and reassurance and for continuously reminding me that I would make it through the many stressful moments of my masters. Thank you for letting me talk your ear off when I was frustrated and for cheering me on when things went well. A big shoutout to my fellow lab mates: Callie Stirling, Laura Corrigan, Matthew Poppleton, and Richard Huang. Thank you for your support and feedback throughout our lab meetings.

This project was made possible by funding from the National Science and Engineering Research Council, York University, The Northern Scientific Training Program, Trent University, and the Ministry of Northern Development, Mines, Natural Resources and Forestry.

TABLE OF CONTENTS

LIST OF FIGURES

LIST OF TABLES

Chapter 1: General Introduction

Climate change is expected to have far-reaching impacts to ecosystem form and function, but the extent of these changes remains unclear in northern regions. Consequences of climate change include increases in global air temperature, changing precipitation patterns, rising sea levels, increase in drought and heat waves, and, most likely, an ice-free Arctic (IPCC, 2021). At northern latitudes, freezing temperatures and the presence of permafrost, defined as any ground material that remains at 0˚C or below for at least two years (Harris et al., 1988), shape northern ecosystems and the adaptations of plants and animals who live there (Vincent et al., 2013). Thus, understanding the controls on thaw dynamics within the ground helps to understand and assess the impacts of climate change on ecosystems and wildlife.

Northern regions are characterized by strong seasonality and extensive snow cover for much of the year, however, climate change is expected to promote a change in land surface albedo that will exacerbate warming of the ground (Serreze and Francis, 2006). Snow has a high albedo compared to vegetation and a trend towards a longer snow free period is expected to allow more radiation to be absorbed by the ground, thus resulting in increased soil temperatures, and promoting permafrost degradation (Serreze and Francis, 2006). Increased temperatures as a result of climate change will create favorable conditions for a transition to a shrubbier vegetation composition (Pearson et al., 2013), which would further alter surface albedo in the summer (Mod and Luoto, 2016).

Impacts of permafrost melt on ecosystems

Permafrost ecosystems amplify the effects of climate change (Schuur et al., 2015) and are more greatly impacted than other regions, with arctic regions warming faster than other parts of the world—a phenomena known as arctic amplification (Serreze and Barry,

2011). As temperatures increase, permafrost begins to thaw, which unlocks stored carbon. Microbes then convert this carbon into greenhouse gases, particularly methane and carbon dioxide, as by-products of their metabolic processes. This process is expected to further amplify global temperature increases (Schuur et al., 2015). Melt of permafrost can result in a transition of land areas from a carbon sink to a carbon source (Schuur et al., 2015). Permafrost melt can also result in various ecosystem changes, including riverbank and coastline erosion, destabilization of infrastructure, and changes in the carbon and hydrological cycle (National Research Council USA, 2014; Rowland et al., 2010).

Northern wetlands may be especially vulnerable to permafrost melt, notably through effects on hydrology. Northern wetlands also contribute significantly to biodiversity through the provision of unique habitat features. For example, the interspersion of open water and drier raised features (e.g., moss hummocks) in wetlands provide a range of nesting and feeding habitats used by migratory water birds. The potential effects of permafrost melt to wetlands are complex and may vary depending on site conditions and timing of transitional effects. Fist, permafrost melt may induce the loss of some wetlands (Woo et al., 1992). Northern wetlands are maintained due to the retention of water near surface above the impermeable permafrost layer, but degradation of permafrost can allow for deep percolation and drainage of wetlands (Woo et al., 1992). Changes in the water balance are also expected as longer snow free periods increase water lost through evapotranspiration, potentially reducing the extent of wetlands (Woo, 1990). Alternatively, climate change and abrupt permafrost melt may result in wetland expansion (Schuur et al., 2015). Increased air temperatures can cause the ground-ice to melt, which would result in the collapse of the ground surface into the volume previously occupied by the ice (Schuur et al., 2015). This would cause the water to move towards to collapsed

regions which will cause more localized thawing and erosion and may result in wetland expansion (Schuur et al., 2015).

Permafrost thaw can alter the availability or quality of habitat for species (Smits et al., 1988). Migratory shorebirds, for example, rely on numerous landform types for survival. They use graminoid fen and shallow open water for feeding (Cunningham et al., 2016), some nest on flat upland beach ridges for a broad field of view against predators (Johnson and Walters, 2011), and some use palsas and peat plateaus for perching or feeding locations (Tsuyuzaki et al., 2008). Melting of permafrost can alter soil moisture content and vegetation composition in wetlands (Mobaek et al., 2009), thereby resulting in changes to habitat quality or availability (Nielsen et al., 1994; Smits et al., 1988). Understanding the effects of permafrost melt and its associated effects on landforms used by wildlife is particularly relevant in subarctic ecosystems where many species are at the southern edge of their range. These populations may be more sensitive to environmental change and disproportionately important for the survival and evolution of the species (Hampe and Petit, 2005; Provan and Maggs, 2012). As such, improving our understanding of permafrost melt and its effects on different landform types is important in understanding how habitat conditions may be altered for northern biodiversity.

The Active Layer

The active layer, defined as the layer of ground above the permafrost layer that undergoes annual freezing and thawing (Burn, 1998), is commonly used to study permafrost (Black, 1976). Biophysical properties of the active layer control heat exchange with the permafrost layer, as well as, gas exchange with the atmosphere (Wojciech Dobiński, 2020). Changes in active layer thickness (ALT) can be used to assess patterns in degradation or aggradation of the permafrost layer. Active layer thermal dynamics (i.e.,

timing of thaw, magnitude of thaw, and rate of thaw) can also be useful indicators of permafrost conditions (Black, 1976; Jorgenson and Osterkamp, 2005; Kim et al., 2021); they can indicate large-scale change and local feedbacks involving the hydrological cycle and above ground properties, such as vegetation and snowpack (Grünberg et al., 2020; Guglielmin et al., 2012; Mauro Guglielmin et al., 2008).

Climate change has resulted in warming permafrost in arctic and isolated permafrost regions (Ding et al., 2019; Wu et al., 2015). Arctic permafrost temperatures and ALT have increased (Vaughan et al., 2013) at an accelerated rate during the past few decades (Ednie and Smith, 2015; Noetzli and Voelksch, 2014). Mean annual ground temperature between the depths of 10-30m has increased by 1.5˚C in the past 30 years (Ednie and Smith, 2015; Noetzli and Voelksch, 2014). Rates of temperature increase of the permafrost layer, however, vary across the world's arctic and isolated permafrost regions due to local factors such as snow cover, slope aspect, vegetation cover, and soil properties (Arzhanov and Mokhov, 2013; Luo et al., 2016; Romanovsky et al., 2007; Wu et al., 2012). These differences in local environmental factors have resulted in varying warming rates and even decreases in permafrost temperatures and ALT (Arzhanov and Mokhov, 2013; Luo et al., 2016; Romanovsky et al., 2007; Wu et al., 2012).

Local environmental factors control active layer thermal regime (Fisher et al., 2016; M. Guglielmin et al., 2008; Hu et al., 2020; Lafrenière et al., 2013; Luo et al., 2016; Subin et al., 2013), but whether they have warming or cooling effects on the ground depends on how these factors interact with each other (Atchley et al., 2016; Subin et al., 2013; Yang et al., 2013). Soil properties, such as soil type and grain size, influence thermal conductivity (Cui et al., 2020). Gravel and sandy soils have higher thermal conductivity rates, so heat is more easily transported through the ground leading to

increased soil temperatures (Cui et al., 2020). Soil moisture is also an important factor in active layer thermal regime. Some studies have shown that more saturated soils increase thermal conductivity of the ground, allowing for increased temperatures (Li et al., 2019). Conversely, more saturated soils can also decrease soil temperatures due to the higher heat capacity of water; it therefore requires more energy to heat up saturated soil than unsaturated (Tatenhove and Olesen, 1994). Snow cover also influences the active layer as it has insulating properties. Variation in the onset of snow and timing of snowmelt can affect active layer thermal regime. Later onset of snow cover and later snowmelt promotes decreases in ground temperature, while earlier snow melt promotes increased ground temperatures and greater active layer depths (Ling and Zhang, 2003). Vegetation is another influential factor for active layer thermal regime as it affects surface albedo, intercepts rainfall, and utilizes ground water and heat for growth (Blok et al., 2011; Loranty et al., 2014; Railton and Sparling, 1973). A transition to a shrubbier landscape would also affect local shading which may decrease soil temperatures and slow carbon release due to permafrost degradation (Blok et al., 2010). Understanding the fine-scale controls on the active layer will aid in predicting how landform types will change in the face of climate change.

Understanding active layer thermal regime at the southern edge of continuous permafrost

Most studies of permafrost have been conducted in the Arctic or in mountainous and isolated permafrost areas rather than subarctic ecosystems at the southern edge of continuous permafrost. However, due to the substantial variation in active layer thickness and thermal regime, even at similar latitudes, understanding fine-scale variation in active layer dynamics in this region is crucial for understanding how these regions will change in response to a warming climate.

The Hudson Bay Lowlands (HBL) have a subarctic climate and are located at the southern extent of continuous permafrost. This region is the largest peatland in North America and is a significant carbon sink (Martini, 2006). The HBL contains a heterogeneous mix of land covers, that differ in soil properties, vegetation, and soil moisture regime. Treeless wetlands (mostly fen) are the dominant land cover with fens and bogs making up approximately 60% of the landscape within the continuous permafrost zone of the HBL in Ontario. Fens are more common near the coast and transitions to greater occurrence of bog approximately 30km inland. Tundra heath and open grasslands occur on the drier upland sites near the coast, characterized by well drained, raised mineral soils. The tundra heath upland typically occurs on relic coastal and inland beach ridges that parallel the Hudson Bay coastline. Although representing only about 2% of the land cover within the continuous permafrost zone, they occur throughout the coastal zone within about 15km of the coast. Extensive areas of palsa formations occur approximately 20 to 30km inland, within the continuous zone of permafrost. This region is also intersected by the 0˚C isotherm for annual air temperature, meaning temperature increases by only a few degrees will result in the melting of ice. The persistence of ice, however, is crucial for maintaining the unique features of this subarctic ecosystem. Climate projections estimate a 10˚C increase by 2080 in the region (McDermid et al., 2015), posing a high risk of permafrost degradation, changes in the hydrological cycle, and shifts in vegetation. It is, therefore, important to understand how environmental conditions control active layer thermal regime and how this relationship may impact the regions response to climate change.

Objectives

The objectives of this thesis were to 1) describe and compare active layer thermal regime (i.e., thaw rates, thaw depths, soil temperatures, thaw period) across different landforms (palsas, fens, and upland tundra heath) and 2) understand how vegetation, soil properties, and weather patterns influence active layer thermal regime across a subarctic wetland complex.

My study site was situated in the Hudson Bay Lowlands (HBLs) of Northern Ontario. It is found within a transition zone between the boreal forest and Arctic, where biota are adapted to the northern climate, but many are found at the southern trailing edge of their distribution which may make them particularly vulnerable to environmental change (Hampe and Petit, 2005; Provan and Maggs, 2012). Three landforms were targeted for the study of active layer thermal regime: upland tundra heath, open graminoid fen, and palsas/peat plateaus. These features were expected to contain unique vegetation cover, soil moisture regime, and soil types that would affect active layer thermal regime. Understanding fine-scale active layer dynamics across the landscape will contribute useful knowledge for land-use planning, habitat and wildlife conservation, and resource management.

Chapter 2: Active layer thermal regime varies across landforms in a subarctic peatland

Abstract

The influence of climate change on permafrost and active layer thickness has far reaching effects on northern ecosystems. Better understanding is needed of the controls on active layer thermal regime at the southern edge of continuous permafrost, where boundary conditions may induce rapid changes in subarctic ecosystem structure. Active layer thickness and thermal regime can vary substantially, even at similar latitudes, due to fine-scale environmental heterogeneity. I investigated how landform, vegetation, and weather patterns affect active layer thermal regime, notably timing, magnitude, and rate of thaw. My study site was located within the Hudson Bay Lowlands of Northern Ontario, a vast subarctic peatland. I measured properties of the active layer in open graminoid fen, upland tundra heath, and palsas, which varied in vegetation cover and soil properties. Active layer thaw patterns differed among landforms. Palsas had the lowest thaw rates and soil temperatures during the thaw period, while tundra heath had the highest values for those metrics. Air temperature was the most influential predictor of thaw patterns, but the effects of temperature appeared to be mediated by vegetation and soil properties. Greater surface soil moisture slowed active layer thaw, while timing of snowmelt was a non-significant predictor of active layer thermal regime in this study. My study clarifies how biophysical properties of prominent landform features can interact with climate to affect active layer thaw. These findings can aid in predicting how climate warming will affect subarctic ecosystems.

Introduction

Climate-induced degradation of permafrost in poleward regions of the planet will have a major impact on ecosystem structure. Better understanding is required of the factors affecting permafrost properties in the subarctic, where the southern extent of continuous permafrost occurs at the interface between the boreal and arctic biomes. Permafrost is defined as any ground material that remains at zero degrees Celsius or below for at least two years (Harris et al., 1988) and currently occurs in almost 24% of ground in the Northern Hemisphere (Zhang et al., 2008). The active layer refers to the area of ground above permafrost that undergoes annual freezing and thawing (Burn, 1998). Thermal dynamics in the active layer have a major control on above and below-ground biotic and abiotic properties, as well as sensitivity to local feedbacks involving hydrology, vegetation, and snowpack.

Across the Northern Hemisphere, the average permafrost temperature has increased by approximately 0.3˚C between 2007-2016 (Biskaborn et al., 2019) and permafrost thaw is projected to increase active layer thickness (ALT) by 30-40% by the end of the 21st century for most permafrost areas (Stendel and Christensen, 2002). The warming of permafrost has now passed a threshold where permafrost is predicted to continue to thaw for hundreds of years in some regions (Randers and Goluke, 2020). Such changes will undoubtedly change northern ecosystems. The amount of thaw in the active layer affects the availability of water and nutrients for biological processes, with increased thaw depth providing more volume for these processes (W. Dobiński, 2020; Hinzman et al., 1991; Kane et al., 1991). Understanding patterns in active layer thaw and

the influential drivers is crucial for understanding the consequences of thaw on the ecosystem.

Active layer thaw dynamics can vary widely across space, even at similar latitudes, due to variation in local environmental control. Features, such as vegetation, snow cover, soil moisture, and soil properties, govern active layer thermal regime at fine scales (Fisher et al., 2016; Mauro Guglielmin et al., 2008; Hu et al., 2020; Lafrenière et al., 2013; Luo et al., 2016; Subin et al., 2013). These factors can have both warming and cooling effects depending on time of year and synergistic interactions involving water and energy balance (Atchley et al., 2016; Subin et al., 2013; Yang et al., 2013). For example, vegetation alters surface albedo, affecting the amount of solar radiation absorbed by the ground (Blok et al., 2011; Loranty et al., 2014) and influences the amount of water that reaches the ground surface (Peng et al., 2019). Increased shading as a result of a transition to a shrubbier landscape can actually cool soil temperatures, which would result in a negative feedback to climate warming (Blok et al., 2010). As such, warming permafrost has been found to both promote and hinder vegetation growth, while also being affected by vegetation (Peng et al., 2019). Precipitation, both rainfall and snow, alter the soil's volumetric water content, which in turn affects thermal conductivity (Subin et al., 2013; Wen et al., 2014) and the latent and specific heat capacity of the ground (Hinkel et al., 2001). Soil moisture can also have varying effects within the same soil column. Closer to the surface, increased soil moisture can result in increased ALT depth due to increased thermal conductivity of the soil (Clayton et al., 2021). Alternatively, increased soil moisture across the entire active layer can result in shallower ALT due to increased latent heat of fusion for thaw (Clayton et al., 2021). The ice of more inundated sites must thaw

before the active layer can begin to thaw. Ice, however, has large latent heat requirements and thus requires a lot of energy to melt. Once the ice melts, the soil is saturated which increases the specific heat requirements of the soil. Combined, there is a greater energy input required to thaw the active layer which can result in shallower thaw depths. Snow is also an important factor as snow cover affects surface albedo (Li et al., 2018), with early melt decreasing albedo and promoting active layer thaw (Lafrenière et al., 2013; Ling and Zhang, 2003). It can also act as an insulator, meaning early onset of snow can trap heat in the ground, promoting greater summer ALT (Ling and Zhang, 2003). Soil properties are important as different soil types have different heat-conducting capacity (Cui et al., 2020) and also allow for different percolation rates and water holding capacity (Aiken and Cotsaris, 1995). Understanding whether these factors have warming or cooling effects on the active layer is important to understanding active layer thermal regime and its effects on ecosystem structure.

The active layer thermal regime and its environmental controls remain poorly understood in the subarctic and across the southern edge of continuous permafrost. In Ontario, the Hudson Bay Lowlands (HBL) intersect the southern edge of continuous permafrost in North America. It is the largest peatland complex in North America and a major carbon sink (Martini, 2006). The area represents a transition zone between boreal forest and Arctic, where most of the biota are adapted to a northern climate and occur at the southern trailing edge of their distributions. Thus, these species may be particularly vulnerable to environmental change (Hampe and Petit, 2005; Provan and Maggs, 2012). The region contains a heterogeneous mix of land covers that differ in vegetation cover, soil moisture regime, and soil properties. The most prominent land cover is treeless

wetlands, notably fens and bogs that make up approximately 60% of the landscape within the continuous permafrost zone of the Ontario HBL. Fens are most common near the coast and transition into primarily bogs about 30km inland. Tundra heath, characterized by well drained soils, make up about 2% of the land cover within the continuous permafrost zone and occur on relic coastal and inland beach ridges that parallel the Hudson Bay coast. They typically occur within 15km of the coast. Extensive areas of palsas, defined as peat mounds with perennially frozen peat cores and predominantly lichen covers, also occur throughout the continuous permafrost zone, approximately 20 to 30km inland. These different land covers are expected to vary in active layer thaw dynamics, but the nature of this variation remains unclear in this landscape.

My objectives were to 1) describe and compare the active layer thermal regime of palsas, fens, and tundra heath and 2) investigate how landform, vegetation, and weather conditions affect the active layer thermal regime in an extensive wetland at the southern edge of continuous permafrost in North America. I used weather station data and ground-based measurements to determine the differences among palsas, fens, and upland tundra heath with respect to the effects of soil moisture, snow cover, temperature, and vegetation composition on active layer thaw patterns.

I expected palsas to have shallower thaw depths than tundra heath and fens due to the combined effects of a thick peat layer and lichen cover that promote greater freezing in the winter and reduced heat absorption in the summer. I expected that the effects of temperature on active layer thaw dynamics (timing, rate, magnitude of thaw) will be modified by site-specific environmental conditions, such as soil moisture and vegetation.

Due to the increased thermal conductivity of water compared to air, I predicted that increased soil moisture would promote active layer thaw.

Methods

Study Site

My study site was located within the HBL in Northern Ontario, overlapping Polar Bear Provincial Park (Burntpoint Creek Research Station, N55.241, W84.318) (Figure 1). This region is dominated by a vast wetland complex, situated southwest of the James Bay and Hudson Bay. The substratum of the HBL is comprised of Precambrian terrain that binds Paleozoic and Mesozoic rock (Martini, 1989). The last glaciation period in the area occurred when the Laurentian Ice Sheet covered the region, which caused a significant amount of subsidence due to its weight (Martini, 2006). Retreat of the ice sheet left the area inundated which, in turn, left a layer of marine silty clays (Martini, 2006). Since the early Holocene, the HBL has been subjected to isostatic rebound and the continual emergence from the sea (Martini, 2006). The area is characterized by tidal flats adjacent to the coast, irregularly shaped inland beach ridges (tundra heath), which show the location of former shorelines, fens, bogs, marshes, peat plateaus, and palsas.

The HBL has a humid microthermal arctic climate (as per the Köppen system) (Chapman et al., 1968) with mean annual temperature at the Burntpoint Creek Research Station ranging from -5.6˚C to -1˚C and total annual rainfall ranging from 234mm to 292mm throughout the study period. No significant trends in air temperature were observed throughout the study period (2009-2021, Mann Kendall Trend Test, $p>0.05$). The area is uncharacteristically cold for its southernly latitude due to the influx of arctic air masses over the relatively flat terrain and from the influx of some arctic water into James Bay and Hudson Bay which has a cooling effect on the landscape (Martini, 1989).

The area is located at the southernly limit of continuous permafrost in Canada, defined as areas where at least 90% of the ground is underlain by permafrost (Heginbottom et al., 1993). Permafrost thickness is relatively shallow in the HBL (<10m) compared to more northern latitudes (Smith and Burgess, 2002). Recent modeling of permafrost within the HBL indicate a reduction of the continuous permafrost zone between Churchill, Manitoba and Polar Bear Provincial Park (Dredge and Dyke, 2020).

Vegetation is primarily low-lying, with lichen and moss growing on the dryer tundra. Lapland rhododendron (*Rhododendron lapponicum*), crowberry (*Empetrum nigrum*), mountain cranberry (*Vaccinium vitis-idaea*), and many graminoids are also common. Low-lying shrubs can also be found, notably dwarf birch (*Betula nana*), willow (*Salix species*), and Labrador tea (*Rhododendron tomentosum*). Stunted coniferous trees, including black spruce (*Picea mariana*), tamarack (*Larix laricina*), and white spruce (*Picea glauca*), also grow, but tree density decreases from south to north. The area also supports many cold-adapted wildlife, such as woodland caribou (*Rangifer tarandus caribou*), moose (*Alces alces*), marten (*Martes species*), arctic fox (*Vulpes lagopus*), and polar bear (*Ursus maritimus*). This is also the southern edge of range of many breeding migratory shorebirds and waterfowl, including white geese (*Chen caerulescens*), dunlin (*Calidris alpina*), whimbrel (*Numenius phaeopus*), and Hudsonian godwits (*Limosa haemastica*).

Data Collection: Weather Station Data

Weather and ground temperature information were collected by the Ontario Ministry of Northern Development, Mines, Natural Resources and Forestry (NDMNRF). Eight continuous data-logging weather stations located in the study area (Figure 1, Figure

S1) were equipped with below-ground thermistor strings (Campbell CS225 Temperature String) to collect hourly soil temperature information. Soil temperature sensors are located every 0.5m along the thermistor string starting at 0m or 0.5m depending on the station and ending at 2m (Figure 1, Table 1). These stations also recorded hourly measurements for air temperature (Campbell HC-S3-XT Relative Humidity and Air Temperature Probe), snow depth (SR50A Sonic Ranger 5KHz Module), and a relative index of near surface soil moisture (CS616-L50 Water Content Reflectometer, installed horizontally 5cm below the surface, pre-set calibration). The Water Content Reflectometer measured volumetric water content as the ratio of the volume of water to the volume of soil. The soil moisture probe used the high dielectric permittivity value of water to detect volumetric water content of the soil (Campbell Scientific, 2016). Given that calibration of the soil moisture units was not feasible for my study, these measurements were interpreted as relative differences in soil moisture for making comparisons among sites and landforms (Migała et al., 2014), rather than absolute value of soil moisture. Although measures of soil moisture at depths corresponding to the measures of soil temperature would be beneficial, they were not available for this study. The stations provided information for varying numbers of years since 2008 (Table 1).

Weather Stations: Vegetation Descriptions

The weather stations were located on upland tundra heath, fen, and palsa landforms. Quantitative vegetation descriptions were collected at each of the weather stations. Five by five-meter plots were measured with the weather station in the center of each plot. Percentage of each vegetation class (e.g., lichen, moss, low-lying shrub) was visually estimated within each quadrat and recorded.

Weather stations Tundra 1 and 2 were found on tundra heath. Vegetation cover at Tundra 1 was 50% moss and lichen, 10% shrub, and 30% forb. Tundra 2 contained a lot of bare soil (50%), lichen (48%), and 2% low-lying shrub. Fen 1 consisted of 90% graminoid, 5% shrub, and 5% moss and lichen. Fen 2 was 70% graminoid, 10% bare soil, and 20% moss. Palsa 1 station was removed and the palsa decayed, preventing me from collecting vegetation measurements. Palsa 2 was 40% lichen, 40% moss, 15% low-lying shrub, and 5% bare soil. Palsa 3 was 60% bare soil, 5% moss, 25% lichen, 5% conifer, and 5% berry shrubs. Palsa 3 was the only station located in the discontinuous permafrost zone and was a decaying palsa as evidenced by erosion and large (approximately $3m^2$) patches of bare soil at the surface (Figure S1g). Palsa 4 consisted of 40% lichen, 30% bare soil, and 30% berry shrubs.

Weather Stations: Soil Descriptions

Soil at weather stations Tundra 1-2 have an upper layer of organic soil (average depth 6.2cm) followed by predominantly sandy and gravel soil. Fen weather stations consisted of upper peat layer (average depth 27.6cm) overtop of mineral soil and were highly saturated, both in soil moisture and surface water. Soil at weather stations Palsa 1-4 consisted of a deep layer of peat (greater than 1.25m (Railton and Sparling, 1973)). Soil profiles could not be obtained for this study, so the depth of each soil horizon is unknow.

Each soil type has its own distinct characteristics that affect movement of water and transmission of heat throughout the soil column. Peat is decayed or decaying organic matter that can hold large amounts of water. Thermal conductivity of dry peat is estimated at 0.06 $Wm^{-1}K^{-1}$ (Letts et al., 2000), while thermal conductivity of thawed saturated peat and frozen peat is approximately 0.48 $Wm^{-1}K^{-1}$ and 1.2 $Wm^{-1}K^{-1}$,

respectively (McClymont et al., 2013). Saturated hydraulic conductivity of peat has been estimated at $4.2x10^{-2}$ ms^{-1} (McClymont et al., 2013) and water-holding capacity is approximately 5.06 g/g (Treat et al., 2014). Mineral soils are mainly composed of minerals or rock and contains little organic matter. Average thermal conductivity of mineral soil is estimated to be 2.93 $Wm^{-1}K^{-1}$ (Letts et al., 2000). Hydraulic conductivity of mineral soil is estimated to be $1.2x10^{-7}$ ms^{-1} (Balland et al., 2008), while water-holding capacity ranges from 0.1 to 0.3 cm^3/cm^3 (Lennartz and Liu, 2019). Sand and gravel are coarse-grained soils with no organic matter. Thermal conductivity is estimated to be 4.44 $Wm^{-1}K^{-1}$ for gravel soils (Hamdhan and Clarke, 2010). Hydraulic conductivity of gravel soils is estimated to be $3x10^{-4}$ ms^{-1} (Lowry et al., 2009), while water-holding capacity ranges from 0.02-0.06 cm/cm (Adamu and Aliyu, 2012).

Data Collection: Manual Active Layer Thickness

Manual measurements of ALT were available for two transects near the Burntpoint Creek Research Station (Figure 2). The fen transect (2012-2021) was typically flooded in spring and dominated by graminoid cover, with a deep peat layer (average depth 27.6cm), varying amounts of surface water saturation, and interspersed with patterned low shrub fen ribs (Riley, 2011). Two stations within this transect were located on the exposed edge of beach ridges, where vegetation began to transition to mossy wet tundra heath. The drier upland tundra heath transect (2014-2021) was not typically flooded in the spring, was characterized by a shallow organic layer (average depth 6.2cm) underlain by gravel and sand, and was interspersed with shrub-rich graminoid fen, open-low shrub, and tundra heath cover. The fen transect consisted of ten stations, approximately 250m apart. The upland tundra heath transect consisted of ten stations,

approximately 150m apart. Stations were marked using metal rods and flagging tape to ensure sampling locations were the same every year. Each year, ALT was manually measured at each station by hammering a steel rod into the ground until frozen ground was reached and measuring depth to ice. To characterize seasonal patterns in thaw, ALT measurements were collected three times each year, in early June, July, and August, referred to as sample period 1, 2, and 3 , respectively.

Analyses

The soil temperature information from the data-logging weather stations were used to describe and compare the active layer thermal regime among the three landforms (tundra heath, fen, palsa). I linearly interpolated soil temperature from the weather stations between each soil temperature probe depth at 0.05m intervals (Table 1). I then plotted soil temperature across depth and time using the ggplot package in R to create soil temperature profiles. The following indices were extracted from the soil temperature profiles as indicators of active layer thermal regime:

1. Seasonal Soil Temperature Change: Change of soil temperature between the 100^{th} and 200^{th} day of year at a depth of 0.5m calculated using the following formula:

$$\text{Seasonal Soil Temperature Change} = (Tsoil_{200} - Tsoil_{100})/100$$

   This time frame was selected to capture the transition from soil temperatures below 0˚C to soil temperatures above 0˚C across all stations and years.

   A depth of 0.5m was selected due to issues with the thermistor string placement at stations Tundra 1 and 2 and Palsa 1. Soil temperature values were not reliable below 1m, so 0.5m represented a reliable depth measurement across all stations.

2. Start of Thaw Index: First day where daily average soil temperature is greater than 0˚C at 0.5m depth. This metric does not represent the actual start of ground thaw. Ground thaw begins at the surface, so the ground has already undergone substantial thawing by the time thaw begins at 0.5m. However, surface soil temperature was not available across all weather stations. This metric was used as a relative measure of the start of the thaw period and for comparison across landforms.
3. Length of Thaw period: Number of days where ground remains thawed (average daily soil temperature >0˚C) at depth of 0.5m
4. Average soil temperature: Average soil temperature at 0.5m during the thaw period
5. Vertical Thaw Rate: Change in depth over time of the 0˚C isotherm between 0.5-1m. It was calculated using the following formula:

    Vertical Thaw Rate = (1m – 0.5.m)/(Day of year when 0˚C isotherm reaches 1m – Day of year when 0˚C isotherm reaches 0.5m)

This metric only follows the 0 ˚C isotherm between 0.5m-1m depths to account for uncertainty in soil temperature measurements below 1m at stations Tundra 1, Tundra 2, and Palsa 1.

Each index of active layer thermal regime was used as a response variable in a linear mixed effect model using the *lme* function in the *nlme* R package (Pinheiro et al., 2022) with landform as a fixed effect and station as a random effect. The effect of landform within each model was compared using the *lsmeans* function in the *lsmeans* R package (Lenth, 2016) with a Tukey adjustment. This function computes the least-squares

means of a given factor and compares them. Since weather stations are present for varying number of years, I removed years where spring or summer air temperature deviated from the years present across all the stations.

The manual ALT transect data was also used to compare active layer depth between transects and across years. I compared ALT between the upland tundra and fen transects over time using a two-way analysis of variance (ANOVA) with transect and year as effects on average ALT values across the three sample periods. I also tested for the presence of a temporal trend in manual ALT using a Man Kendall Trend test using the *MannKendall* function in the *Kendall* package in R (McLeod, 2011). I also compared ALT between the three sample periods using a two-way ANOVA on average ALT at each transect during each sample period across all years with transect and sample period as effects.

To investigate how weather conditions affect active layer thermal regime, I extracted the following weather metrics from the weather station data:

1. Percent Thaw Days: Percentage of the first 150 days of the year with an average daily air temperature greater than 0˚C
2. Day of Last Snow: Last day of year when snow is recorded on the ground prior to the start of thaw. The snow sensor is accurate to the nearest centimeter, and we used the first day of the year where snow depth was 1cm or less as day of last snow.
3. Early Season Soil Moisture: Average soil moisture (%), measured 5cm below surface and following ground thaw at this depth, for the 20 days prior to the start

of the thaw period at 0.5m below surface. Ground thaw at 5cm was confirmed during this timeframe by the detection of soil moisture by the probes.

Each weather metric from the weather stations was used as a predictor for each of the indicators of active layer thermal regime in a generalized additive model (GAM). The indicators of active layer thermal regime across all years were pooled across landform (tundra heath, fen, palsa). The GAM was selected to account for possible non-linear relationships between the weather and active layer metrics. I ran these models in R using the *mgcv* package (Wood, 2017), smoothing parameter *k* was set to 4 to avoid overfitting using thin plate regression splines, and the Maximum Likelihood method was used for estimating the smoothing parameter. Non-linear terms were fit with splines (Wood, 2006). GAMs assume that the predictor value is measured without error. In practice, however, we assume that predictor variables are measured with less error than response variables. Due to small sample size of the indicators of active layer thermal regime, separate models were used to evaluate the effect of each of the weather metrics. Second-order Akaike information criterion (AICc) values were used to compare models with and without landform as an interacting effect to select the model of best fit. AICc was selected to correct for small sample size. AICc values were also used to rank models for weather predictors within each response variable grouping. To keep sample size consistent across models with same response variable, missing predictor values were assigned the average value across years and sites.

Results

Active Layer Thermal Regime Comparison

Differences in active layer thermal regime were evident among tundra heath, fens and palsas (Figure 3, Figure S2). Palsas had the lowest soil temperature during the thaw period, and thaw depth was shallowest among the three landforms (Figure 3). Conversely, tundra heath had the warmest soil temperature during the thaw period (Figure 3, darker red color), and thaw depth was greater. Palsa 1 was the only palsa that did not have shallower thaw depth in comparison to other landforms (Figure S8); however, it had collapsed, and surface water had inundated much of the original palsa.

Seasonal soil temperature change was significantly greater at tundra heath sites than palsas ($p=0.01$), averaging 0.147˚C/day and 0.073˚C/day, respectively (Figure 4a, Tables 2-3). Seasonal soil temperature change of fens, averaging 0.077 ˚C/day, was not significantly different than either tundra heath or palsas ($p>0.05$, Figure 4a, Tables 2-3). The start of thaw index at palsas was significantly later than at tundra heath sites, averaging day of year 196 and 144, respectively ($p=0.004$, Figure 4b, Tables 2-3). Start of the thaw index was also significantly later at palsas than fens ($p=0.03$). Start of the thaw index in fens, averaging day of year 161, was not significantly different than at tundra heath (day of year 144) ($p=0.44$, Figure 4b, Tables 2-3). The thaw period was longest at the tundra heath and fens and shortest at the palsas (Figure 4c. Tables 2-3), averaging 159**,** 162, and 103 days, respectively. However, no significant differences between landform were detected ($p>0.05$). Average soil temperature during the thaw period was significantly higher at the tundra heath sites, averaging approximately 6.5˚C, than at the palsas, which averaged 2.1˚C ($p=0.02$, Figure 4d, Tables 2-3). Average soil temperature

during the thaw period at the fens was also relatively high, averaging 4.8 ˚C, but did not vary significantly from the tundra heath or palsas ($p>0.05$), despite visual differences (Figure 4d, Tables 2-3). Vertical thaw rate had the widest distribution at the tundra heath, averaging 0.20m/day, compared to the palsas and fens, which averaged 0.018m/day and 0.015m/day, respectively (Figure 4e, 4f, Tables 2-3). However, no significant differences in calculated least-squares means were detected ($p>0.05$).

Manual Active Layer Thickness Comparison

Two-way ANOVAs were used to compare ALT across the two transects and years (Table 4). There was no significant interaction between transect and year ($F_{6,403}=1.48$, $p=0.183$), but I found a significant year effect, indicating strong annual variation in thaw depth ($F_{6,403}=3.38$, $p=0.003$, Figure 5a), but this variation was not directional. The Mann-Kendall trend test detected no significant temporal trend in the upland tundra transect (tau= -0.048, p=1) nor in the fen transect (tau= -0.057, p=0.917), consistent with the absence of a temporal trend in ambient air temperature.

The two-way ANOVA assessing the effects of transect and sample period revealed a significant effect of transect ($p<0.0001$) and sample period ($p<2E-16$) (Table 4). There was also a significant interaction between transect and sample period ($p=0.0014$). A Tukey post-hoc analysis revealed a significant difference between the fen and tundra transects during sample period 2 or early July ($p= 0.000003$), but no significant differences were found between the two transects during sample period 1 (early June) or sample period 3 (early August, $p>0.05$ for both, Figure 5b).

Effects of Weather on Active Layer Thermal Regime

AICc values ranked by response variable suggest that, overall, percent thaw days was the most influential predictor of active layer dynamics in this study (Table 5, Table S1, Figure S3-S11). Models with percent thaw days had the lowest AICc value for all indicators of active layer thermal regime, except seasonal soil temperature change where the model for day of last snow had a lower AICc value than the model for percent thaw days (Table 5. Table S1).

GAMs indicate that average soil temperature and vertical thaw rate were each significantly affected by percent thaw days and its interaction with landform (Table 5, Table S1). Models of best fit for seasonal soil temperature change, start of the thaw index, and length of the thaw period did not include landform as an interaction effect (Table 5, Table S1). Average soil temperature during the thaw period was significantly affected by percent thaw days in palsas ($p=0.011$) with increased thaw days resulting in increased soil temperatures (Figures 6 & 7, Table 5). Start of the thaw index varied significantly with percent thaw days across all landforms ($p=0.004$) with increased percentage of thaw days resulting in an earlier start to the thaw period at 0.5m within the active layer (Figure 6 & 7, Table 5). The start of the thaw index began following a gradual increase in air temperature (Figures S4-S11). Length of the thaw period was significantly affected by percent thaw days ($p=0.004$) with increased percent thaw days resulting in longer thaw periods (Figures 6 & 7, Table 5). Seasonal soil temperature change and vertical thaw rate were not significantly related to percent thaw days ($p=0.17$, Figures 6, Table 5). The relationship between air temperature profiles and soil temperature profiles was also inspected visually (Figure 3). As expected, there is a lag between the start of rise in air

temperature in the spring and rise in ground temperature. Between landforms, however, there are differences in the progression of ground thaw as air temperature hits zero degrees Celsius. As temperature hits 0˚C, ground temperatures at the tundra heath also sits around 0˚C (white color), fen ground temperatures are still frozen and sit just below 0˚C (light blue color), and palsas are also still frozen but the darker blue colors of the soil temperature profiles indicate that soil temperature is cooler than in the fens.

Seasonal soil temperature change and vertical thaw rate were correlated with day of last snow and its interaction with landform, but the interaction with landform was not significant for the other models (Table 5, Table S1). Seasonal soil temperature change was significantly correlated with day of last snow in tundra heath only ($p=0.017$), and the trend was found to represent a quadratic relationship (Figure 7, Table 5). Day of last snow did not have a significant effect on any other indices of active layer thermal regime (Figures 6 & 7, Table 5, $p>0.05$ for all).

Soil moisture varied significantly among landforms and evidence from our GAMs suggested that soil moisture did not improve the explanatory power of thermal regime response models when landform was included as a factor (Table S1). Independent GAMs for the effect of soil moisture and landform indicated that AICc values were lower for landform in the univariate models (Table S1). However, visual inspection of the scatter plots suggested a probable effect of soil moisture on response variables that was potentially confounded with landform level differences (Figure 6). I report trends found in the univariate soil moisture models to assess the apparent direct effect of soil moisture on active layer thermal regime. Seasonal soil temperature change and average soil temperature during the thaw period were significantly and negatively correlated with soil

moisture ($p=0.0022$ and $p= 0.013$, respectively, Figure 7, Table 5). Length of the thaw period and vertical thaw rate were significantly correlated with soil moisture ($p=0.0086$ and $p=0.025$, respectively), where both metrics decreased non-linearly in response to increased soil moisture until an asymptote (Figure 7, Table 5). Start of the thaw index was significantly correlated with soil moisture ($p=0.0017$), where greater soil moisture resulted in a delayed start to the thaw period until an asymptote (Figure 7, Table 5).

Discussion

I found that active layer thermal regime differed among tundra heath, fens, and palsas. Thaw rates and soil temperatures were greatest at the tundra heath sites and lowest at palsas. The greater thaw depth recorded may be evidence of the increased thaw the resulted in its collapse. As expected, air temperature, as indicated by percentage of thaw days, was a significant predictor of active layer thermal regime, but site-specific environmental factors appear to mediate some of those effects. Palsas experienced the least amount of thaw compared to fens and tundra heath. Contrary to what we expected, increased soil moisture at the surface did not promote active layer thaw. My findings are consistent with the widely recognized overarching importance of weather patterns driving annual variation in active layer thickness (Abramov et al., 2019; Wu et al., 2015).

As expected, air temperature was the most important predictor of active layer thermal regime in my study, with increased percent thaw days resulting in an earlier start of thaw index, longer thaw periods, and greater soil temperatures in the palsas. However, some of the effects of temperature were mediated by landform-specific properties. This was demonstrated through the non-significance of percent thaw days for some of the landforms and for some of the metrics (Figure 7). It was also evidenced by the variation in progression of thaw across landforms as air temperature reached zero degrees Celsius (Figure 3). It is likely that site-specific environmental factors, notably soil properties, vegetation, and soil moisture, are mediating the effects of temperature and contributing to variation in active layer thermal regime detected between landforms (Almeida et al., 2014; Railton and Sparling, 1973).

Soil properties that affect heat conduction may explain variation among palsas, fens, and tundra heath in active layer thaw patterns. Organic matter thickness varies among sites and palsas had the thickest peat layer (>1.25m), followed by fens (27.6cm) and tundra heath (6.2cm). Greater thickness of organic matter is correlated with smaller ALT values due to the insulative properties of organic soil (Fisher et al., 2016). This relationship, however, is dependent on soil moisture, with increased soil moisture increasing thermal conductivity of peat and, therefore, decreasing it ability to insulate (Fisher et al., 2016; Zoltai and Tarnocai, 1971). For example, Palsa 2 had greater soil moisture and greater thaw depth thaw Palsa 3 (figures S9, S10). In general, the thick and dry peat layer of palsas have low thermal conductivity which helps them remain relatively cool year-round and retain their ice cores (Nelson et al., 1985; Railton and Sparling, 1973). It also helps create a negative energy balance needed during palsa formation (Railton and Sparling, 1973). Fens and tundra heath had much thinner organic layers, which resulted in less insulation and greater thaw depth (Fisher et al., 2016). Fens also remain saturated for most of the season; saturated peat has been found to have greater thermal conductivity than dry peat which would also result in greater thaw compared to palsas (Fisher et al., 2016; Nelson et al., 1985). Furthermore, peat of fens was underlain by mineral soil which has greater thermal conductivity than peat (Hinzman et al., 1991). Despite the increased thermal conductivity, fens have still been found to have shallower maximum thaw depths than drier landforms, like the tundra heath, due to higher ice content of the fens (Woo and Xia, 1996). Greater amounts of latent heat are required to melt ground ice prior to the start of ground thaw, thus reducing energy available for ground thaw (Woo and Xia, 1996). Tundra sites have a dry, but thin organic layer. While thermal conductivity of the organic layer may be low, there is insufficient thickness to

provide adequate insulation. Furthermore, tundra heath organic soil is underlain by coarse-grained gravel, which has high thermal conductivity, thus allowing for greater transmission of heat throughout the active layer and promoting active layer thaw (Cui et al., 2020; Iijima et al., 2017; Shiklomanov et al., 2010). These properties explain the greater thaw seen at the tundra heath sites compared to palsas and fens.

Vegetation can influence soil temperature and thus ALT though multiple pathways, including effects on shading, snow accumulation, and albedo (Cannone et al., 2006; Fisher et al., 2016; Guo et al., 2018; Hu et al., 2020); however, I was unable to confirm the importance of these factors using direct measurements. No sites had significant tree cover for shading and, although palsa sites typically had greater amounts of shrub cover, the density and height of shrubs was relatively low, and the greater elevation of palsas in the generally flat terrain also provided more wind exposure that may counter the effects of snow accumulation. Although lichen, common on palsas and tundra heath, may give rise to relatively higher surface albedos compared to fen vegetation (Lafleur et al., 1997; Matthias et al., 2000; Railton and Sparling, 1973; Stoy et al., 2012) and potentially reduce het loss, tundra heath and palsa had the highest and lowest soil temperatures, respectively. Edaphic factors in combination with ambient air temperature may have had a stronger influence in my study, although vegetation may interact with soil moisture conditions to affect active layer thermal regime (Fisher et al., 2016).

Timing of snow melt did not affect active layer thermal regime in my study; however, snow is widely known for its ability to insulate the soil and delayed snowmelt can delay the start of the thaw period in the active layer, thus decreasing ground

temperature (Ling and Zhang, 2003). I was unable to assess the effects of snow depth and its effect on winter and summer energy balance and suggest that further studies collect detailed snow information to help clarify its effect on active layer thermal regime.

Contrary to what I expected, lower soil moisture at the surface was positively related to thaw. Water has higher heat capacity than air, and therefore takes more energy to heat up more saturated soils than drier soils (Clayton et al., 2021; Tatenhove and Olesen, 1994). The tundra heath sites had the lowest soil moisture values of all three landforms. Since soils on the tundra heath sites were the least saturated, they require less energy than the palsas and fens to warm up which would explain my findings. Although I was unable to measure soil moisture at greater depths below surface, the tundra heath sites were known to have a deep layer of coarse sediment within the depth profile of soil temperatures, suggestive of drier conditions further down (Migała et al., 2014), compared to a deep organic layer characteristic of the fens. An alternative explanation is that increased thaw depth actually decreased surface soil moisture by allowing surface water to move down the thawing front, lowering the water table and thus decreasing soil moisture at the surface (Yang et al., 2013). As the soil moisture probes were only located at the surface, I cannot confirm the influence of such factors. Due to the known variation in soil moisture across different depth in the same soil column (Clayton et al., 2021), future studies in this study area should assess the effects of soil moisture at different depths on active layer thermal regime.

Manual ALT in the tundra heath transect was greater than in the fen transect, however, significant differences were only detected between the two transects during the second sample period, or early July. Overall, greater thaw occurred in the tundra transect

between sample period two and three (June to July), whereas greater thaw occurred in the fen transect between sample period two and three (July to August) (Figure 5). These findings are consistent with observations from the weather stations that indicated more rapid thaw in in the drier tundra heath sites and slower thaw on the fen that had greater amount of peat and soil moisture. As ground thaw commences, fens are highly saturated both in soil moisture and surface water, but as the summer progresses, water content in the fens decreases. The GAMs demonstrated that decreased soil moisture was positively related to thaw, which may explain the increased thaw of fens in later summer when conditions were drier. The similar maximum thaw depth between these transects suggest perceived differences in surface cover and below ground properties of these sites did not result in different ground temperatures in late summer.

The patterns of active layer thermal regime represent local dynamics at the southern edge of continuous permafrost, which may differ from patterns within core areas of continuous permafrost and colder climates. Although annual variation in active layer thickness was evident, I did not find a definitive temporal trend. Deeper thaw and thickening of the active layer has been seen in the high Arctic, with increases in ALT of 3%-6% occurring between 2008-2012 (Sobota and Nowak, 2014) and corresponding to increases in air temperature (Wawrzyniak et al., 2016). Subarctic regions have been found to have more muted responses to warming than the high Arctic (Fraser et al., 2018). Consistent with my findings however, there is also significant spatial variation in ALT in the high Arctic, including among sites at similar latitudes where the general climate would be similar (Sobota and Nowak, 2014). Across the Northern Hemisphere, soil

moisture was found to be a significant contributor to ALT, particularly in North America, whereas snow depth was not (Wang et al., 2018).

Despite finding significant differences among the three landforms in my indicators of active layer thermal regime, my choice of indices and errors in measurements may have influenced my results. My ability to detect differences in the effects of soil moisture between landforms may have been hindered by the use of the soil moisture probes. The calibration of the soil moisture probes was pre-set for mineral soil and therefore did not account for the more complex structure and small bulk density of organic soil (Bircher et al., 2016). Organic soils have greater porosity and larger surface area than mineral soil, thus allowing for greater water holding capacity and a larger amount of bound water which alters the dielectric constant (Bircher et al., 2016). The soil moisture probes are, therefore, potentially underestimating actual soil moisture values (Bircher et al., 2016). Furthermore, the soil moisture probes were inserted at the surface into the organic layers of our three landforms and therefore didn't detect soil moisture of the underlying soil types or depths. My findings are interpreted as a relative index of soil moisture at surface for comparisons among landforms and the relative importance of my soil moisture index in explaining observed variation in the active layer. Further, Yang et al. (2013) found thaw surface soil moisture is correlated with thaw depth early in the ground's thaw period. Since my active layer metrics incorporate soil temperatures early in the ground's thaw period, I can establish that surface soil values impacted the assessed active layer thermal regime metrics. Furthermore, soil type differs within each soil column. Each soil type has its own distinct characteristics, each having its own thermal conductivity, heat capacity, percolation rates, and water holding capacity. These factors will affect both soil

temperature and soil moisture, meaning that surface soil moisture does not capture the soil moisture conditions of underlying soil strata. Despite the limitations of the probes, variation in soil moisture regime between the three landforms was still supported by past studies (Migała et al., 2014; Railton and Sparling, 1973). Calibration of these data and generation of reliable absolute measures will be important for prediction and where mechanistic understanding is needed for the magnitude of effects to active layer properties in response to absolute values of soil moisture, and the important influence of soil moisture at different depths (Clayton et al., 2021), but such examination was beyond the scope of this study. An additional study may be needed to assess the accuracy of the soil moisture measurements by recalibrating the probes for organic soil and comparing the data to the data calibrated for mineral soil.

Some of the active layer thermal regime metrics may have limited my ability to detect certain patterns. Vertical thaw rate, for example, may have been too sensitive to extreme weather days. Average vertical thaw rate at the tundra heath weather stations was 0.2m/day, meaning that the 0˚C isotherm would have passed between 0.5m and 1.0m in only 2.5 days. Given the thin organic layer of the tundra heath and the well-drained gravel soils, quick thawing at these sites could occur with even a small number of unusually warm days. Next, seasonal soil temperature change may not have detected the full extent of variation of ground thaw at 0.5m. Day of year 100 to 200 was selected as a relative metric to assess a transition between frozen ground and thawed ground across the three landforms. However, rates of thaw could have been drastically different had the date range been shifted by only a few days, especially considering how quickly heat was transmitted through the ground at the tundra heath sites. As such, this metric could be

improved to account for the day-to-day variability in soil temperature at this depth. While a depth of 0.5m was selected for several metrics because of the ability to compare across all landforms, this would have also impacted interpretation of results. This depth would have intersected different soil types across the different landforms. Soil temperature at a given point in time under similar climatic conditions would be different within a peat layer, mineral layer, or gravel layer. The above soil layers, notably thickness of the soil organic layer, would have also influenced the gradient of heat down to assessed ground depth. As such, some of the variation in active layer metrics detected by the GAMs is likely due to the soil horizon and not the assessed predictor. Despite limitations so the selected metrics, metrics similar to those in this study have been used previously to assess active layer thaw patterns (Wright et al., 2009; Wu et al., 2015). Wu et al. (2015) compared the onset and duration of thaw at 0.5m across different landforms, equivalent to the start of thaw index and length of thaw period in my study. At tundra-heath-like sites, onset of thaw occurred around May 8 and duration of thaw lasted 170 days (Wu et al., 2015). Start of thaw index at the tundra heath averaged day of year 144 (late May) and the length of the thaw period was estimated to be 170 days in my study. Wright et al. (2009) assessed the relationship between spring thaw rate and air temperature, similar to my metric of vertical thaw rate. Spring thaw rates were based off a 35-day window at the start of ground thaw. Contrary to my results, they found significant a strong correlation between spring thaw rates and air temperature (Wright et al., 2009).

Current climate projections estimate a 10˚C increase in annual air temperature by 2080 in the HBL (McDermid et al., 2015) posing high risk of permafrost degradation, changes in the hydrological cycle, and shifts in vegetation (Riordan et al., 2006). Based

on my results, temperature is a significant predictor of active layer thermal regime but may be mediated by site-specific environmental factors. These increases, however, are expected to cause a shift in vegetation towards a "greener" landscape, which in turn, through changes in albedo, could increase ground temperatures, thaw rates, and ultimately promote permafrost degradation (Peng et al., 2019). Furthermore, there is evidence suggesting that air temperature may diminish the impact of soil moisture and snow cover as air temperatures continue to rise (Wang et al., 2018). The ultimate degradation of permafrost is predicted under the context of climate change, but the extent and rate of this melt may be difficult to predict given the site-specific environmental factors that can mediate the effects of climate change.

Conclusion

I found that active layer thermal regime differs among tundra heath, fens, and palsas, and thaw patterns are influenced by air temperature. However, in certain cases, the effects of temperature are likely mediated by site-specific environmental factors, notably vegetation and soil properties. These fine-scale environmental factors also contribute to the distinct patterns in active layer thaw that are not necessarily supported by other studies. Active layer thermal regime is controlled by complex interactions between environmental factors, such as snow cover, vegetation, organic layer, and soil properties. Since every landscape has their own unique vegetation composition, soil moisture regime, soil types, and snow fall patterns, active layer thermal regime will vary across regions even at similar latitudes. As such, it is important to understand these relationships at fine-scales to try to understand to effects of climate change at local-scales and predict how these interactions might be altered and how some of these factors might promote thaw or mediate the effects of climate change.

Figures and Tables

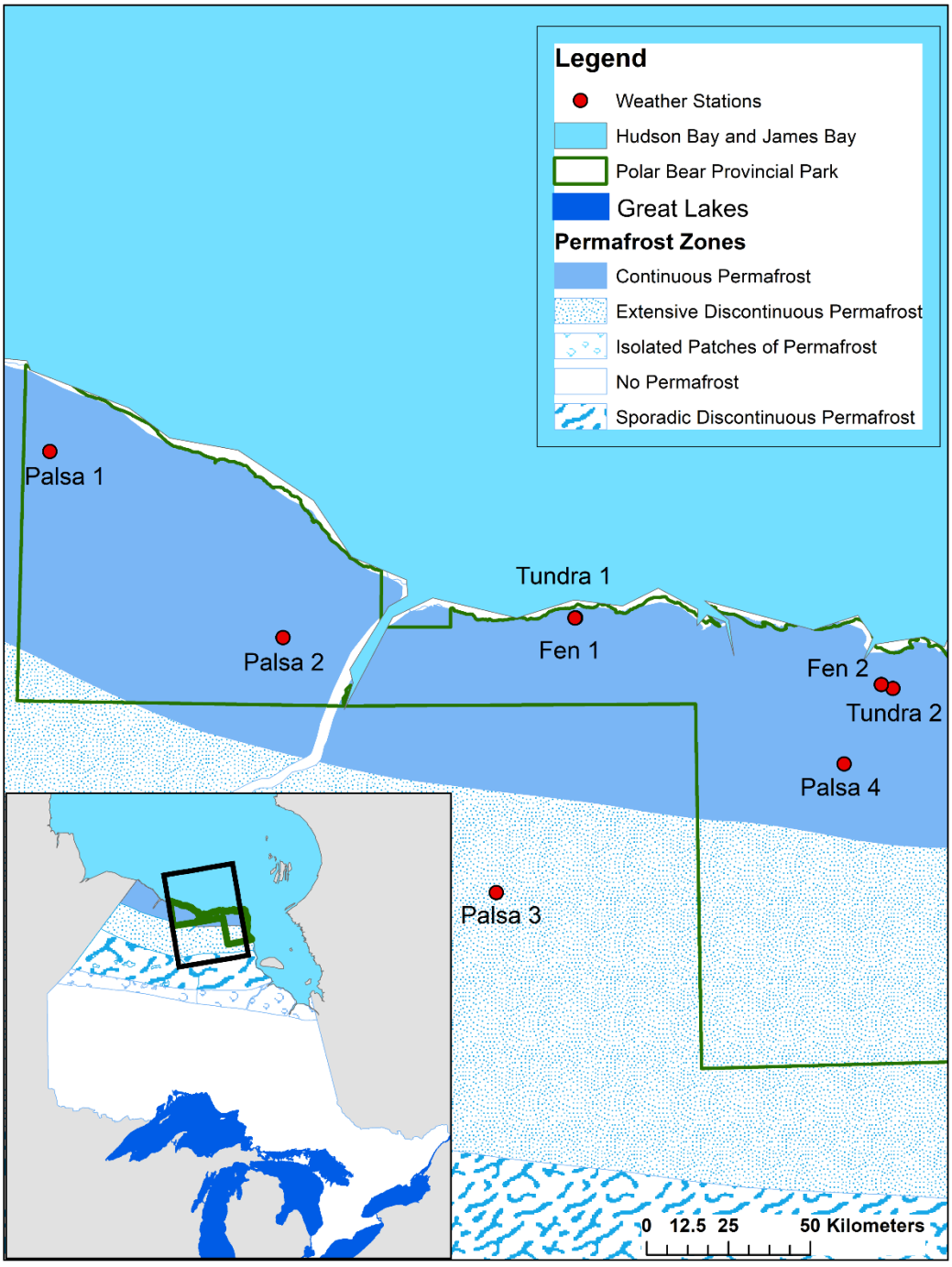

Figure 1. Location of the data-logging weather stations and their associated permafrost zone. The names of weather stations are indicative of landform. Inset map indicates the location of our study area in comparison to the province of Ontario. Tundra 1 and Fen 1 locations are identical on the map due to their proximity of each other.

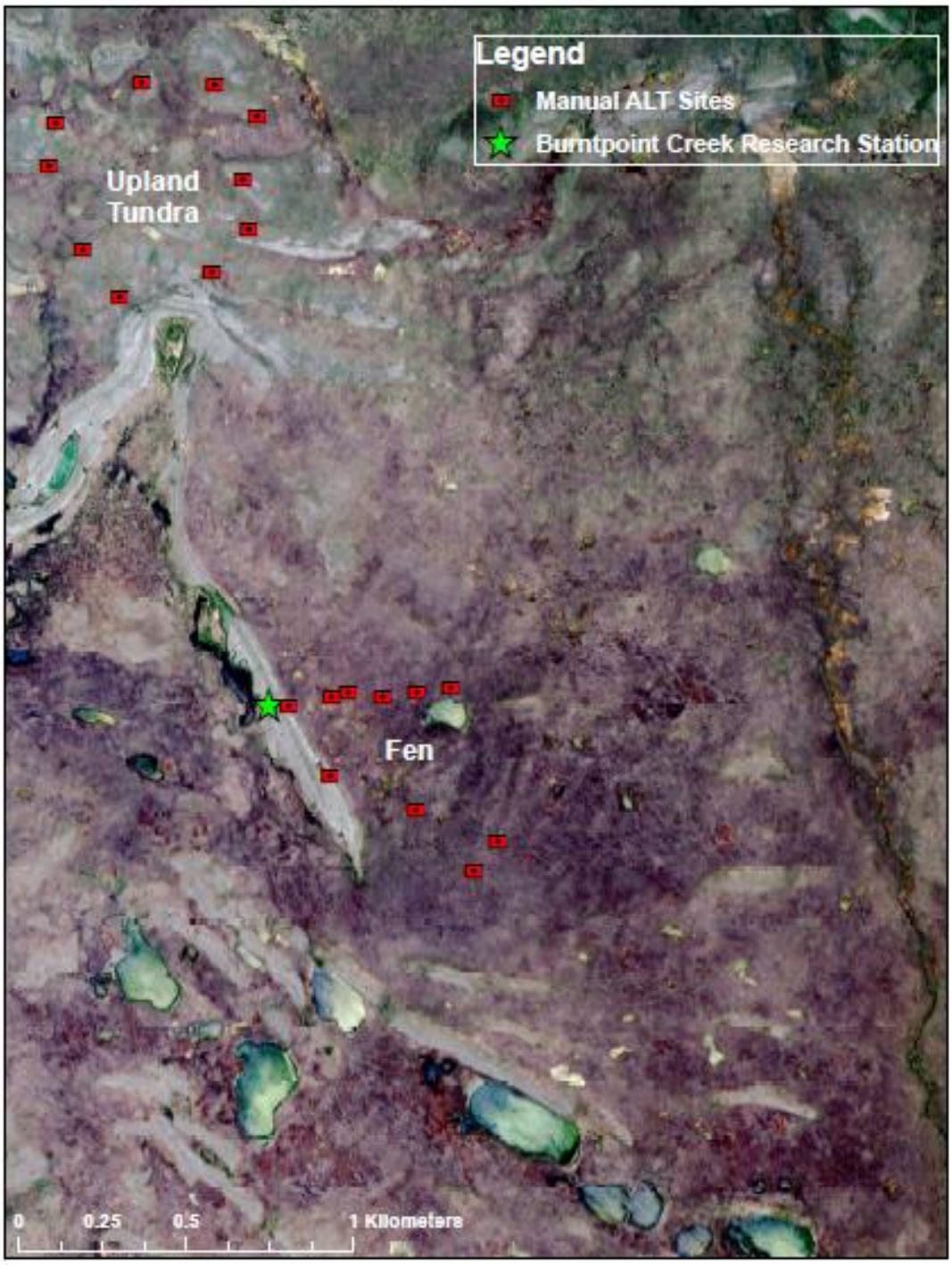

Figure 2. Location of the manual active layer thickness (ALT) transects in relation to the Burntpoint Creek Research Station and their associated sampling sites.

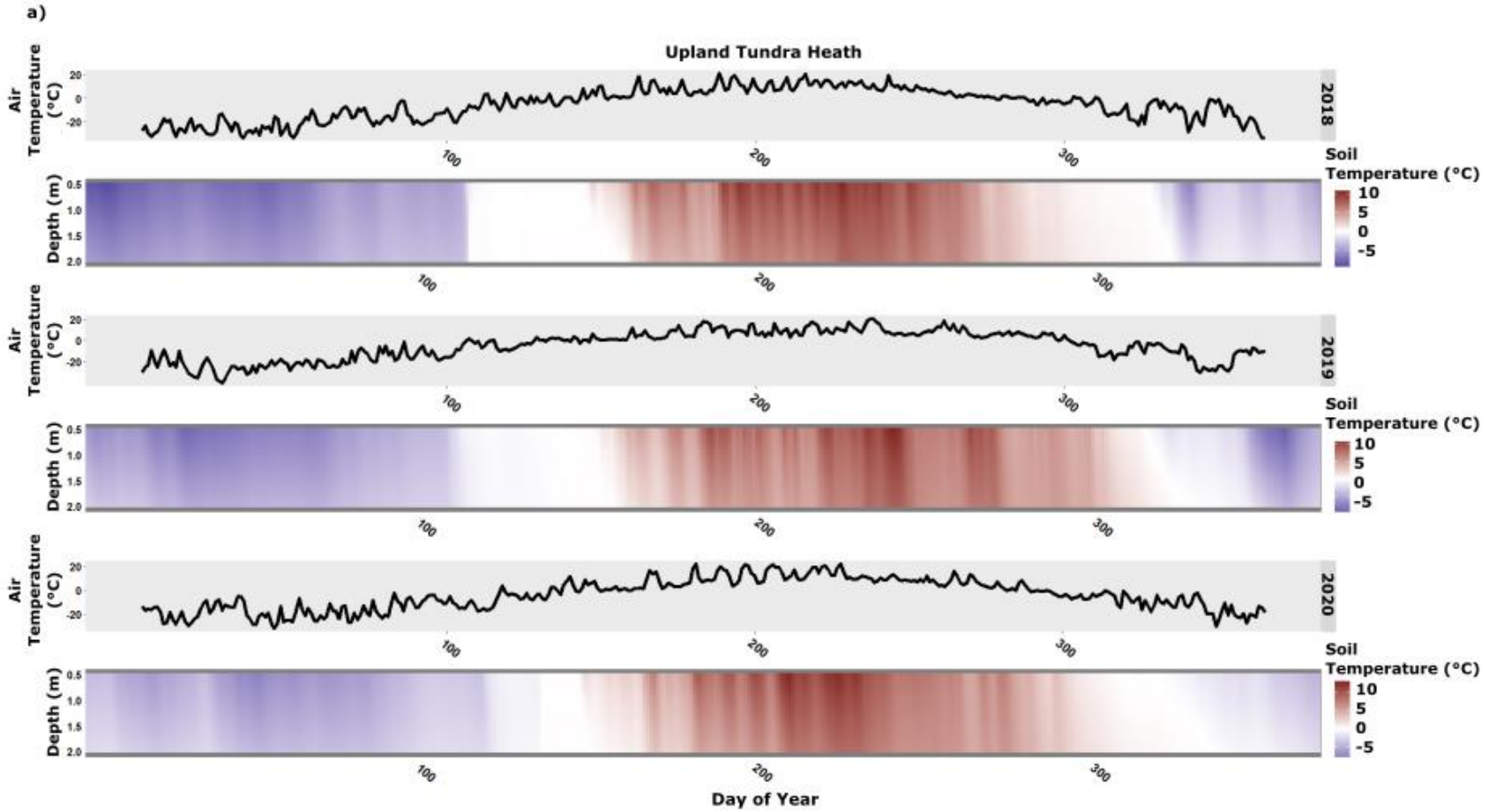
a)
Upland Tundra Heath
Air Temperature (°C)
20
0
-20
2018
100
200
300
Depth (m)
0.5
1.0
1.5
2.0
Soil Temperature (°C)
10
5
0
-5
2019
2020
Day of Year

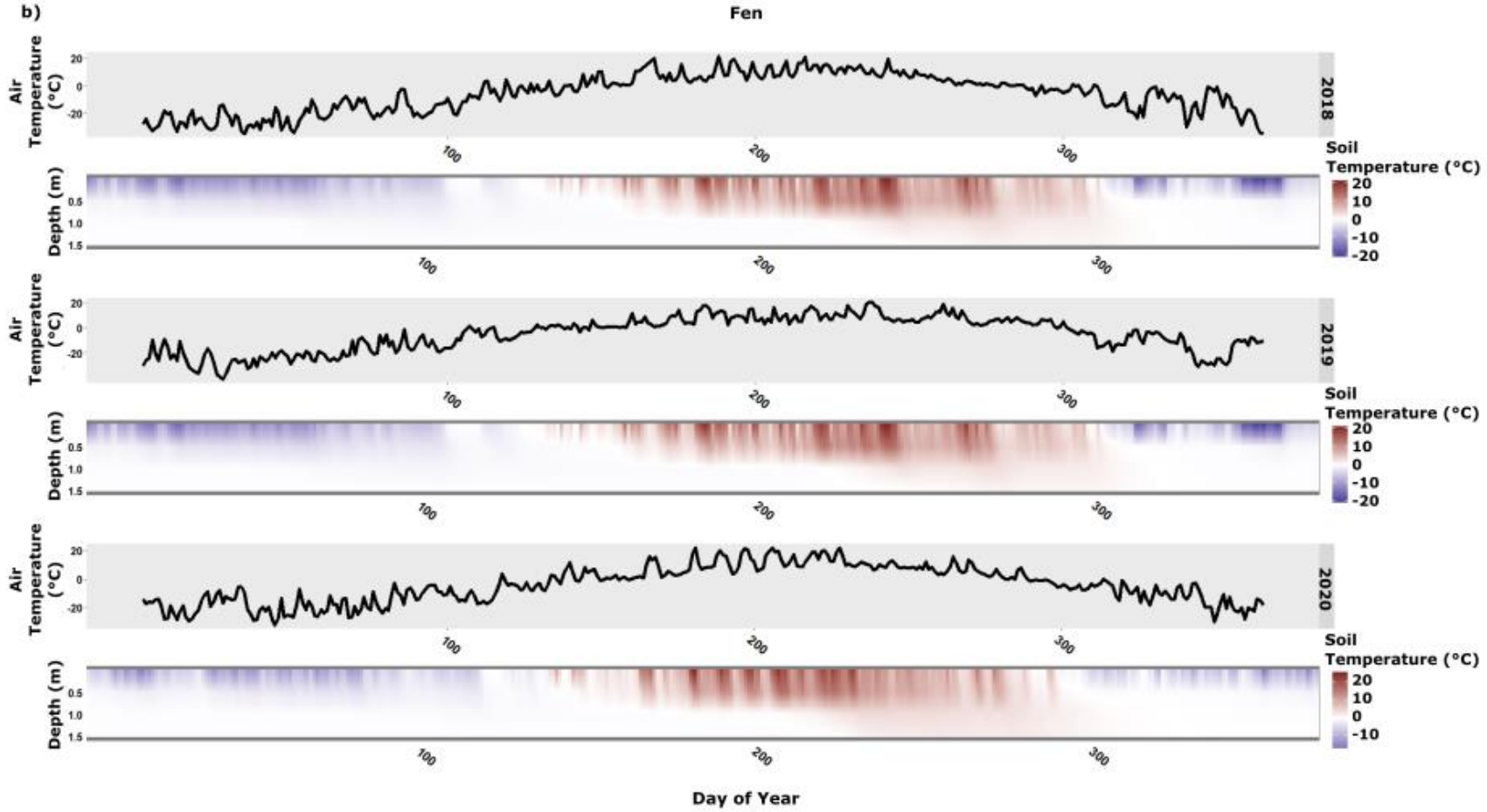
b)
Fen
Air Temperature (°C)
20
0
-20
2018
100
200
300
Depth (m)
0.5
1.0
1.5
Soil Temperature (°C)
20
10
0
-10
-20
2019
2020
Day of Year

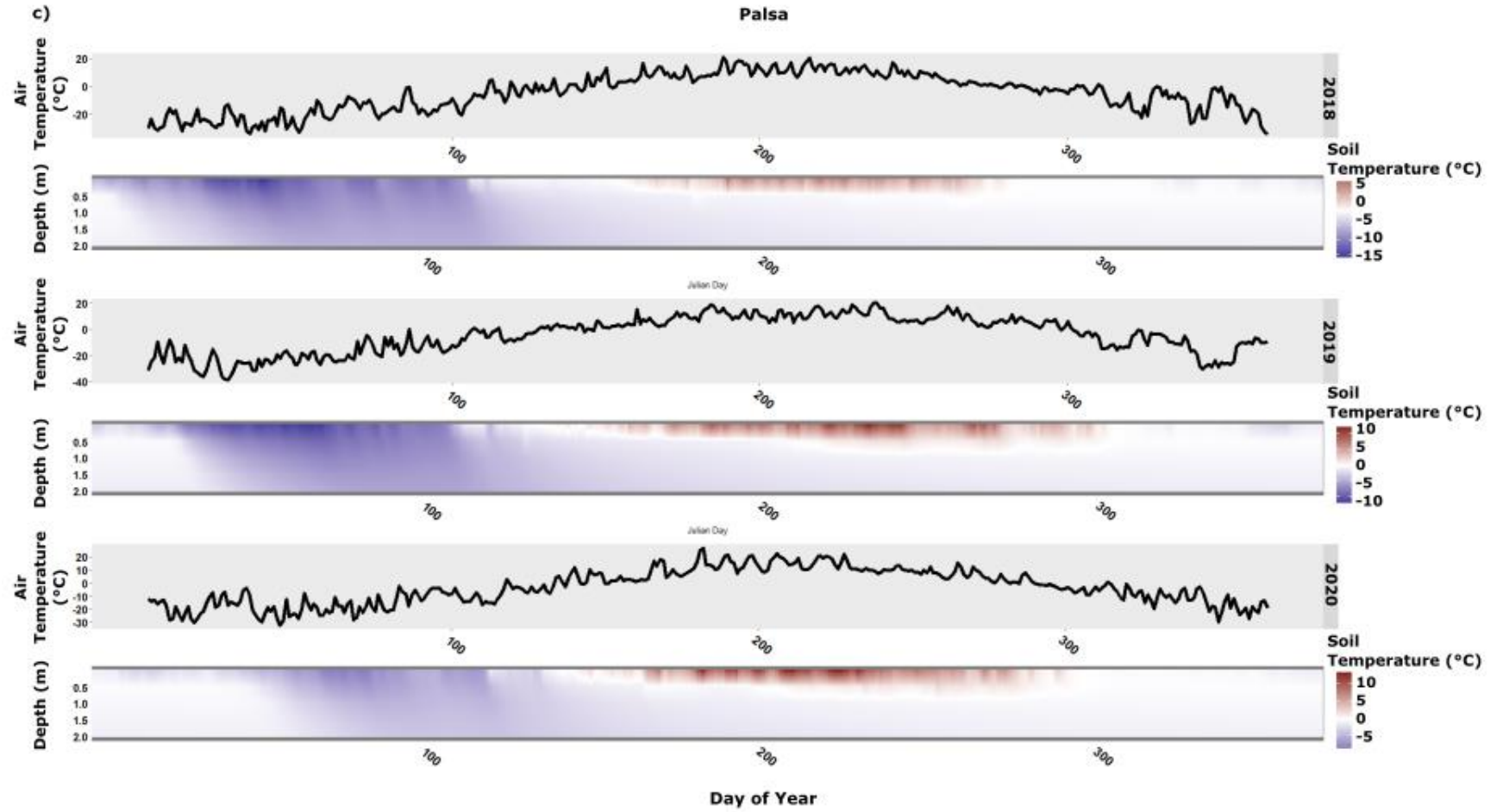

Figure 3. Air temperature and soil temperature profiles across depth and time of a a) tundra heath (Tundra 1), b) fen (Fen 1), and c) palsa (Palsa 4) for years 2018, 2019, and 2020. Red indicates soil temperatures greater than 0˚C, blue is less than 0˚C, and white represents the 0˚C isotherm. Grey indicates that there is no data for that day. Soil temperature data originates from weather station data.

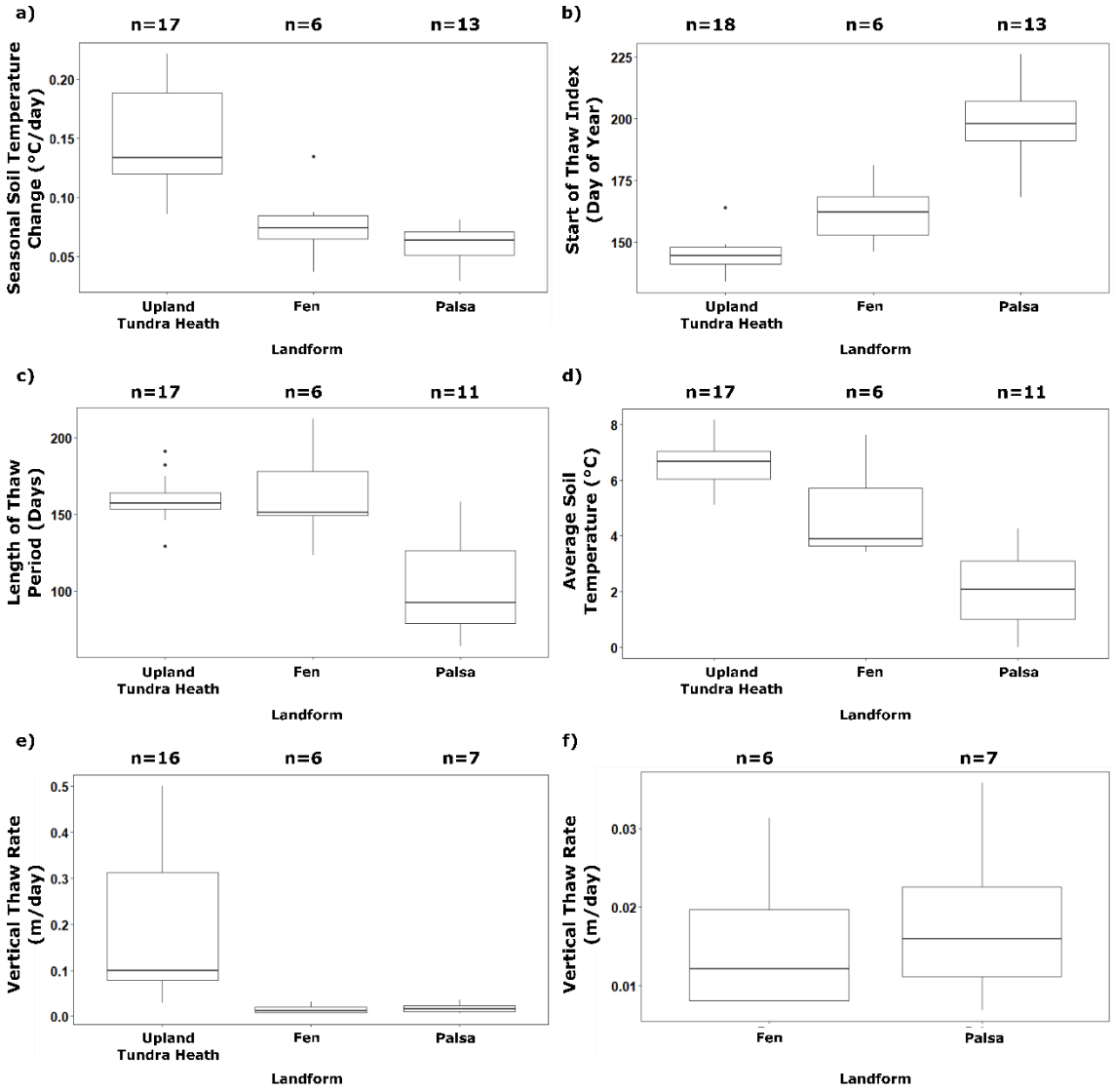

Figure 4. Effect of landform on different indicators of active layer thermal regime extracted from soil temperature profiles where data originates from weather stations: a) seasonal soil temperature change, b) start of the thaw index, c) length of the thaw period, d) average soil temperature, e) vertical thaw rate, and f) a zoom in of vertical thaw rate on the fen and palsa sites. Sample size of each group is indicated at the top of each figure. Sample size originates from the number of each metric extracted from each landform. Not all years could be utilized for each metric if there was an incomplete year worth of data. Within each box, the horizontal black line signifies median values. Boxes extend from the 25th to the 75th percentile of each group's distribution, while vertical lines represent the most extreme values within 1.5 interquartile range of the 25th and 75th percentile for each group. Single data points represent outliers.

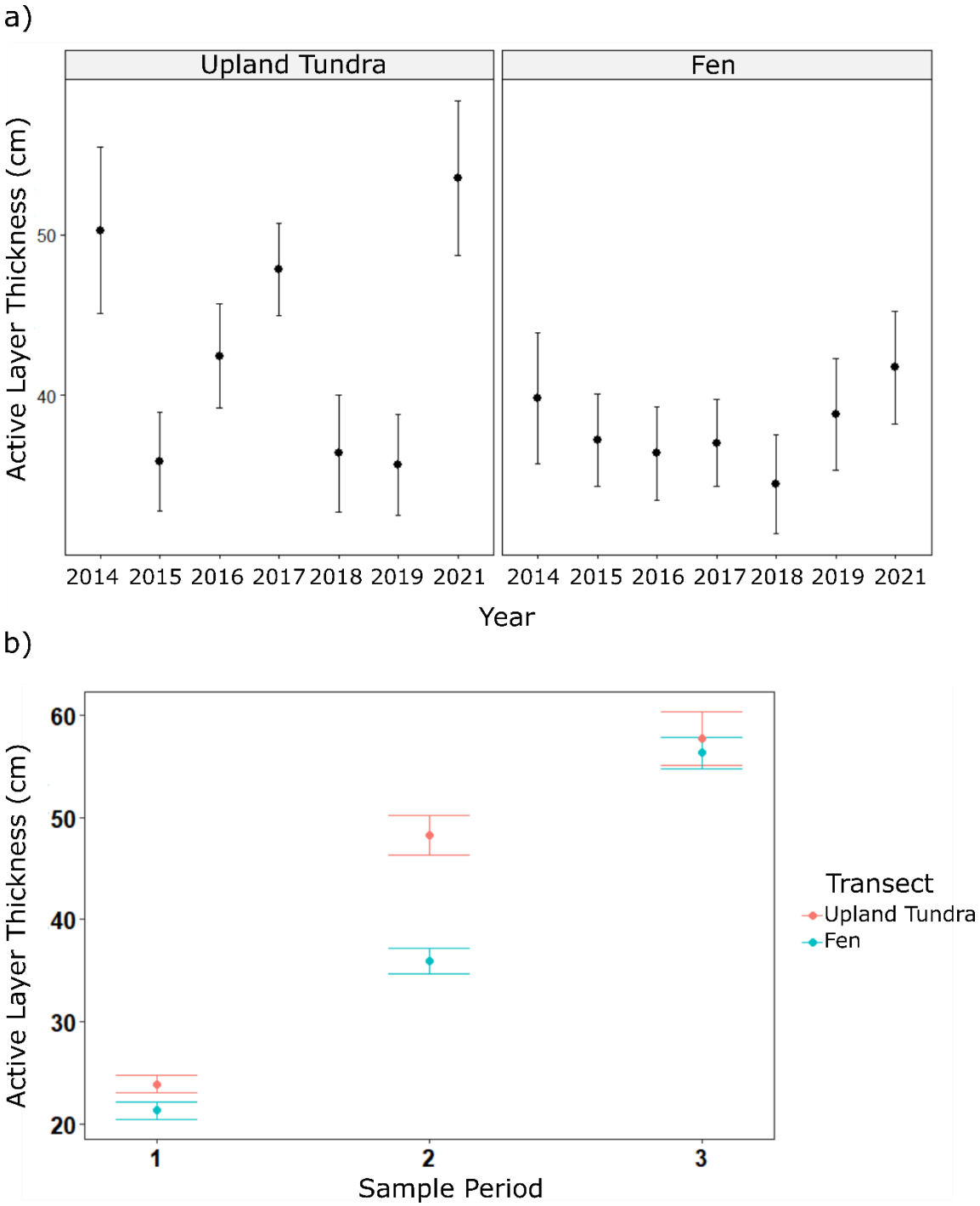

Figure 5. a) Mean active layer thickness (cm) of all sample periods averaged across year for the upland tundra and fen transect and b) average active layer thickness (cm) for each sample period across all years for the upland tundra and fen transect.

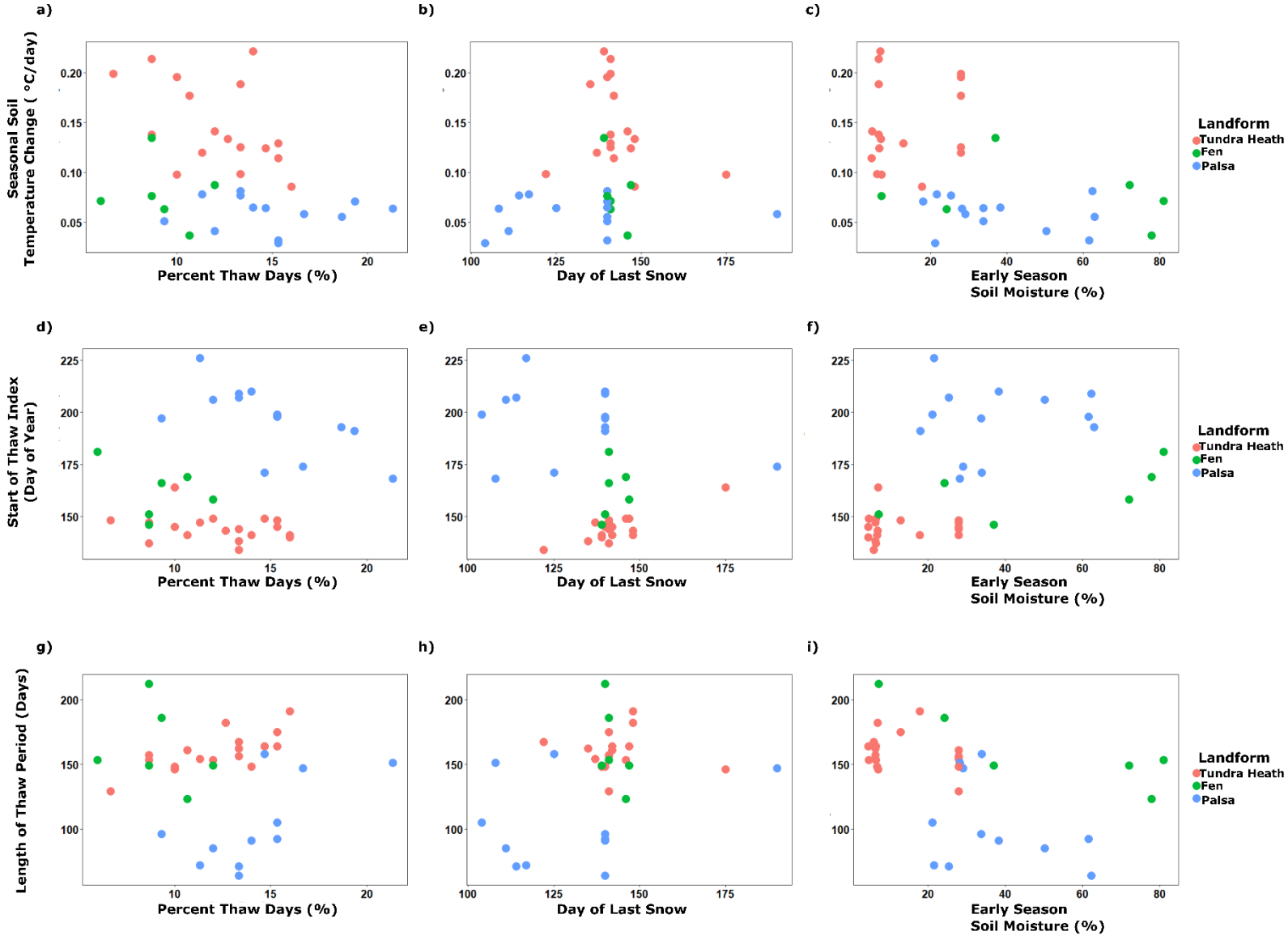
a)
b)
c)
d)
e)
f)
g)
h)
i)
Seasonal Soil Temperature Change (°C/day)
Start of Thaw Index (Day of Year)
Length of Thaw Period (Days)
Percent Thaw Days (%)
Day of Last Snow
Early Season Soil Moisture (%)
Landform
Tundra Heath
Fen
Palsa

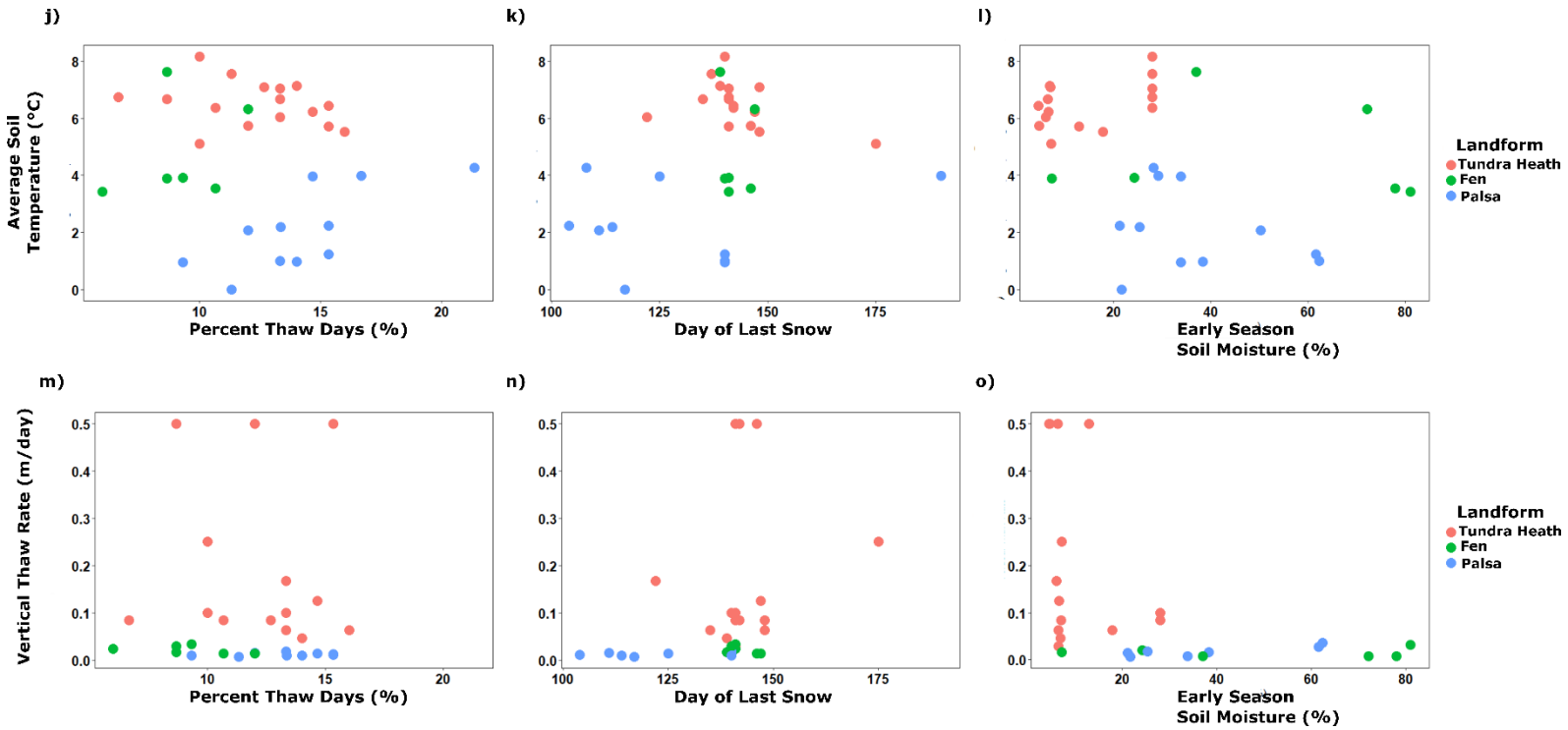

Figure 6. Scatterplots of raw data for seasonal soil temperature change against a) percent thaw days, b) day of last snow, and c) early season soil moisture, start of thaw index against d) percent thaw days, e) day of last snow, and f) early season soil moisture, length of the thaw period against g) percent thaw days, h) day of last snow, and i) early season soil moisture, average soil temperature against j) percent thaw days, k) day of last snow, and l) early season soil moisture, vertical thaw rate against m) percent thaw days, n) day of last snow, and o) early season soil moisture. Response variables were extracted from soil temperature profiles and all data originates from weather station data.

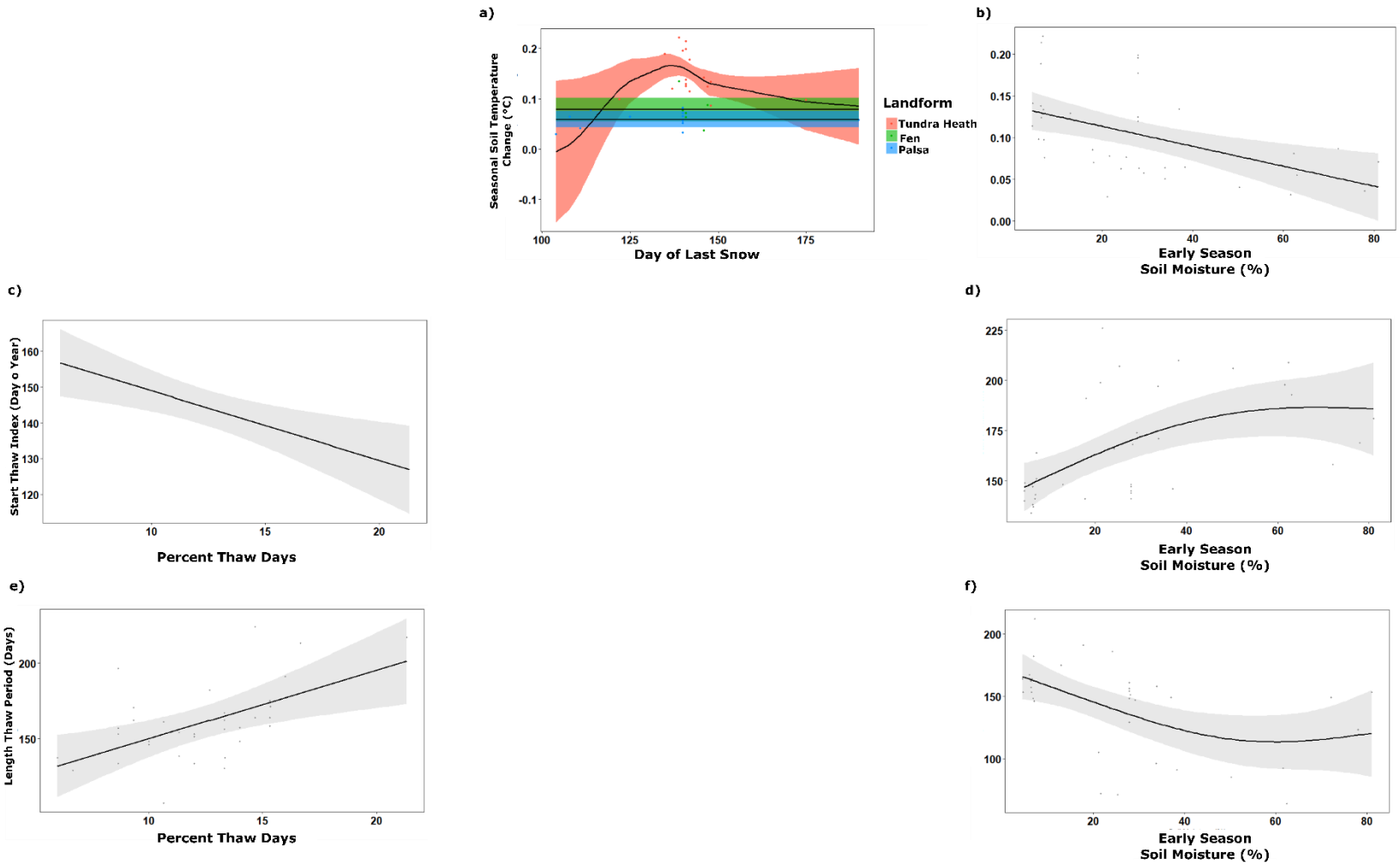
a)
Seasonal Soil Temperature Change (°C)
0.2
0.1
0.0
-0.1
100
125
150
175
Day of Last Snow
Landform
Tundra Heath
Fen
Palsa
b)
0.20
0.15
0.10
0.05
0.00
20
40
60
80
Early Season Soil Moisture (%)
c)
Start Thaw Index (Day o Year)
160
150
140
130
120
10
15
20
Percent Thaw Days
d)
225
200
175
150
20
40
60
80
Early Season Soil Moisture (%)
e)
Length Thaw Period (Days)
200
150
10
15
20
Percent Thaw Days
f)
200
150
100
20
40
60
80
Early Season Soil Moisture (%)

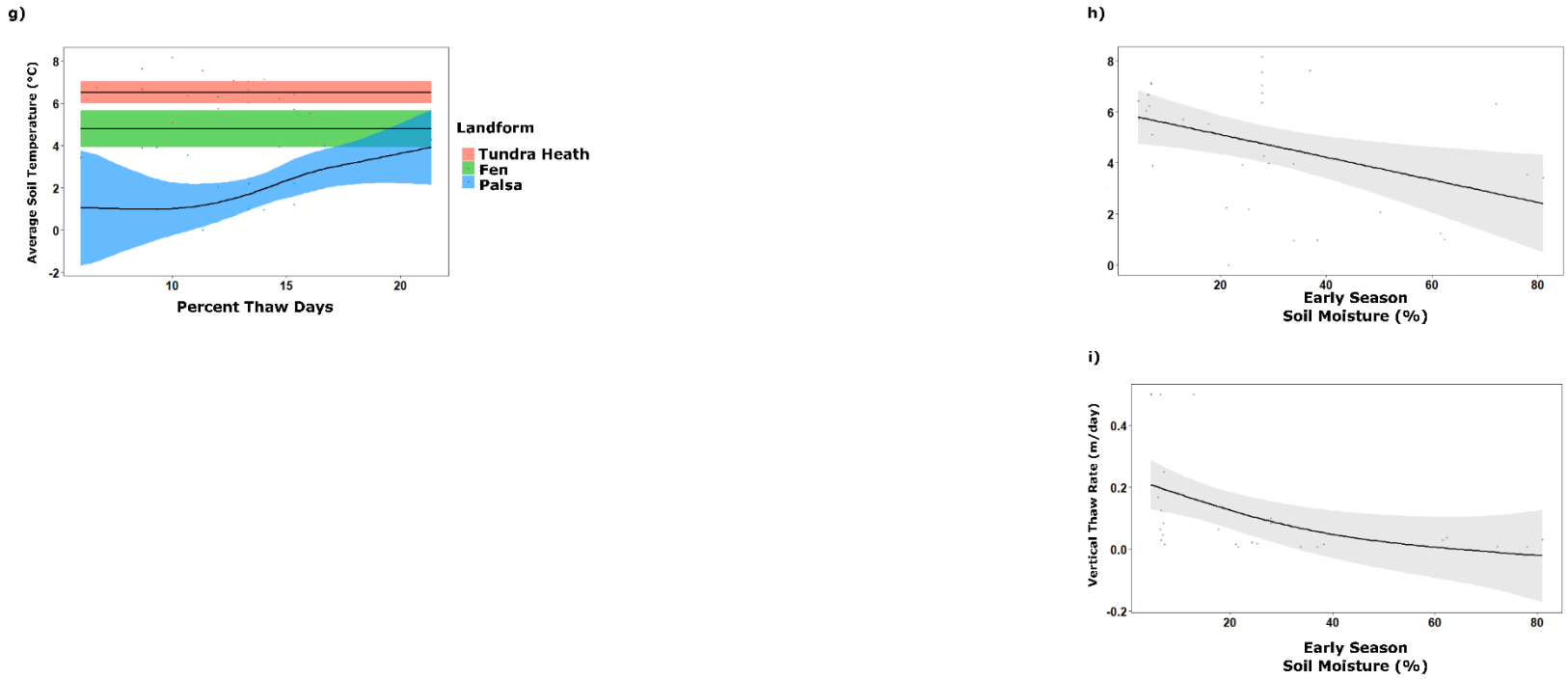

Figure 7. GAM trends for seasonal soil temperature change against a) day of last snow, and b) early season soil moisture, start of thaw index against c) percent thaw days and d) soil moisture, length of the thaw period against e) percent thaw days and f) soil moisture, average soil temperature against g) percent thaw days and h) soil moisture, and i) vertical thaw rate against soil moisture. Plots were only produced for significant interactions. Bands represents 96% point-wise confidence bands. Plots with multi-color confidence bands represent models where the interaction with landform was the model of best fit. Plots with grey confidence bands represent models where no interaction with landform was the model of best fit. Data originates from weather station data.

Table 1. Weather Station site descriptions.

Station	Landform	Years	Soil	Vegetation	Permafrost Zone	Soil Temperature Sensor Depths (m)
Tundra 1	Tundra Heath	2008-2021	Upper peat layer Sandy/gravel soil	Lichen Moss Low-lying shrub	Continuous	0.5, 1.0, 1.5, 2.0
Tundra 2	Tundra Heath	2009-2020	Upper peat layer Sandy/gravel soil	Lichen Moss Low-lying shrub	Continuous	0.5, 1.0, 1.5, 2.0
Fen 1	Fen	2017-2021	Upper peat layer Mineral soil	Graminoids	Continuous	0.0, 0.5, 1.0, 1.5
Fen 2	Fen	2017-2021	Upper peat layer Mineral soil	Graminoids	Continuous	0.0, 0.5, 1.0, 1.5, 2.0
Palsa 1	Palsa	2008-2014	Deep peat layer	Lichen Low-lying shrub	Continuous	0.5, 1.0, 1.5, 2.0
Palsa 2	Palsa	2016-2019	Deep peat layer	Lichen Low-lying shrub	Continuous	0.0, 0.5, 1.0, 1.5, 2.0
Palsa 3	Palsa	2016-2019	Deep peat layer	Lichen Low-lying shrub	Discontinuous	0.0, 0.5, 1.0, 1.5, 2.0
Palsa 4	Palsa	2017-2021	Deep peat layer	Lichen Low-lying shrub	Continuous	0.0, 0.5, 1.0, 1.5, 2.0

Table 2. Results of linear mixed effect models assessing differences in indices of active layer thermal regime. Landform was set as a fixed effect and station as a random effect. Indices of active layer thermal regime were extracted from the soil temperature profiles, where the data originated from the weather stations. Tundra heath referred to as Tundra.

Model	Fixed Effects					Random Effects	
	Value	Std. Error	df	t-value	p-value	Intercept	Residual
Seasonal Soil Temperature Change						0.016	0.030
Tundra	0.145	0.013	28	10.77	0.00		
Fen	-0.067	0.021	5	-3.14	0.025		
Palsa	-0.087	0.018	5	-4.87	0.005		
Start Thaw Index						9.08	10.04
Tundra	144.5	6.84	29	21.12	0.00		
Fen	17.33	10.24	5	1.69	0.151		
Palsa	52.60	8.68	5	6.06	0.002		
Length Thaw Period						22.38	19.11
Tundra	159.77	16.49	26	9.69	0.00		
Fen	2.22	24.15	5	0.092	0.93		
Palsa	-61.73	20.79	5	-2.97	0.031		
Average Soil Temperature						1.15	0.85
Tundra	6.50	0.84	26	7.74	0.00		
Fen	-1.71	1.22	5	-1.40	0.22		
Palsa	-4.59	1.05	5	-4.36	0.007		
Vertical Thaw Rate						0.08	0.11
Tundra	0.199	0.061	23	3.29	0.003		
Fen	-0.178	0.093	4	-1.91	0.114		
Palsa	-0.187	0.081	4	-2.32	0.068		

Table 3. Results of the least-squares means test with a Tukey adjustment for each index of active layer thermal regime. Tundra heath sites are referred to as tundra. Indices of active layer thermal regime were extracted from the soil temperature profiles, where data originates from weather stations.

Index and Contrast	Estimate	SE	df	t-ratio	p-value
Seasonal Soil Temperature Change					
Tundra-Fen	0.068	0.022	5	3.15	0.06
Tundra-Palsa	0.087	0.018	5	4.87	**0.01**
Fen-Palsa	0.019	0.020	5	0.93	0.64
Start Thaw Index					
Tundra-Fen	-17.3	10.2	5	-1.69	0.30
Tundra-Palsa	-52.6	8.68	5	-6.06	**0.004**
Fen-Palsa	-35.3	9.30	5	-3.79	**0.03**
Length Thaw Period					
Tundra-Fen	-2.23	24.1	5	-0.092	0.99
Tundra-Palsa	61.73	20.8	5	2.97	0.07
Fen-Palsa	63.96	21.7	5	2.94	0.07
Average Soil Temperature					
Tundra-Fen	1.71	1.22	5	1.40	0.41
Tundra-Palsa	4.59	1.05	5	4.36	**0.02**
Fen-Palsa	2.88	1.09	5	2.64	0.10
Vertical Thaw Rate					
Tundra-Fen	0.18	0.093	5	1.91	0.22
Tundra-Palsa	0.19	0.081	5	2.32	0.14
Fen-Palsa	0.0097	0.089	5	0.11	0.99

Table 4. Results of two-way analysis of variance (ANOVA) on manual active layer thickness transect data for a) year and transect as effects and b) sample period and transect as effects.

Effect	df	Sum Squares	Mean Squares	F-value	p-value
a)					
Year	6	7606	1267.7	3.382	**0.003**
Transect	1	2895	2895.4	7.725	**0.006**
Year: Transect	6	3330	555.0	1.481	0.183
Residuals	403	151047	374.8		
b)					
Sample Period	2	83029	41515	223.53	**<2E-16**
Transect	1	3024	3024	16.28	**6.5E-05**
Sample Period: Transect	2	2491	1246	6.71	0.001
Residuals	411	76333	186		

Table 5. Results of selected Generalized Additive Models (GAMs) pooled by response variable. AICc values for each response are ranked. Tundra heat sites are referred to as tundra. Data originates from weather station data.

Model Parameters	Linear Terms				Smoothed Terms				Deviance Explained	AICc	Sample Size (n)
	Estimate	SE	t	P	edf	Ref.df	F	P	(%)		
Seasonal Soil Temperature Change									72.7	-138.94	36
Tundra	0.13	0.010	12.96	**5.8E-14**							
Fen	-0.05	0.016	-3.42	**0.0018**							
Palsa	-0.07	0.013	-5.59	**4.1E-06**							
Last snow: Tundra					2.42	3	3.3	**0.017**			
Last Snow: Fen					1.6E-05	3	0	0.226			
Last Snow: Palsa					2.4E-05	3	0	0.958			
Seasonal Soil Temperature Change									64.8	-135.17	36
Tundra	0.14	0.008	17.84	**<2E-16**							
Fen	-0.07	0.017	-4.68	**5.1E-05**							
Palsa	-0.08	0.014	-5.82	**1.8E-06**							
Thaw Days					1	1	2.73	0.108			
Seasonal Soil Temperature Change									24.4	-113.66	36

Soil Moisture					1		1	11.0	**0.0022**		
Start Thaw Index										84.6%	289.08	37
Tundra	143.67	2.57	55.90	**<2E-16**							
Fen	11.27	5.48	2.05	**0.048**							
Palsa	56.73	4.29	13.21	**9.9E-15**							
Thaw Days					1		1	9.29	**0.004**		
Start Thaw Index										80.3	298.22	37
Tundra	144.61	2.94	49.16	**<2E-16**							
Fen	17.33	5.78	2.99	**0.0052**							
Palsa	51.27	4.72	10.87	**1.9E-12**							
Last Snow					1		1	0.041	0.841		
Start Thaw Index										33.3	339.41	37
Soil Moisture					1.69		2.04	7.60	**0.0017**		
Length Thaw Period										66.1	315.63	34
Tundra	160.21	5.43	29.53	**<2E-16**							
Fen	15.69	11.42	1.37	0.18							
Palsa	-66.12	9.19	-7.19	**5.2E-08**							
Thaw Days					1		1	9.916	**0.004**		
Length Thaw Period										55.7	324.67	34
Tundra	158.68	6.31	25.14	**<2E-16**							
Fen	2.65	12.12	0.22	0.83							
Palsa	-54.27	10.55	-5.14	**1.6E-05**							
Last Snow					1		1	0.362	0.552		

Length Thaw Period									34.6	337.74	37
Soil Moisture					1.79	2.14	5.18	**0.0086**			
Average Soil Temperature									80.6%	112.42	34
Tundra	6.53	0.263	24.80	**<2E-16**							
Fen	-1.73	0.515	-3.36	**0.002**							
Palsa	-4.87	0.475	-10.23	**3.4E-11**							
Thaw Days: Tundra					6.1E-05	3	0	0.562			
Thaw Days: Fen					1.6E-05	3	0	0.339			
Thaw Days: Palsa					1.65	3	2.63	**0.011**			
Average Soil Temperature									74.3	118.67	34
Tundra	6.54	0.305	21.42	**<2E-16**							
Fen	-1.73	0.586	-2.96	**0.0059**							
Palsa	-4.48	0.510	-8.78	**8.7E-10**							
Last Snow					1	1	0.036	0.852			
Average Soil Temperature									17.7	152.86	34
Soil Moisture					1	1	6.89	**0.013**			
Vertical Thaw Rate									31.4	-24.54	29
Tundra	0.199	0.035	5.63	**6.4E-06**							
Fen	-0.184	0.067	-2.71	**0.012**							
Palsa	-0.181	0.064	-2.83	**0.0089**							
Thaw Days : Tundra					1.5E-06	3	0	0.596			
Thaw Days : Fen					2E-06	3	0	0.987			
Thaw Days : Palsa					3.2E-06	3	0	0.995			

Vertical Thaw Rate									31.4	-24.54	29
Tundra	0.199	0.035	5.63	**6.4E-06**							
Fen	-0.184	0.068	-2.71	**0.012**							
Palsa	-0.181	0.064	-2.83	**0.008**							
Last Snow : Tundra					5.5E-06	3	0	0.875			
Last Snow: Fen					2.1E-06	3	0	0.971			
Last Snow: Palsa					2.3E-06	3	0	0.988			
Vertical Thaw Rate									27.1	-23.63	29
Soil Moisture					1.41	1.69	3.79	0.025			

Chapter 3: General Discussion

Active layer thermal dynamics were studied within an extensive subarctic peatland complex at the southern edge of continuous permafrost in Northern Ontario. There was no visual evidence of a temporal trend (2014-2021) in active layer thickness (ALT), suggesting that permafrost may not be degrading in our study site during the assessment period. There is evidence of global-scale degradation of permafrost, but this trend is not always evident at fine scales (Fisher et al., 2016; M. Guglielmin et al., 2008; Hu et al., 2020; Lafrenière et al., 2013; Luo et al., 2016; Subin et al., 2013). I did find, however, that active layer thermal regime was controlled by fine-scale environmental factors, notably vegetation and soil properties. These site-specific physical factors can have varying effects on the active layer and involve interactions with climate and local weather patterns (e.g., snow), thus contributing to fine and course-scale variation in thermal regimes across landscapes (Atchley et al., 2016; Subin et al., 2013; Yang et al., 2013). Understanding spatial and temporal variation in the active layer at a range of geographical scales is important to improve predictions of the response of northern ecosystems to climate change (Shiklomanov and Nelson, 2003).

Although a deepening active layer was not evident during my study period, degradation of permafrost can alter the hydrological cycle in northern regions. Permafrost thaw is expected to cause draining of water held above permafrost (Walvoord and Kurylyk, 2016) and alter tundra vegetation, especially non-vascular plants (Schuur and Mack, 2018). Mosses and lichen may be particularly vulnerable (Osterkamp et al., 2009). This may compromise the integrity of some landforms in our study area, like palsas which rely on the high albedo of lichen to maintain their ice cores (Railton and Sparling,

1973). Altering of vegetation will affect albedo and may result in palsa degradation (Railton and Sparling, 1973). Thaw is also expected to cause changes in geomorphology, especially in ice-rich permafrost areas (Schuur and Mack, 2018). Specifically, it will likely cause microtopographic patterns of subsided ground, eventually leading to thermokarst development (Jorgenson, 2013), which promote channeling of the water, and further degradation of permafrost through thermal erosion (Jorgenson, 2013). These hydrological changes can alter permafrost terrain faster than temperature change alone (Shur and Jorgenson, 2007). In my study site, alteration of permafrost terrain can have severe implication for tundra wildlife who rely on various landform types, both wet and dry, for their survival.

Vegetation influences patterns of active layer thermal regime. I found that thaw and soil temperature of the active layer was greater in tundra heath where vegetation consists of moss, lichen, and low-lying shrub which has relatively low albedo and surface roughness compared to palsas and fens. Thaw rates and soil temperatures of the active layer were lowest in palsas, which are dominated by lichen. Climate warming may have complex and counter-effective outcomes to plant growth. Increase in atmospheric carbon that is anticipated from warming (Schuur and Mack, 2018) may stimulate plant growth and affect surface albedo depending on dominant plant forms (Burke et al., 2017; McGuire et al., 2016). Transition from non-vascular plants and graminoids towards shrubs and conifers would cause a decrease in albedo (Loranty et al., 2014; Pearson et al., 2013). Decrease in albedo would result in increased absorption of solar radiation, thus promoting active layer thaw. Alternatively, increased cover of shrubs and conifers would also result in greater shading and lower soil temperatures (Blok et al., 2010).

The Southern Edge of Continuous Permafrost

My study provides new information to address gaps in understanding active layer dynamics at the southern edge of continuous permafrost in North America. The subarctic climate and continuous permafrost extends further south in this region than similar latitudes due to the influx of arctic water into James Bay and Hudson Bay which cools the adjacent landscape (Martini, 1989) and the extensive flat terrain that is exposed to arctic air masses. Patterns of active thermal regime may differ here compared to Arctic environments, evidenced by temporal trends in ALT (Sobota and Nowak, 2014; Wawrzyniak et al., 2016) and in the magnitude of response to warming (Fraser et al., 2018). Much research has already been conducted in Canadian subarctic environments, notably around the Scotty Creek Watershed in the Northwest Territories. They have noticed increased active layer thickness and a reduction in permafrost extent by 38% between 1947-2008 (Quinton et al., 2011). They have also noted changes in land-cover types, such as expansion of wetlands and shrinkage of permafrost peat plateaus (Quinton et al., 2011). Such changes may result in changes to the carbon cycle, as wet features have been found to release significantly more methane than dry features (McLaughlin and Webster, 2014). Permafrost thaw has also resulted in increased runoff and therefore draining of water from the Scotty Creek Watershed due to increased connectivity of wetlands to the drainage basin (Haynes et al., 2018).

Climate projections currently estimate a 10˚C increase in air temperature in the HBL by 2080 (McDermid et al., 2015) and, at the zero-degree isotherm, this poses a severe risk of permafrost and ground ice melt, changes in hydrology, and changes in vegetation composition (Riordan et al., 2006). This makes it crucial to understand how

fine-scale variation in environmental conditions control active layer thermal regime and potentially mediate the effects of climate change.

Knowledge gaps, future work, and recommendations

Due to variation in local environmental conditions, ALT and active layer dynamics can vary spatially at both fine and course scales. Studies, however, are often limited in geographic extent with most comparing active layer dynamics across a few sites and ALT samples extending 0.5 degree of latitude and longitude in size, which can limit accurate representation of natural variability in the active layer needed for evaluation of the active layer (Shiklomanov and Nelson, 2003). I found that ALT varies across dry and wet sites, but there is also variation within each landform. Future studies would benefit from sampling of the active layer within each landform at closer proximities to better understand fine-scale variation in thaw depth. Understanding the natural variability in ALT and its association to the arrangement and state of habitat features (e.g., interspersion of hummocks in fens) within the study area could be beneficial to understanding habitat availability in the face of climate change.

In this study, I was unable to adequately assess the effects of snow on active layer thermal regime. I suggest that further studies in the region collect more detailed snow information, including depth, which may affect water retention and thermal buffering.

Understanding the interactions between permafrost dynamics and wildlife is important in the development of management plans. Climate change can disrupt wildlife through alteration of habitat. Seasonal thaw of the active layer controls water release and is associated with vegetation. In addition, ALT is affected by climate, hydrology, soil, and

insulating properties at the surface (Wright et al., 2009; Yi et al., 2018), making ALT highly variable. Permafrost thaw can also lead to the draining of wetlands (Woo et al., 1992). Changes in any of these ecosystem components may alter the reliability of resources and thus influence habitat selection (Shochat et al., 2002). As shown in this thesis, active layer thaw patterns vary in relation to soil moisture, vegetation, and soil properties, which all affect the quality and availability of habitat. Few studies have addressed the important relationship between permafrost and the active layer and habitat. Studies have found a relationship between size of arctic fox dens and ALT (Nielsen et al., 1994; Smits et al., 1988) and others have noted the effect of permafrost melt on soil moisture and the subsequent consequences to shorebird nest site availability (Cunningham et al., 2016). Future work should assess the relationship between permafrost and wildlife habitat to contribute to more accurate assessment of wildlife vulnerability in northern ecosystems.

Conclusion

Permafrost degradation can have far reaching impacts to ecosystems and people, including vegetation shifts, geomorphological changes, positive feedback loops with regional climate systems, and effects on transportation and infrastructure. To understand the global effects of permafrost melt, it is crucial to understand permafrost and active layer dynamics at a site-level and what drives changes in these layers. My study identifies important sources of variation in active layer dynamics within a peatland complex in Northern Ontario. I found that air temperature and soil moisture were significant predictors of active layer thermal regime, with increased air temperature and decreased soil moisture both promoting thaw. Soil properties also influenced active layer thaw

patterns, with coarser grained soil, like the gravel soil of the tundra heath, promotes thaw. Vegetation was also associated with variation in active layer thermal regime across landforms; the lichen cover of palsas increasing albedo and thus lowering soil temperature. The moss, lichen, and low-lying shrubs of tundra heath, however, lower albedo and allow for greater soil temperatures and thus more thaw. This information will be useful in understanding how the active layer will respond to variations in climate and for the creation of mitigation measures and adaptive management strategies.

References

Abramov, A., Davydov, S., Ivashchenko, A., Karelin, D., Kholodov, A., Kraev, G., Lupachev, A., Maslakov, A., Ostroumov, V., Rivkina, E., Shmelev, D., Sorokovikov, V., Tregubov, O., Veremeeva, A., Zamolodchikov, D., Zimov, S., 2019. Two decades of active layer thickness monitoring in northeastern Asia. Polar Geogr. 1–17. https://doi.org/10.1080/1088937X.2019.1648581

Adamu, G.K., Aliyu, A.K., 2012. Determination of the influence of texture and organic matter on soil water holding capacity in and around Tomas Irrigation, Dambatta Local Government Kano State. Res. J. Environ. Earth Sci. 4, 1038–1044.

Aiken, G., Cotsaris, E., 1995. Soil and Hydrology: their effect on NOM. Journal-American Water Work. Assoc. 87, 36–45. https://doi.org/https://doi.org/10.1002/j.1551-8833.1995.tb06299.x

Almeida, I.C.C., Schaefer, C.E.G.R., Fernandes, R.B.A., Pereira, T.T.C., Nieuwendam, A., Pereira, A.B., 2014. Active layer thermal regime at different vegetation covers at Lions Rump, King George Island, Maritime Antarctica. Geomorphology 225, 36–46. https://doi.org/10.1016/j.geomorph.2014.03.048

Arzhanov, M.M., Mokhov, I.I., 2013. Temperature trends in the permafrost of the Northern Hemisphere: Comparison of model calculations with observations. Dokl. Earth Sci. 449, 319–323. https://doi.org/10.1134/S1028334X1303001X

Atchley, A.L., Coon, E.T., Painter, S.L., Harp, D.R., Wilson, C.J., 2016. Influences and interactions of inundation, peat, and snow on active layer thickness. Geophys. Res. Lett. 43, 5116–5123. https://doi.org/https://doi.org/10.1002/2016GL068550

Balland, V., Pollacco, J.A.P., Arp, P.A., 2008. Modeling soil hydraulic properties for a wide range of soil conditions. Ecol. Modell. 219, 300–316. https://doi.org/10.1016/J.ECOLMODEL.2008.07.009

Bircher, S., Andreasen, M., Vuollet, J., Vehviläinen, J., Rautiainen, K., Jonard, F., Weihermüller, L., Zakharova, E., Wigneron, J.P., H Kerr, Y., 2016. Soil moisture sensor calibration for organic soil surface layers. Geosci. Instrumentation, Methods Data Syst. 5, 109–125. https://doi.org/10.5194/GI-5-109-2016

Biskaborn, B.K., Smith, S.L., Noetzli, J., Matthes, H., Vieira, G., Streletskiy, D.A., Schoeneich, P., Romanovsky, V.E., Lewkowicz, A.G., Abramov, A., Allard, M., Boike, J., Cable, W.L., Christiansen, H.H., Delaloye, R., Diekmann, B., Drozdov, D., Etzelmüller, B., Grosse, G., Guglielmin, M., Ingeman-Nielsen, T., Isaksen, K., Ishikawa, M., Johansson, M., Johannsson, H., Joo, A., Kaverin, D., Kholodov, A., Konstantinov, P., Kröger, T., Lambiel, C., Lanckman, J.-P., Luo, D., Malkova, G., Meiklejohn, I., Moskalenko, N., Oliva, M., Phillips, M., Ramos, M., Sannel, A.B.K., Sergeev, D., Seybold, C., Skryabin, P., Vasiliev, A., Wu, Q., Yoshikawa, K., Zheleznyak, M., Lantuit, H., 2019. Permafrost is warming at a global scale. Nat. Commun. 10. https://doi.org/10.1038/s41467-018-08240-4

Black, R.F., 1976. Periglacial features indicative of permafrost: Ice and soil wedges. Quat. Res. 6, 3–26. https://doi.org/10.1016/0033-5894(76)90037-5

Blok, D., Heijmans, M.M.P.D., Schaepman-Strub, G., Kononov, A.V., Maximov, T.C., Berendse, F., 2010. Shrub expansion may reduce summer permafrost thaw in Siberian tundra. Glob. Chang. Biol. 16, 1296–1305. https://doi.org/https://doi.org/10.1111/j.1365-2486.2009.02110.x

Blok, D., Schaepman-Strub, G., Bartholomeus, H., Heijmans, M.M.P.D., Maximov, T.C., Berendse, F., 2011. The response of Arctic vegetation to the summer climate: relation between shrub cover,NDVI, surface albedo and temperature. Environ. Res. Lett. 6, 035502. https://doi.org/10.1088/1748-9326/6/3/035502

Burke, E.J., Ekici, A., Huang, Y., Chadburn, S.E., Huntingford, C., Ciais, P., Friedlingstein, P., Peng, S., Krinner, G., 2017. Quantifying uncertainties of permafrost carbon-climate feedbacks. Biogeosciences 14, 3051–3066. https://doi.org/10.5194/BG-14-3051-2017

Burn, C.R., 1998. The active layer: two contrasting definitions. Permafr. Periglac. Process. 9, 411–416. https://doi.org/https://doi.org/10.1002/(SICI)1099-1530(199810/12)9:4%3C411::AID-PPP292%3E3.0.CO;2-6

Campbell Scientific, 2016. CS616 and CS625 Water Content Reflectometers.

Cannone, N., Evans, C.J.E., Guglielmin, M., 2006. Interactions between climate, vegetation and the active layer in soils at two Maritime Antarctic sites. Antarct. Sci. 18, 323–333. https://doi.org/10.1017/S095410200600037X

Chapman, L.J., Thomas, M.K.-, Canada Meteorological Branch, D. of T., 1968. The climate of Northern Ontario, 6th ed. Queen's Printer, Ottawa, Canada.

Clayton, L.K., Schaefer, K., Battaglia, M.J., Bourgeau-Chavez, L., Chen, J., Chen, R.H., Chen, A., Bakian-Dogaheh, K., Grelik, S., Jafarov, E., Liu, L., Michaelides, R.J., Moghaddam, M., Parsekian, A.D., Rocha, A. V., Schaefer, S.R., Sullivan, T., Tabatabaeenejad, A., Wang, K., Wilson, C.J., Zebker, H.A., Zhang, T., Zhao, Y., 2021. Active layer thickness as a function of soil water content. Environ. Res. Lett. 16, 055028. https://doi.org/10.1088/1748-9326/ABFA4C

Cui, F.-Q., Liu, Z.-Y., Chen, J.-B., Dong, Y.-H., Jin, L., Peng, H., 2020. Experimental Test and Prediction Model of Soil Thermal Conductivity in Permafrost Regions. Appl. Sci. 10, 2476. https://doi.org/10.3390/APP10072476

Cunningham, J.A., Kesler, D.C., Lanctot, R.B., 2016. Habitat and social factors influence nest-site selection in Arctic-breeding shorebirds. Auk 133, 364–377. https://doi.org/https://doi.org/10.1642/AUK-15-196.1

Ding, Y., Zhang, S., Zhao, L., Li, Z., Kang, S., 2019. Global warming weakening the inherent stability of glaciers and permafrost. Sci. Bull. 64, 245–253. https://doi.org/10.1016/J.SCIB.2018.12.028

Dobiński, Wojciech, 2020. Permafrost active layer. Earth-Science Rev. https://doi.org/10.1016/j.earscirev.2020.103301

Dobiński, W., 2020. Permafrost active layer. Earth-Science Rev. 208, 103301. https://doi.org/https://doi.org/10.1016/j.earscirev.2020.103301

Dredge, L.A., Dyke, L.D., 2020. Landscapes and Landforms of the Hudson Bay Lowlands, in: Landscapes and Landforms of Eastern Canada. Springer, pp. 211–227. https://doi.org/https://doi.org/10.1007/978-3-030-35137-3_8

Ednie, M., Smith, S., 2015. Permafrost temperature data 2008-2014 from community-based monitoring sites in Nunavut.

Fisher, J.P., Estop-Aragonés, C., Thierry, A., Charman, D.J., Wolfe, S.A., Hartley, I.P., Murton, J.B., Williams, M., Phoenix, G.K., 2016. The influence of vegetation and soil characteristics on active-layer thickness of permafrost soils in boreal forest. Glob. Chang. Biol. 22, 3127–3140. https://doi.org/https://doi.org/10.1111/gcb.13248

Fraser, R.H., Kokelj, S. V., Lantz, T.C., McFarlane-Winchester, M., Olthof, I., Lacelle, D., 2018. Climate Sensitivity of High Arctic Permafrost Terrain Demonstrated by Widespread Ice-Wedge Thermokarst on Banks Island. Remote Sens. 10, 954. https://doi.org/10.3390/RS10060954

Grünberg, I., Wilcox, E.J., Zwieback, E.J., Marsh, P., Boike, J., 2020. Linking tundra vegetation, snow, soil temperature, and permafrost. Biogeosciences 17, 4261–4279. https://doi.org/https://doi.org/10.5194/bg-17-4261-2020

Guglielmin, Mauro, Ellis Evans, C.J., Cannone, N., 2008. Active layer thermal regime under different vegetation conditions in permafrost areas. A case study at Signy Island (Maritime Antarctica). Geoderma 144, 73–85. https://doi.org/10.1016/j.geoderma.2007.10.010

Guglielmin, M., Evans, C.J.E., Cannone, N., 2008. Active layer thermal regime under different vegetation conditions in permafrost areas. A case study at Signy Island (Maritime Antarctic). Geoderma 144, 73–85. https://doi.org/10.1016/j.geoderma.2007.10.010

Guglielmin, M., Worland, M.R., Cannone, N., 2012. Spatial and temporal variability of ground surface temperature and active layer thickness at the margin of maritime Antarctica, Signy Island. Geomorphology2 155–156, 20–33. https://doi.org/https://doi.org/10.1016/j.geomorph.2011.12.016

Guo, W., Liu, H., Anenkhonov, O.A., Shangguan, H., Sandanov, D.V., Korolyuk, A.Y., Hu, G., Wu, X., 2018. Vegetation can strongly regulate permafrost degradation at its southern edge through changing surface freeze-thaw processes. Agric. For. Meteorol. 252, 10–17. https://doi.org/https://doi.org/10.1016/j.agrformet.2018.01.010

Hamdhan, I.N., Clarke, B.G., 2010. Determination of thermal conductivity of coarse and fine sand soils, in: Proceedings World Geothermal Congress. Bali, Indonesia, pp. 25–29.

Hampe, A., Petit, R.J., 2005. Conserving biodiversity under climate change: the rear edge matters. Ecol. Lett. 8, 461–467. https://doi.org/10.1111/j.1461-0248.2005.00739.x

Harris, S.A., H.M., F., Heginbottom, J.A., Johnston, G.H., Ladanyi, B., Sego, D.C., van Everdingen, R.O., 1988. Glossary of permafrost and related ground-ice terms.

Ottawa, Canada.

Haynes, K.M., Connon, R.F., Quinton, W.L., 2018. Permafrost thaw induced drying of wetlands at Scotty Creek, NWT, Canada. Environ. Res. Lett. 13, 114001. https://doi.org/https://doi.org/10.1088/1748-9326/aae46c

Heginbottom, J.A., Brown, J.A., Melnikov, E.S., Ferrians Jr., O.J., 1993. Permafrost, in: Permafrost: Sixth International Conference, Beijing Proceedings, Volume 2. South China University of Technology Press, Wushan, Guangzhou, China, pp. 1132–1136.

Hinkel, K.M., Paetzold, F., Nelson, F.E., Bockheim, J.G., 2001. Patterns of soil temperature and moisture in the active layer and upper permafrost at Barrow, Alaska: 1993–1999. Glob. Planet. Change 29, 293–309. https://doi.org/10.1016/S0921-8181(01)00096-0

Hinzman, L.D., Kane, D.L., Gieck, R.E., Everett, K.R., 1991. Hydrologic and thermal properties of the active layer in the Alaskan Arctic. Cold Reg. Sci. Technol. 19, 95–110. https://doi.org/10.1016/0165-232X(91)90001-W

Hu, G., Zhao, L., Li, R., Wu, X., Wu, T., Xie, C., Zhu, X., Hao, J., 2020. Thermal properties of active layer in permafrost regions with different vegetation types on the Qinghai-Tibetan Plateau. Theor. Appl. Climatol. 139, 983–993. https://doi.org/https://doi.org/10.1007/s00704-019-03008-2

Iijima, Y., Park, H., Konstantinov, P.Y., Pudov, G.G., Fedorov, A.N., 2017. Active-Layer Thickness Measurements Using a Handheld Penetrometer at Boreal and Tundra Sites in Eastern Siberia. Permafr. Periglac. Process. 28, 306–313. https://doi.org/10.1002/PPP.1908

IPCC, 2021. Summary for Policymakers. In: Climate Change 2021: The Physical Science Basis. Contribution of Working Group I to the Sixth Assessment Report of the Intergovernmental Panel on Climate Change, in: Masson-Delmotte, V., Zhai, P., Chen, Y., Goldfarb, L., Gomis, M.I., Matthews, J.B.R., Berger, S., Huang, M., Yelekçi, O., Yu, R., Zhou, B., Lonnoy, E., Maycock, T.K., Waterfield, T., Leitzell, K., Caud, N. (Eds.), .

Johnson, M., Walters, J.R., 2011. Proximate and ultimate factors that promote aggregated breeding in the Western Sandpiper. Zool. Res. 32, 128–140. https://doi.org/10.3724/SP.J.1141.2011.02128

Jorgenson, M.T., 2013. Thermokarst terrains, in: Shroder, J.F., Giardino, R., Harbor, J. (Eds.), Treatise on Geomorphology. Academic Press, San Diego, pp. 313–324.

Jorgenson, M.T., Osterkamp, T.E., 2005. Response of boreal ecosystems to varying modes of permafrost degradation. Can. J. For. Ecol. Res. 35, 2100–2111. https://doi.org/https://doi.org/10.1139/x05-153

Kane, D.L., Hinzman, L.D., Zarling, J.P., 1991. Thermal response of the active layer to climate warming in a permafrost environment. Cold Reg. Sci. Technol. 19, 111–122. https://doi.org/https://doi.org/10.1016/0165-232X(91)90002-X

Kim, K., Lee, J., Ju, H., Jung, J.Y., Chae, N., Chi, J., Kwon, M.J., Lee, B.Y., Wagner, J.,

Kim, J.S., 2021. Time-lapse electrical resistivity tomography and ground penetrating radar mapping of the active layer of permafrost across a snow fence in Cambridge Bay, Nunavut Territory, Canada: correlation interpretation using vegetation and meteorological data. Geosci. J. 25, 877–890. https://doi.org/https://doi.org/10.1007/s12303-021-0021-7

Lafleur, P.M., McCaughey, J.H., Joiner, D.W., Bartlett, P.A., Jelinski, D.E., 1997. Seasonal trends in energy, water, and carbon dioxide fluxes at a northern boreal wetland. J. Geophys. Res. Atmos. 102, 29009–29020. https://doi.org/10.1029/96JD03326

Lafrenière, M.J., Laurin, E., Lamoureux, S.F., 2013. The impact of snow accumulation on the active layer thermal regime in high arctic soils. Vadose Zo. J. 12, vzj2012.0058. https://doi.org/https://doi.org/10.2136/vzj2012.0058

Lennartz, B., Liu, H., 2019. Hydraulic functions of peat soils and ecosystem service. Front. Environ. Sci. 7. https://doi.org/https://doi.org/10.3389/fenvs.2019.00092

Lenth, R.V., 2016. Least-Squares Means: The R Package lsmeans. J. Stat. Softw. 69, 1–33. https://doi.org/https://doi.org/10.18637/jss.v069.i01

Letts, M.G., Roulet, N.T., Comer, N.T., Skarupa, M.R., Verseghy, D.L., 2000. Parametrization of peatland hydraulic properties for the Canadian land surface scheme. Atmosphere-Ocean 38, 141–160. https://doi.org/10.1080/07055900.2000.9649643

Li, Q., Ma, M., Wu, X., Yang, H., 2018. Snow Cover and Vegetation-Induced Decrease in Global Albedo From 2002 to 2016. J. Geophys. Res. Atmos. 123, 124–138. https://doi.org/10.1002/2017JD027010

Li, R., Zhao, L., Wu, T., Wang, Q., Ding, Y., Yao, J., Wu, X., Hu, G., Xiao, Y., Du, Y., Zhu, X., Qin, Y., Yang, S., Bai, R., Du, E., Liu, G., Zou, D., Qiao, Y., Shi, J., 2019. Soil thermal conductivity and its influencing factors at the Tanggula permafrost region on the Qinghai–Tibet Plateau. Agric. For. Meteorol. 264, 235–246. https://doi.org/10.1016/J.AGRFORMET.2018.10.011

Ling, F., Zhang, T., 2003. Impact of the Timing and Duration of Seasonal Snow Cover on the Active Layer and Permafrost in the Alaskan Arctic. Permafr. Periglac. Process. 14, 141–150. https://doi.org/https://doi.org/10.1002/ppp.445

Loranty, M.M., Berner, L.T., Goetz, S.J., Jin, Y., Randerson, J.T., 2014. Vegetation controls on northern high latitude snow-albedo feedback: observations and CMIP5 model simulations. Glob. Chang. Biol. 20, 594–606. https://doi.org/10.1111/GCB.12391

Lowry, C.S., Fratta, D., Anderson, M.P., 2009. Ground penetrating radar and spring formation in a groundwater dominated peat wetland. J. Hydrol. 373, 68–79. https://doi.org/10.1016/J.JHYDROL.2009.04.023

Luo, D.L., Wu, Q., Jin, H., Marchenko, S.S., Lü, L., Gao, S., 2016. Recent changes in the active layer thickness across the northern hemisphere. Environ. Earth Sci. 75, 555.

https://doi.org/10.1007/s12665-015-5229-2

Martini, I.P., 2006. Chapter 3 The cold-climate peatlands of the Hudson Bay Lowland, Canada: brief overview of recent work. Dev. Earth Surf. Process. 9, 53–84. https://doi.org/https://doi.org/10.1016/S0928-2025(06)09003-1

Martini, I.P., 1989. The Hudson Bay Lowland: major geologic features and assets. Coast. Lowl. 25–34. https://doi.org/10.1007/978-94-017-1064-0

Matthias, A.D., Fimbres, A., Sano, E.E., Post, D.F., Accioly, L., Batchily, A.K., Ferreira, L.G., 2000. Surface Roughness Effects on Soil Albedo. Soil Sci. Soc. Am. J. 64, 1035–1041. https://doi.org/https://doi.org/10.2136/sssaj2000.6431035x

McClymont, A.F., Hayashi, M., Bentley, L.R., Christensen, B.S., 2013. Geophysical imaging and thermal modeling of subsurface morphology and thaw evolution of discontinuous permafrost. J. Geophys. Res. Earth Surf. 118, 1826–1837. https://doi.org/10.1002/JGRF.20114

McDermid, J., Fera, S., Hogg, A., 2015. Climate change projections for Ontario: An updated synthesis for policymakers and planners. Peterborough, ON.

McGuire, A.D., Koven, C., Lawrence, D.M., Clein, J.S., Xia, J., Beer, C., Burke, E., Chen, G., Chen, X., Delire, C., Jafarov, E., MacDougall, A.H., Marchenko, S., Nicolsky, D., Peng, S., Rinke, A., Saito, K., Zhang, W., Alkama, R., Bohn, T.J., Ciais, P., Decharme, B., Ekici, A., Gouttevin, I., Hajima, T., Hayes, D.J., Ji, D., Krinner, G., Lettenmaier, D.P., Luo, Y., Miller, P.A., Moore, J.C., Romanovsky, V., Schädel, C., Schaefer, K., Schuur, E.A.G., Smith, B., Sueyoshi, T., Zhuang, Q., 2016. Variability in the sensitivity among model simulations of permafrost and carbon dynamics in the permafrost region between 1960 and 2009. Global Biogeochem. Cycles 30, 1015–1037. https://doi.org/10.1002/2016GB005405

McLaughlin, J., Webster, K., 2014. Effects of Climate Change on Peatlands in the Far North of Ontario, Canada: A Synthesis. Arctic, Antarct. Alp. Res. 46, 84–102. https://doi.org/10.1657/1938-4246-46.1.84

McLeod, A.I., 2011. Kendall rank correlation and Mann-Kendall trend test [WWW Document]. URL https://cran.r-project.org/package=Kendall

Migała, K., Wojtuń, B., Szymański, W., Muskała, P., 2014. Soil moisture and temperature variation under different types of tundra vegetation during the growing season: A case study from the Fuglebekken catchment, SW Spitsbergen. Catena 116, 10–18. https://doi.org/https://doi.org/10.1016/j.catena.2013.12.007

Mobaek, R., Mysterud, A., Egil Loe, L., Holand, Ø., Austrheim, G., 2009. Density dependent and temporal variability in habitat selection by a large herbivore; an experimental approach. Oikos 118, 209–218. https://doi.org/10.1111/j.1600-0706.2008.16935.x

Mod, H.K., Luoto, M., 2016. Arctic shrubification mediates the impacts of warming climate on changes to tundra vegetation. Environ. Res. Lett. 11, 124028. https://doi.org/10.1088/1748-9326/11/12/124028

National Research Council USA, 2014. Opportunities to Use Remote Sensing in Understanding Permafrost and Related Ecological Characteristics: Report of a Workshop. The National Academic Press, Washington, DC.

Nelson, F.E., Outcalt, S.I., Goodwin, C.W., Hinkel, K.M., 1985. Diurnal Thermal Regime in a Peat-Covered Palsa, Toolik Lake, Alaska [WWW Document]. Arctic. URL https://www.jstor.org/stable/40511003?casa_token=Ev3mM1FLjWEAAAAA%3AL9xdWThpchTqQzvoa-T8gnT64VPaFF8278m8-v01y2qPOaoBAMyI9MU16k4-4SlEYAbQnMh-bwyG-meJzm9dn1vLRxxyQiCRh4hayaO4jA1_fnlPK10&seq=1#metadata_info_tab_contents (accessed 10.1.21).

Nielsen, S.M., Pedersen, V., Klitgaard, B.B., 1994. Arctic Fox (Alopex lagopus) Dens in the Disko Bay Area, West Greenland. Arctic 47, 327–333.

Noetzli, J., Voelksch, I., 2014. Organisation and analysis of temperature data measured within the Swiss Permafrost Monitoring Network (PERMOS), in: EGU General Assembly Conference Abstracts. Vienna, Austria, pp. EGU2014-11376.

Osterkamp, T.E., Jorgenson, M.T., Schuur, E.A.G., Shur, Y.L., Kanevskiy, M.Z., Vogel, J.G., Tumskoy, V.E., 2009. Physical and ecological changes associated with warming permafrost and thermokarst in Interior Alaska. Permafr. Periglac. Process. 20, 235–256. https://doi.org/10.1002/PPP.656

Pearson, R.G., Phillips, S.J., Loranty, M.M., Beck, P.S.A., Damoulas, T., Knight, S.J., Goetz, S.J., 2013. Shifts in Arctic vegetation and associated feedbacks under climate change. Nat. Clim. Chang. 3, 673–677. https://doi.org/10.1038/nclimate1858

Peng, X., Zhang, T., Frauenfeld, O.W., Wang, S., Qiao, L., Du, R., Mu, C., 2019. Northern Hemisphere Greening in Association with Warming Permafrost. J. Geophys. Res. Biogeosciences 125, e2019JG005086. https://doi.org/https://doi.org/10.1029/2019JG005086

Pinheiro, J., DebRoy, S., Sarkar, D., Team, R.C., 2022. nlme: Linear and Nonlinear Mixed Effects Models. R package version 3.1-155.

Provan, J., Maggs, C.A., 2012. Unique genetic variation at a species' rear edge is under threat from global climate change. Proc. R. Soc. B Biol. Sci. 279, 39–47. https://doi.org/10.1098/rspb.2011.0536

Quinton, W.L., Hayashi, M., Chasmer, L.E., 2011. Permafrost-thaw-induced land-cover change in the Canadian subarctic: implications for water resources. Hydrol. Process. 25, 152–158. https://doi.org/10.1002/hyp.7894

Railton, J.B., Sparling, J.H., 1973. Preliminary studies on the ecology of palsa mounds in northern Ontario. Can. J. Bot. 51, 1037–1044. https://doi.org/10.1139/B73-128

Randers, J., Goluke, U., 2020. An earth system model shows self-sustained thawing of permafrost even if all man-made GHG emissions stop in 2020. Sci. Rep. 10. https://doi.org/https://doi.org/10.1038/s41598-020-75481-z

Riley, J.L., 2011. Wetlands of the Ontario Hudson Bay Lowlands: A Regional Overview.

Toronto, ON.

Riordan, B., Verbyla, D., McGuire, A.D., 2006. Shrinking ponds in subarctic Alaska based on 1950-2002 remotely sensed images. J. Geophys. Res. Biogeosciences 111. https://doi.org/10.1029/2005JG000150

Romanovsky, V.E., Sazonova, T.S., Balobaev, V.T., Shender, N.I., Sergueev, D.O., 2007. Past and recent changes in air and permafrost temperatures in eastern Siberia. Glob. Planet. Change 56, 399–413. https://doi.org/10.1016/J.GLOPLACHA.2006.07.022

Rowland, J.C., Jones, C.E., Altmann, G., Bryan, R., Crosby, B.T., Geernaert, G.L., Hinzman, L.D., Kane, D.L., Lawrence, D.M., Mancino, A., Marsh, P., McNamara, J.P., Romanovsky, V.E., Toniolo, H., Travis, B.J., Trochim, E., Wilson, C.J., 2010. Arctic landscapes in transition: Responses to thawing permafrost. Eos (Washington. DC). 91, 229–230. https://doi.org/10.1029/2010EO260001

Schuur, E.A.G., Mack, M.C., 2018. Ecological response to permafrost thaw and consequences for local and global ecosystem services. Annu. Rev. Ecol. Evol. Syst. 49, 279–301.

Schuur, E.A.G., McGuire, A.D., Schädel, C., Grosse, G., Harden, J.W., Hayes, D.J., Hugelius, G., Koven, C.D., Kuhry, P., Lawrence, D.M., Natali, S.M., Olefeldt, D., Romanovsky, V.E., Schaefer, K., Turetsky, M.R., Treat, C.C., Vonk, J.E., 2015. Climate change and the permafrost carbon feedback. Nature 520, 171–179. https://doi.org/10.1038/nature14338

Serreze, M.C., Barry, R.G., 2011. Processes and impacts of Arctic amplification: A research synthesis. Glob. Planet. Change 77, 85–96. https://doi.org/10.1016/j.gloplacha.2011.03.004

Serreze, M.C., Francis, J.A., 2006. The arctic amplification debate. Clim. Change 76, 241–264. https://doi.org/10.1007/s10584-005-9017-y

Shiklomanov, N.I., Nelson, F.E., 2003. Statistical representation of landscape-specific active layer variability, in: Proceedings of the International Permafrost Conference. Swets & Zeitlinger, The Netherlands, Zurich, Switzerland.

Shiklomanov, N.I., Streletskiy, D.A., Nelson, F.E., Hollister, R.D., Romanovsky, V.E., Tweedie, C.E., Bockheim, J.G., Brown, J., 2010. Decadal variations of active-layer thickness in moisture-controlled landscapes, Barrow, Alaska. J. Geophys. Res. Biogeosciences 115. https://doi.org/10.1029/2009JG001248

Shochat, E., Abramsky, Z., Pinshow, B., Whitehouse, M.E.A., 2002. Density-dependent habitat selection in migratory passerines during stopover: What causes the deviation from IFD? Evol. Ecol. 16, 469–488. https://doi.org/10.1023/A:1020851801732

Shur, Y.L., Jorgenson, M.T., 2007. Patterns of permafrost formation and degradation in relation to climate and ecosystems. Permafr. Periglac. Process. 18, 7–19. https://doi.org/10.1002/PPP.582

Smith, S.L., Burgess, M.., 2002. A digital database of permafrost thickness in Canada. https://doi.org/https://doi.org/10.4095/213043

Smits, C.M.M., Smith, C.A.S., Slough, B.G., 1988. Physical Characteristics of Arctic Fox (Alopex lagopus) Dens in Northern Yukon Territory, Canada. Arctic 41, 12–16.

Sobota, I., Nowak, M., 2014. Changes in the dynamics and thermal regime of the permafrost and active layer of the high arctic coastal area in north-west spitsbergen, svalbard. Geogr. Ann. Ser. A, Phys. Geogr. 96, 227–240. https://doi.org/10.1111/GEOA.12045

Stendel, M., Christensen, J.H., 2002. Impact of global warming on permafrost conditions in a coupled GCM. Geophys. Res. Lett. 29, 10-1-10–4. https://doi.org/https://doi.org/10.1029/2001GL014345

Stoy, P.C., Street, L.E., Johnson, A.V., Prieto-Blanco, A., Ewing, S.A., 2012. Temperature, Heat Flux, and Reflectance of Common Subarctic Mosses and Lichens under Field Conditions: Might Changes to Community Composition Impact Climate-Relevant Surface Fluxes? Arctic, Antarct. Alp. Res. 44, 500–508. https://doi.org/https://doi.org/10.1657/1938-4246-44.4.500

Subin, Z.M., Koven, C.D., Riley, W.J., Torn, M.S., Lawrence, D.M., Swenson, S.C., 2013. Effects of Soil Moisture on the Responses of Soil Temperatures to Climate Change in Cold Regions. J. Clim. 26, 3139–3158. https://doi.org/https://doi.org/10.1175/JCLI-D-12-00305.1

Tatenhove, F.G.M. Van, Olesen, O.B., 1994. Ground temperature and related permafrost characteristics in west greenland. Permafr. Periglac. Process. 5, 199–215. https://doi.org/10.1002/PPP.3430050402

Treat, C.C., Wollheim, W.M., Varner, R.K., Grandy, A.S., Talbot, J., Frolking, S., 2014. Temperature and peat type control CO2 and CH4 production in Alaskan permafrost peats. Glob. Chang. Biol. 20, 2674–2686. https://doi.org/10.1111/GCB.12572

Tsuyuzaki, S., Sawada, Y., Kushida, K., Fukuda, M., 2008. A preliminary report on the vegetation zonation of palsas in the Arctic National Wildlife Refuge, northern Alaska, USA. Ecol. Res. 23, 787–793. https://doi.org/https://doi.org/10.1007/s11284-007-0437-1

Vaughan, D G, Comiso, J.C., Allison, I, Carrasco, J, Kaser, G, Kwok, R, Mote, P., Murray, T., Paul, F., Ren, J., Rignot, E., Solomina, O., Steffen, K., Zhang, T., Stocker, [, Qin, D., Plattner, G.-K., Tignor, M., Allen, S.K., Boschung, J., Nauels, A., Xia, Y., Bex, V., Midgley, P.M., Vaughan, David G, Allison, Ian, Carrasco, Jorge, Kaser, Georg, Kwok, Ronald, 2013. Observations: Cryosphere. In: Climate Change 2013: The Physical Science Basis. Contribution of Working Group I to the Fifth Assessment Report of the Intergovernmental Panel on Climate Change. Cambridge University Press, Cambridge, United Kingdom.

Vincent, W.F., Lemay, M., Allard, M., Wolfe, B.., 2013. Adapting to Permafrost Change: A Science Framework. Eos (Washington. DC). 94, 373–375. https://doi.org/https://doi.org/10.1002/2013EO420002

Walvoord, M.A., Kurylyk, B.L., 2016. Hydrologic Impacts of Thawing Permafrost—A Review. Vadose Zo. J. 15, vzj2016.01.0010.

https://doi.org/10.2136/VZJ2016.01.0010

Wang, C., Wu, D., Kong, Y., Li, R., Shi, H., 2018. Changes of Soil Thermal and Hydraulic Regimes in Northern Hemisphere Permafrost Regions over the 21st Century. Arctic, Antarct. Alp. Res. 49, 305–319. https://doi.org/10.1657/AAAR0016-026

Wawrzyniak, T., Osuch, M., Napiorkowski, J., Westermann, S., 2016. Modelling of the thermal regime of permafrost during 1990-2014 in Hornsund, Svalbard. Polish Polar Res. 37, 219–242. https://doi.org/10.1515/popore-2016-0013

Wen, Z., Niu, F., Yu, Q., Wang, D., Feng, W., Zheng, J., 2014. The role of rainfall in the thermal-moisture dynamics of the active layer at Beiluhe of Qinghai-Tibetan plateau. Environ. Earth Sci. 71, 1195–1204. https://doi.org/https://doi.org/10.1007/s12665-013-2523-8

Woo, M., 1990. Consequences of Climatic Change for Hydrology in Permafrost Zones. J. Cold Reg. Eng. 4, 15–20. https://doi.org/10.1061/(ASCE)0887-381X(1990)4:1(15)

Woo, M., Xia, Z., 1996. Effects of Hydrology on the Thermal Conditions of the Active LayerPaper presented at the 10th Northern Res. Basin Symposium (Svalbard, Norway — 28 Aug./3 Sept. 1994). Hydrol. Res. 27, 129–142. https://doi.org/10.2166/NH.1996.0024

Woo, M.K., Lewkowicz, A.G., Rouse, W.R., 1992. Response of the canadian permafrost environment to climatic change. Phys. Geogr. 13, 287–317. https://doi.org/10.1080/02723646.1992.10642459

Wood, S., 2017. Generalized Additive Models: An Introduction with R, 2nd ed. Chapman and Hall/CRC, Boca Raton.

Wood, S.N., 2006. Generalized Additive Models: An Introduction with R. Chapman and Hall/CRC, Boca Raton, FL.

Wright, N., Hayashi, M., Quinton, W.L., 2009. Spatial and temporal variations in active layer thawing and their implication on runoff generation in peat-covered permafrost terrain. Water Resour. Res. 45, W05414. https://doi.org/10.1029/2008WR006880

Wu, Q., Hou, Y., Yun, H., Liu, Y., 2015. Changes in active-layer thickness and near-surface permafrost between 2002 and 2012 in alpine ecosystems, Qinghai–Xizang (Tibet) Plateau, China. Glob. Planet. Change 124, 149–155. https://doi.org/10.1016/J.GLOPLACHA.2014.09.002

Wu, Q., Zhang, T., Liu, Y., 2012. Thermal state of the active layer and permafrost along the Qinghai-Xizang (Tibet) Railway from 2006 to 2010. Cryosphere 6, 607–612. https://doi.org/10.5194/TC-6-607-2012

Yang, Z.., Gao, J.X., Zhao, L., Xu, X.L., Ouyang, H., 2013. Linking thaw depth with soil moisture and plant community composition: effects of permafrost degradation on alpine ecosystems on the Qinghai-Tibet Plateau. Plant Soil 367, 687–700. https://doi.org/https://doi.org/10.1007/s11104-012-1511-1

Yi, Y., Kimball, J.S., Chen, R.H., Moghaddam, M., Reichle, R.H., Mishra, U., Zona, D., Oechel, W.C., 2018. Characterizing permafrost active layer dynamics and sensitivity to landscape spatial heterogeneity in Alaska. Cryosphere 12, 145–161. https://doi.org/10.5194/tc-12-145-2018

Zhang, T., Barry, R.G., Knowles, K., Heginbottom, J.A., Brown, J., 2008. Statistics and characteristics of permafrost and ground-ice distribution in the Northern Hemisphere. Polar Geogr. 31, 47–68. https://doi.org/https://doi.org/10.1080/10889379909377670

Zoltai, S.C., Tarnocai, C., 1971. Properties of a Wooded Palsa in Northern Manitoba. Arct. Alp. Res. 3, 115–129. https://doi.org/https://doi.org/10.1080/00040851.1971.12003602

Appendix A: Weather Station Images

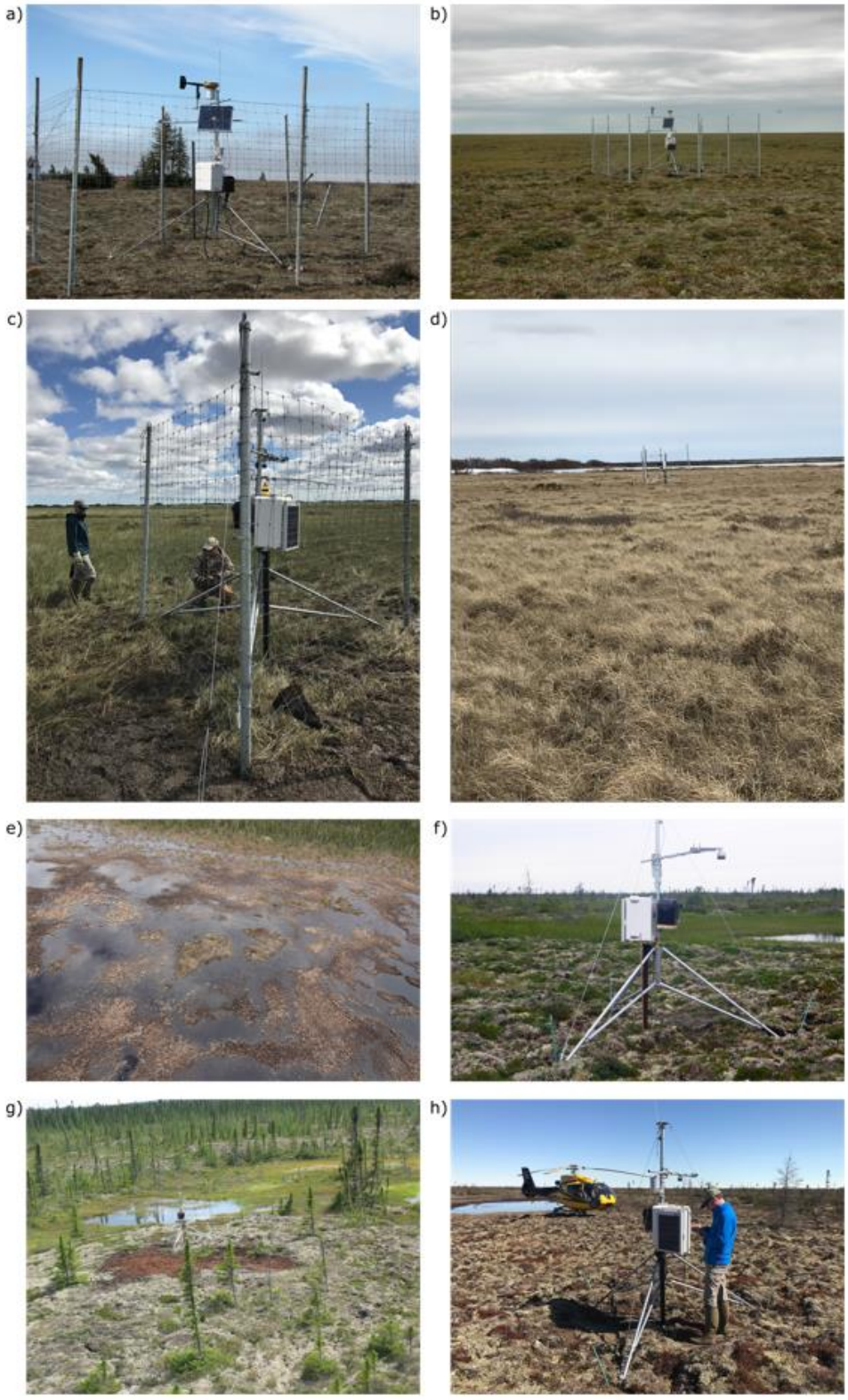

Figure S1. Images of the a) Tundra 1, b) Tundra 2, c) Fen 1, d) Fen 2, e) Palsa 1, f) Palsa 2, g) Palsa 3, and h) Palsa 4 weather stations.

Appendix B: Frequency Distribution of Active Layer Metrics

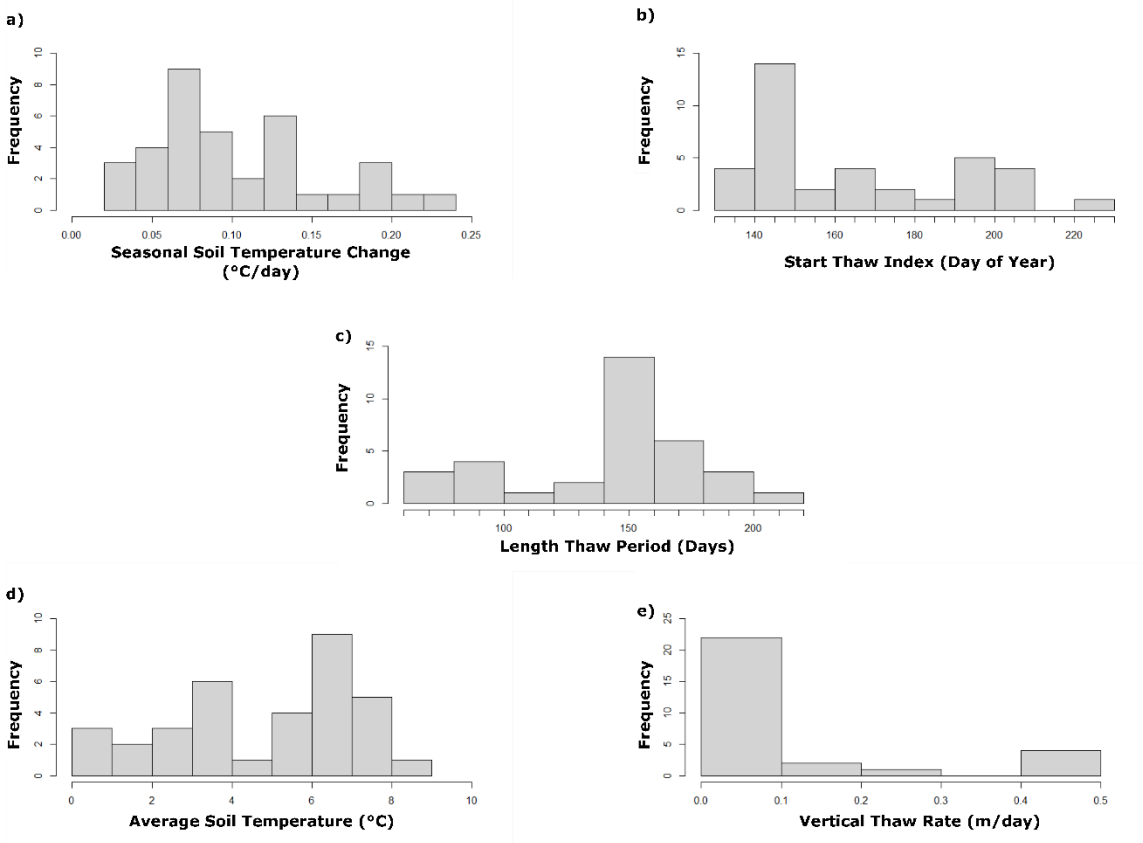

Figure S2. Frequency distribution of active layer thermal regime metrics a) seasonal soil temperature change, b) start of the thaw index, c) length of the thaw period, d) average soil temperature, and e) vertical thaw rate across all landforms. Metrics were extracted from soil temperature profiles where data originates from weather station data.

Appendix C: Diagnostic Plots for GAM Models

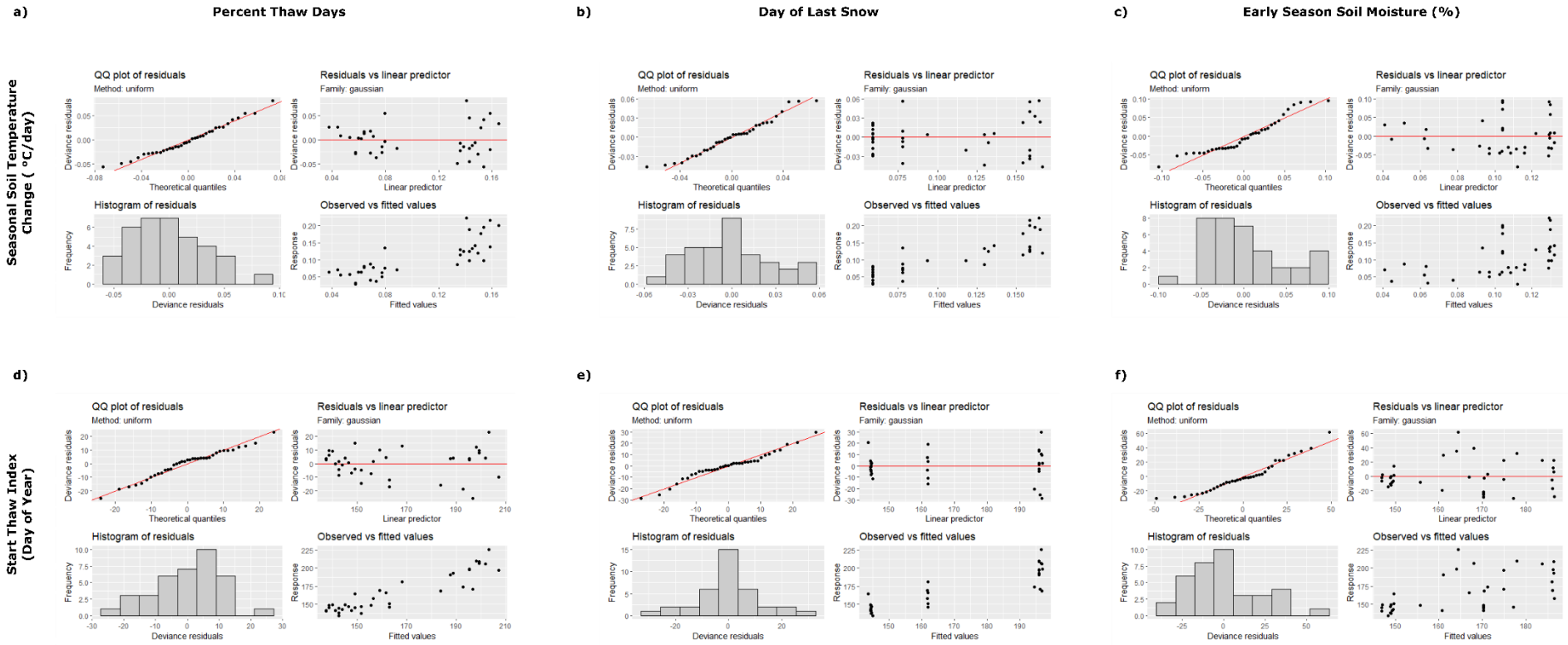

g)

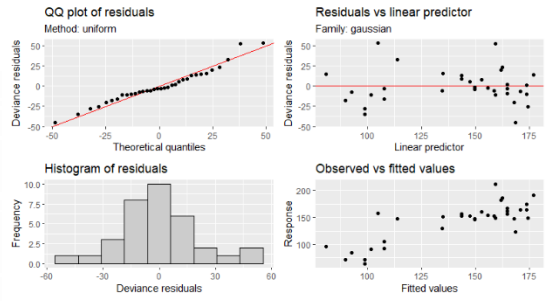

h)

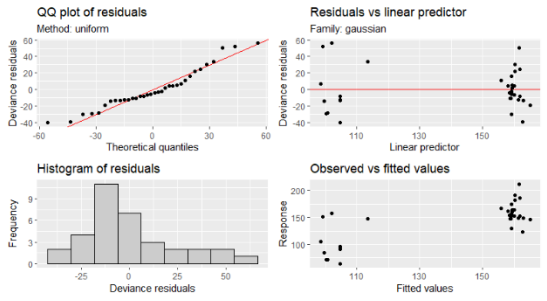

i)

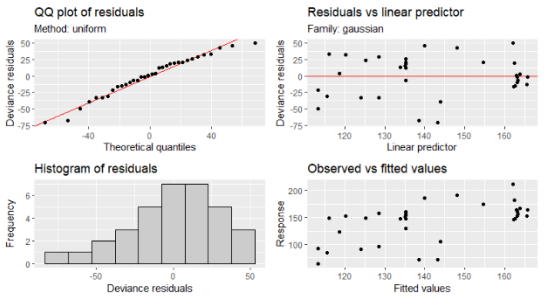

Length Thaw Period (Days)

j)

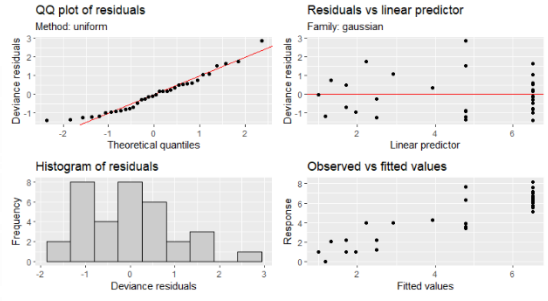

k)

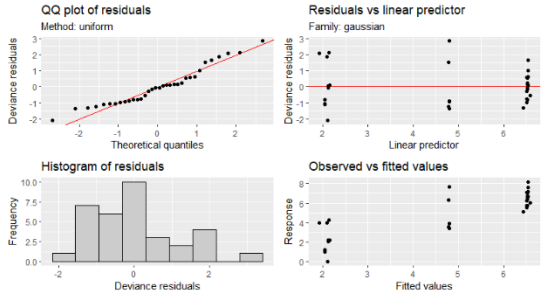

l)

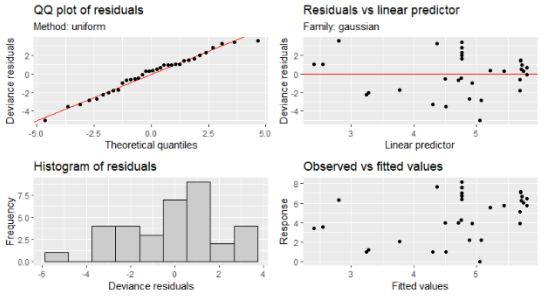

Average Soil Temperature (°C)

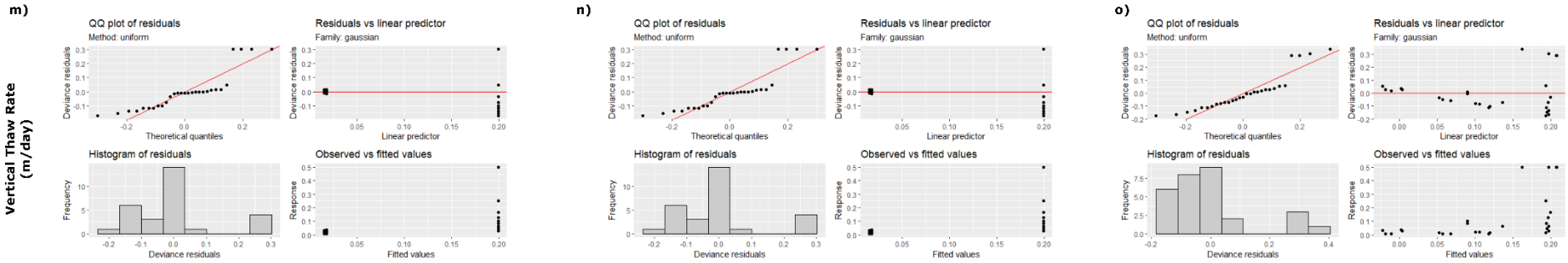

Figure S3. Diagnostic plots for the selected GAM Models. The top row is seasonal soil temperature change against a) percent thaw days, b) day of last snow, and c) soil moisture (%). Row 2 is start of thaw index against d) percent thaw days, e) day of last snow, and f) soil moisture. Row 3 is length of the thaw period against g) percent thaw days, h) day of last snow, and i) soil moisture. Row 4 is average soil temperature against j) percent thaw days, k) day of last snow, and l) soil moisture. The final row is vertical thaw rate against m) percent thaw days, n) day of last snow, and o) soil moisture. Data for these models came from weather station data.

Appendix D: Tundra 1 Air Temperature and Soil Temperature Profiles

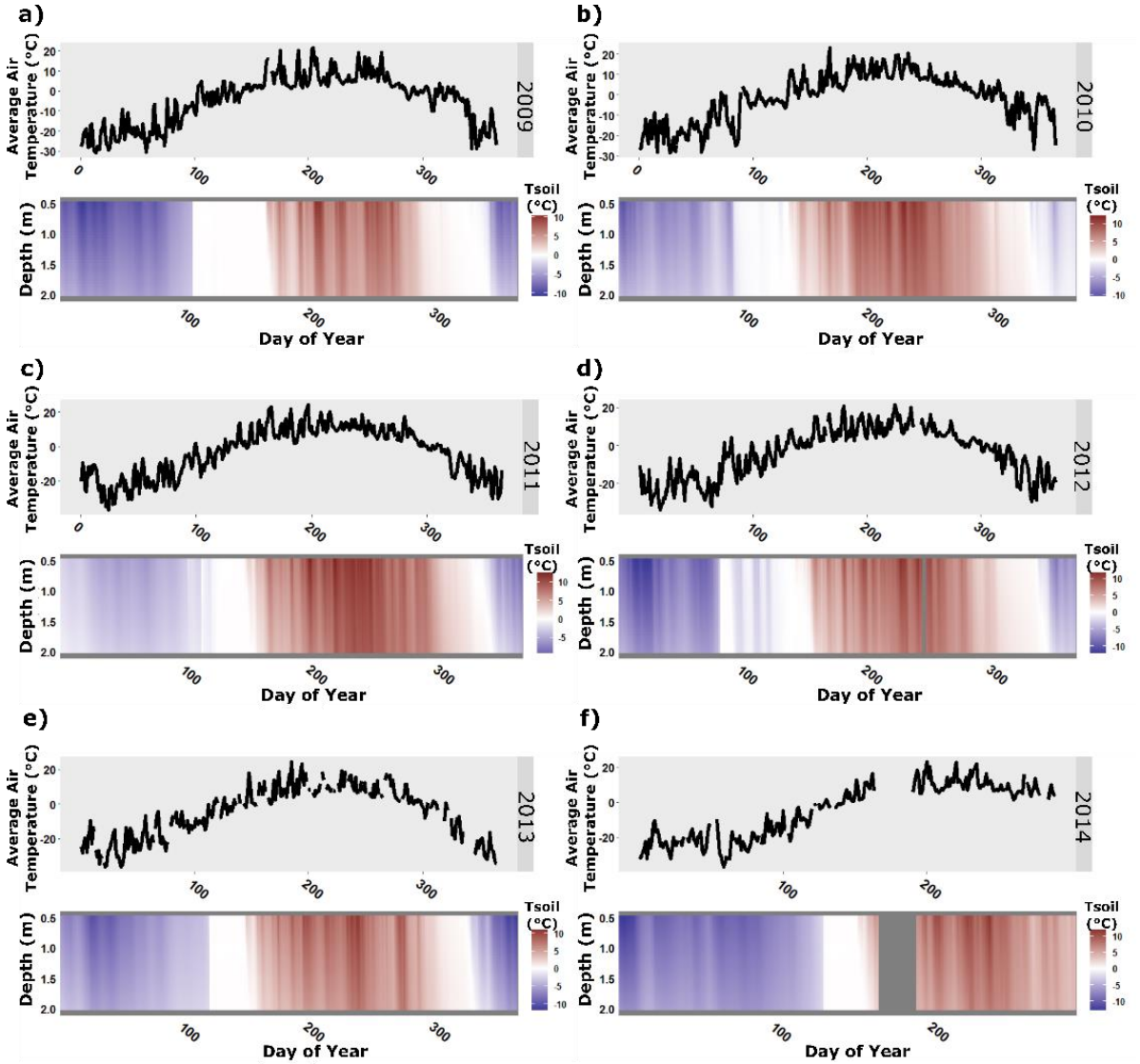

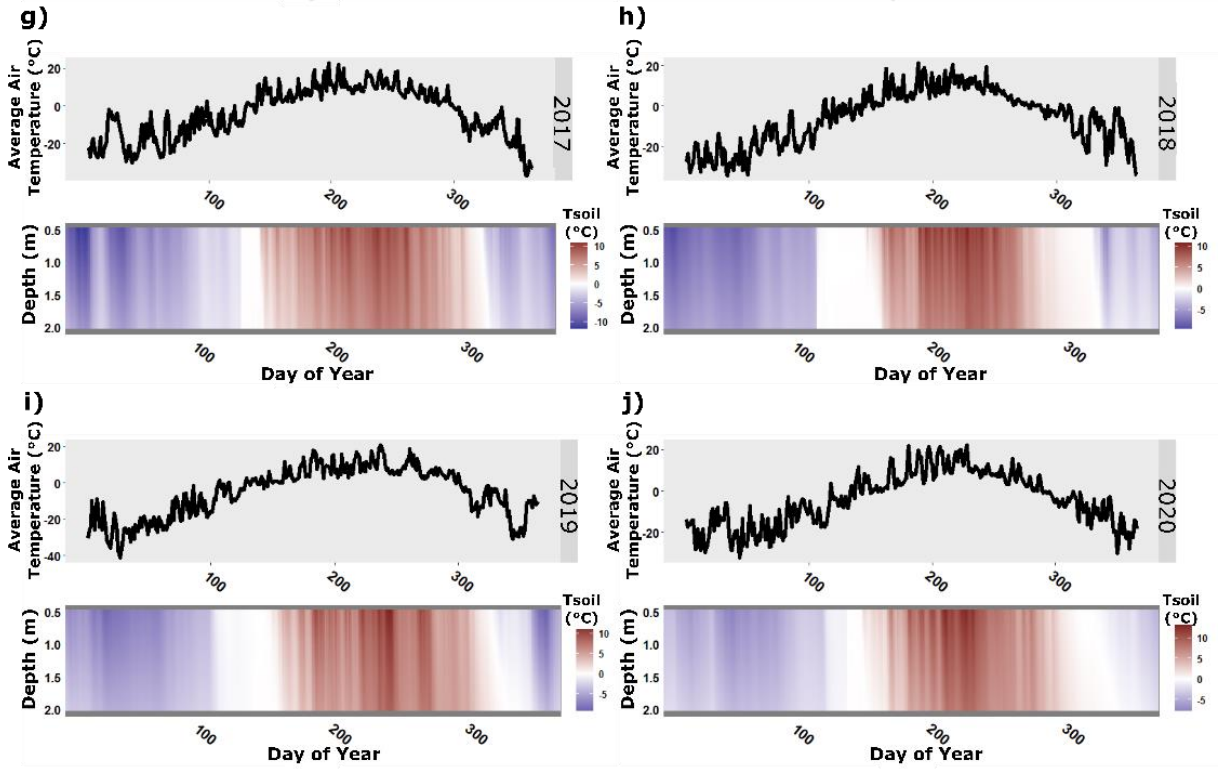

Figure S4. Daily average air temperature and soil temperature profiles across years at Station Tundra 1. Data originates from weather station data.

Appendix E: Tundra 2 Air Temperature and Soil Temperature Profiles

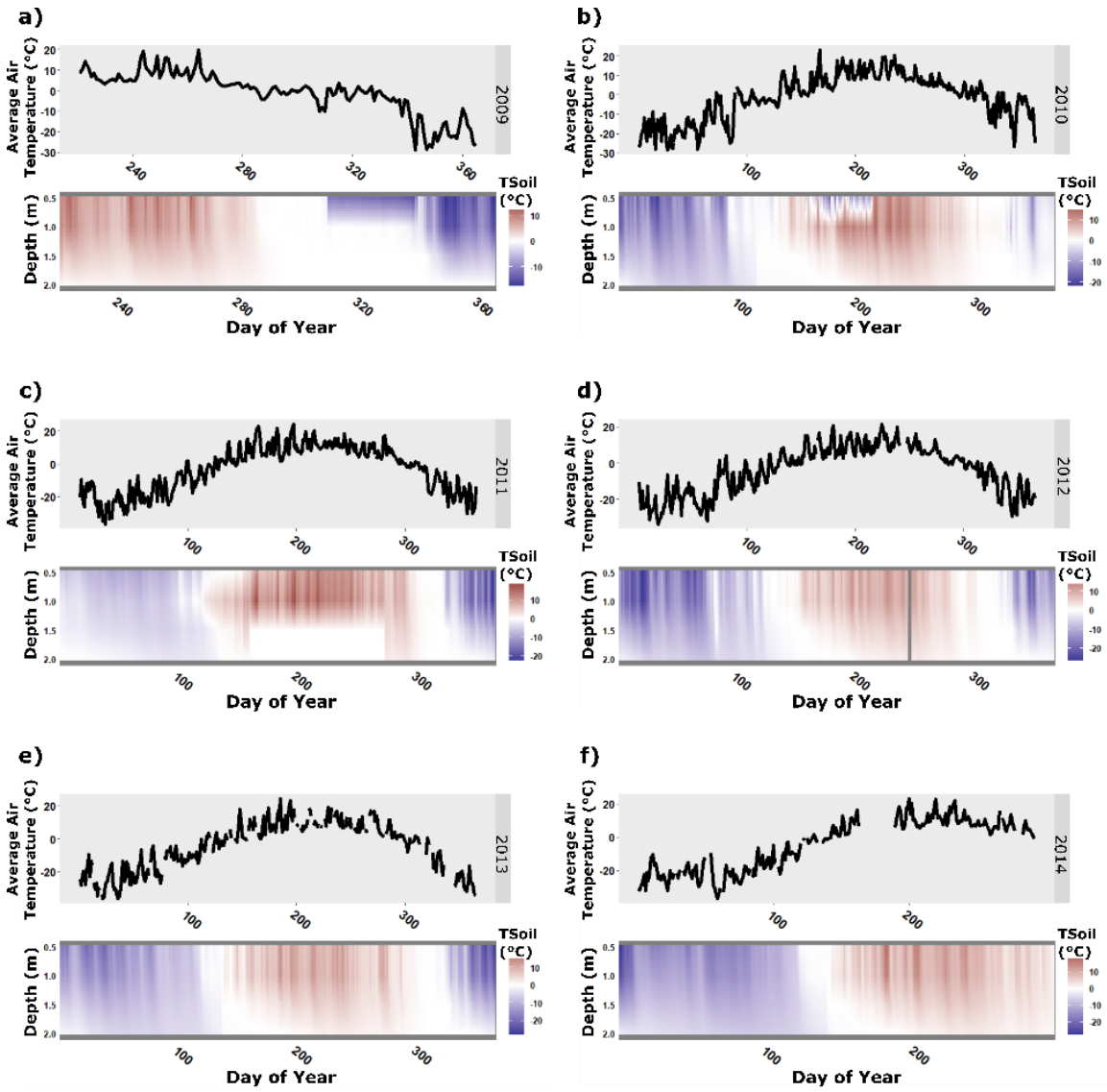

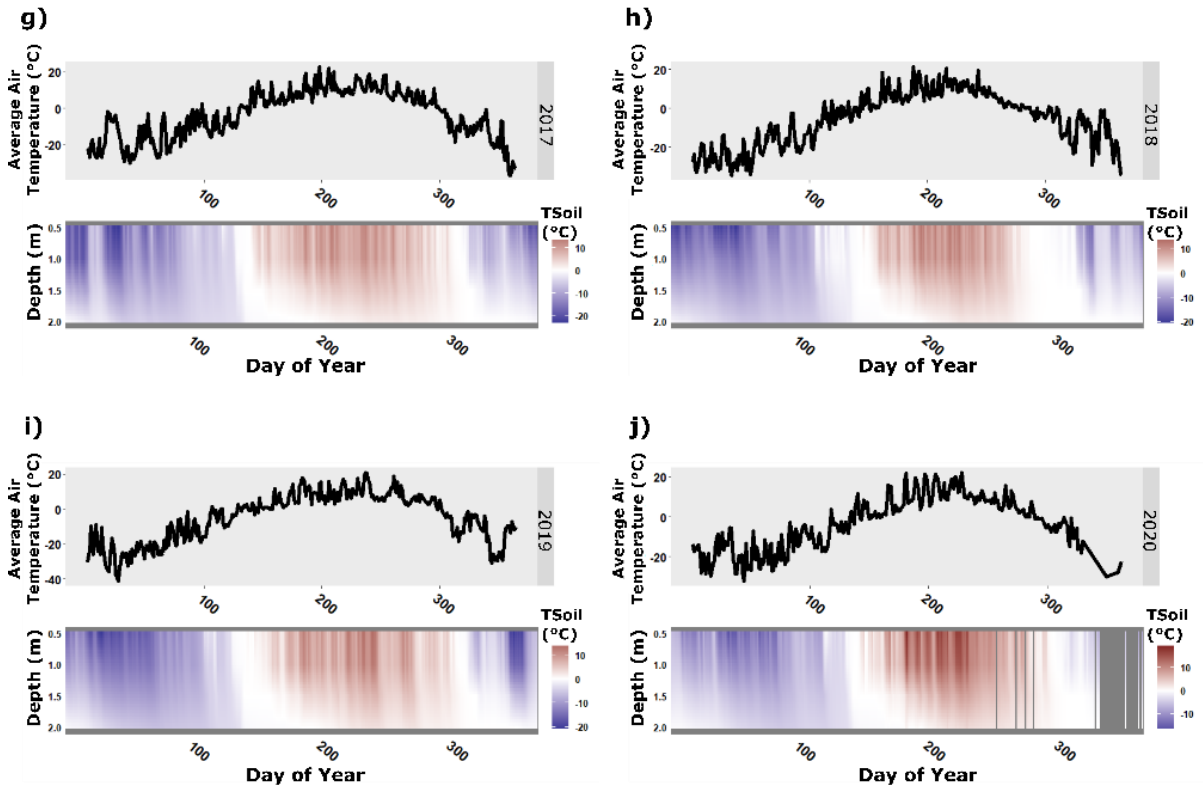

Figure S5. Daily average air temperature and soil temperature profiles across years at Station Tundra 2. Data originates from weather station data.

Appendix F: Fen 1 Air Temperature and Soil Temperature Profiles

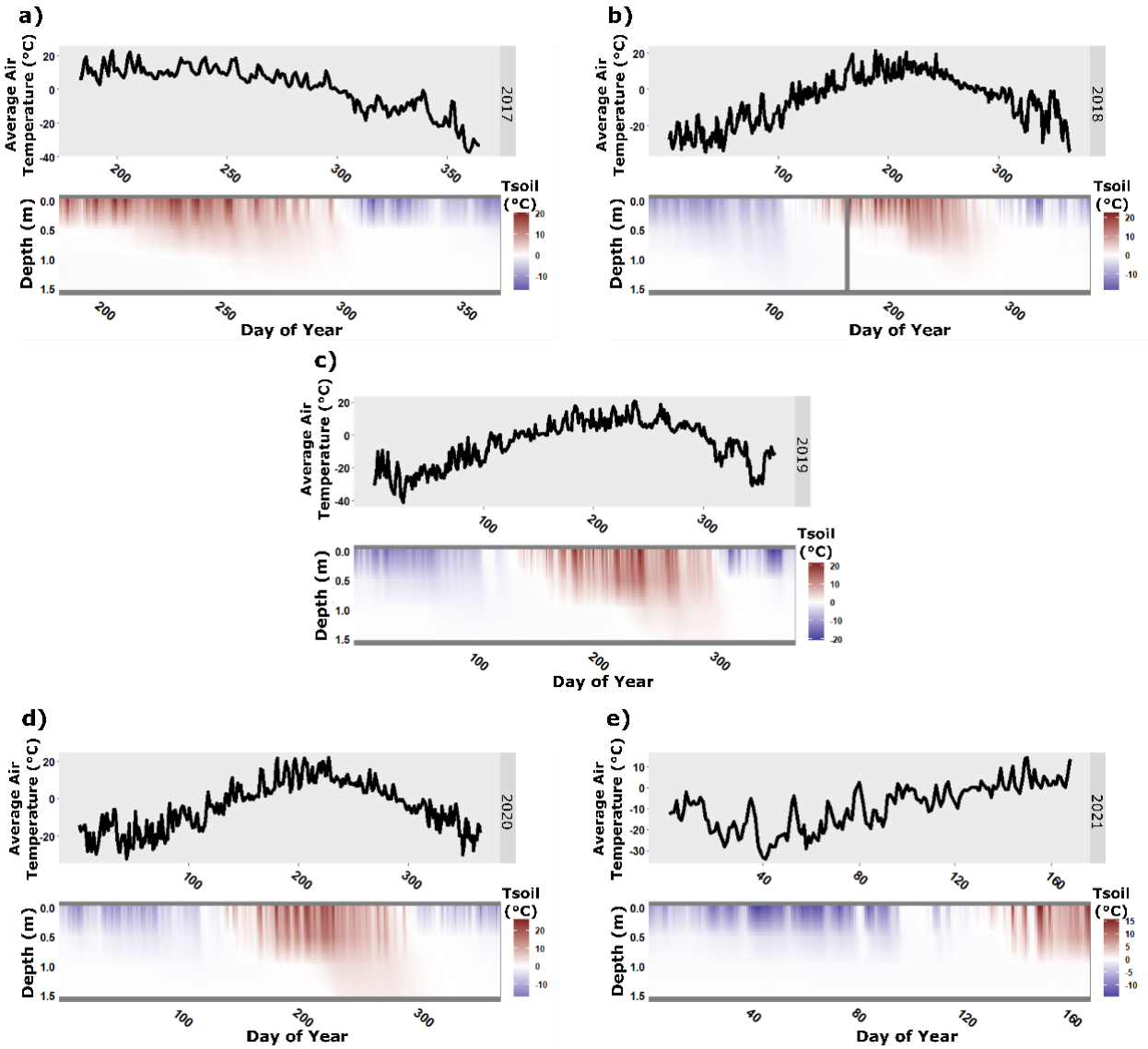

Figure S6. Daily average air temperature and soil temperature profiles across years at Station Fen 1. Data originates from weather station data.

Appendix G: Fen 2 Air Temperature and Soil Temperature Profiles

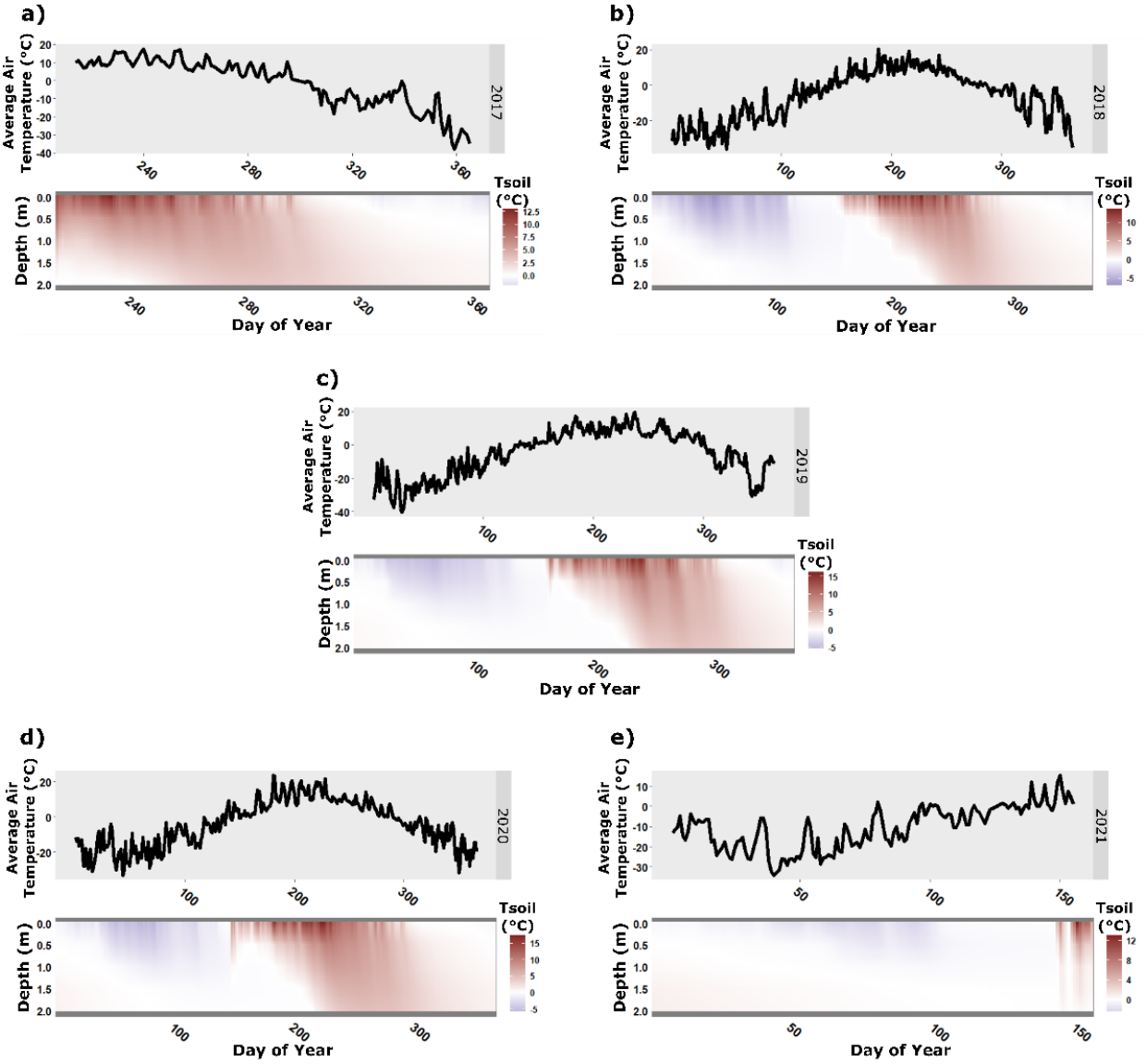

Figure S7. Daily average air temperature and soil temperature profiles across years at Station Fen 2. Data originates from weather station data.

Appendix H: Palsa 1 Air Temperature and Soil Temperature Profiles

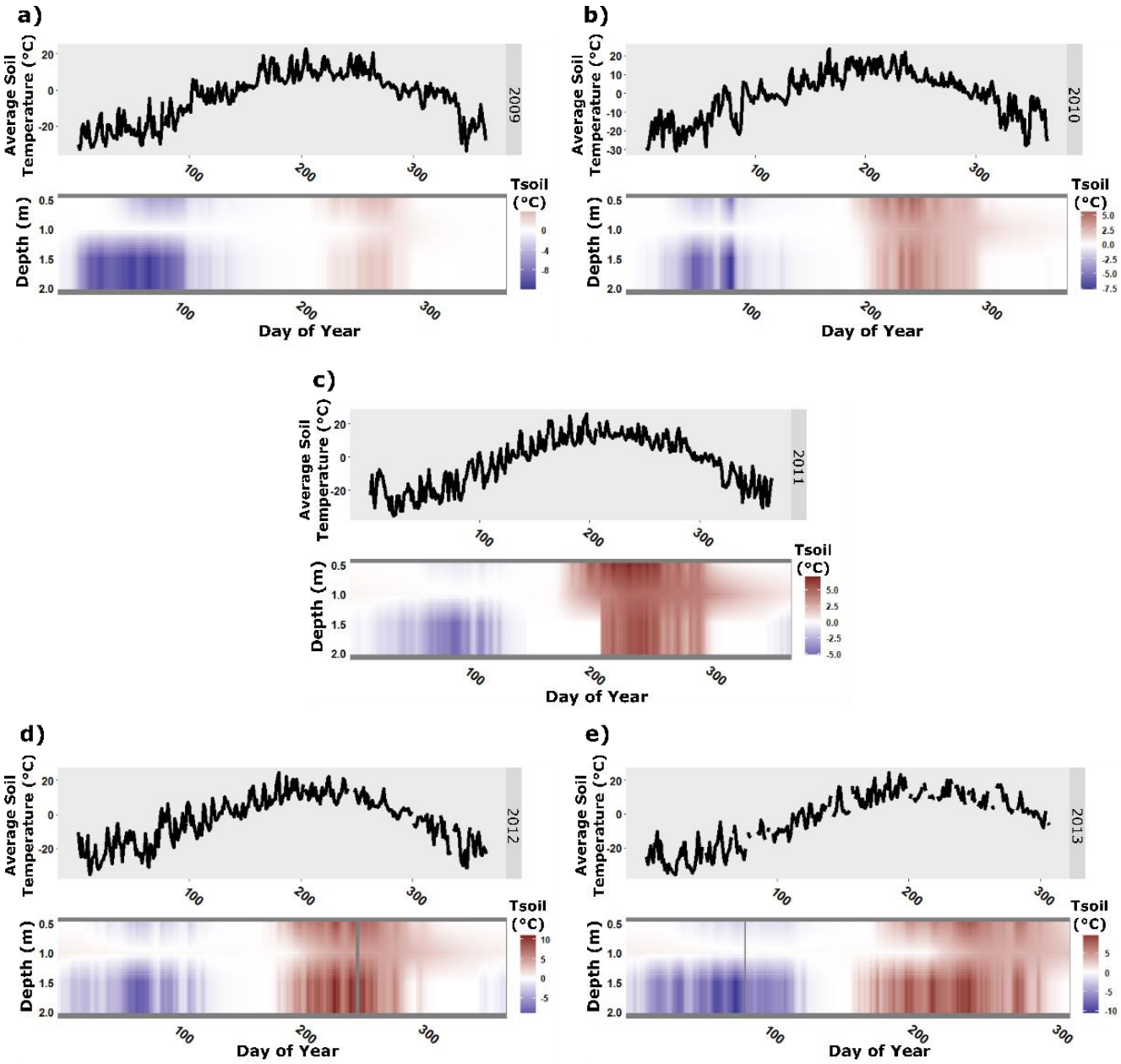

Figure S8. Daily average air temperature and soil temperature profiles across years at Station Palsa 1. Data originates from weather station data.

Appendix I: Palsa 2 Air Temperature and Soil Temperature Profiles

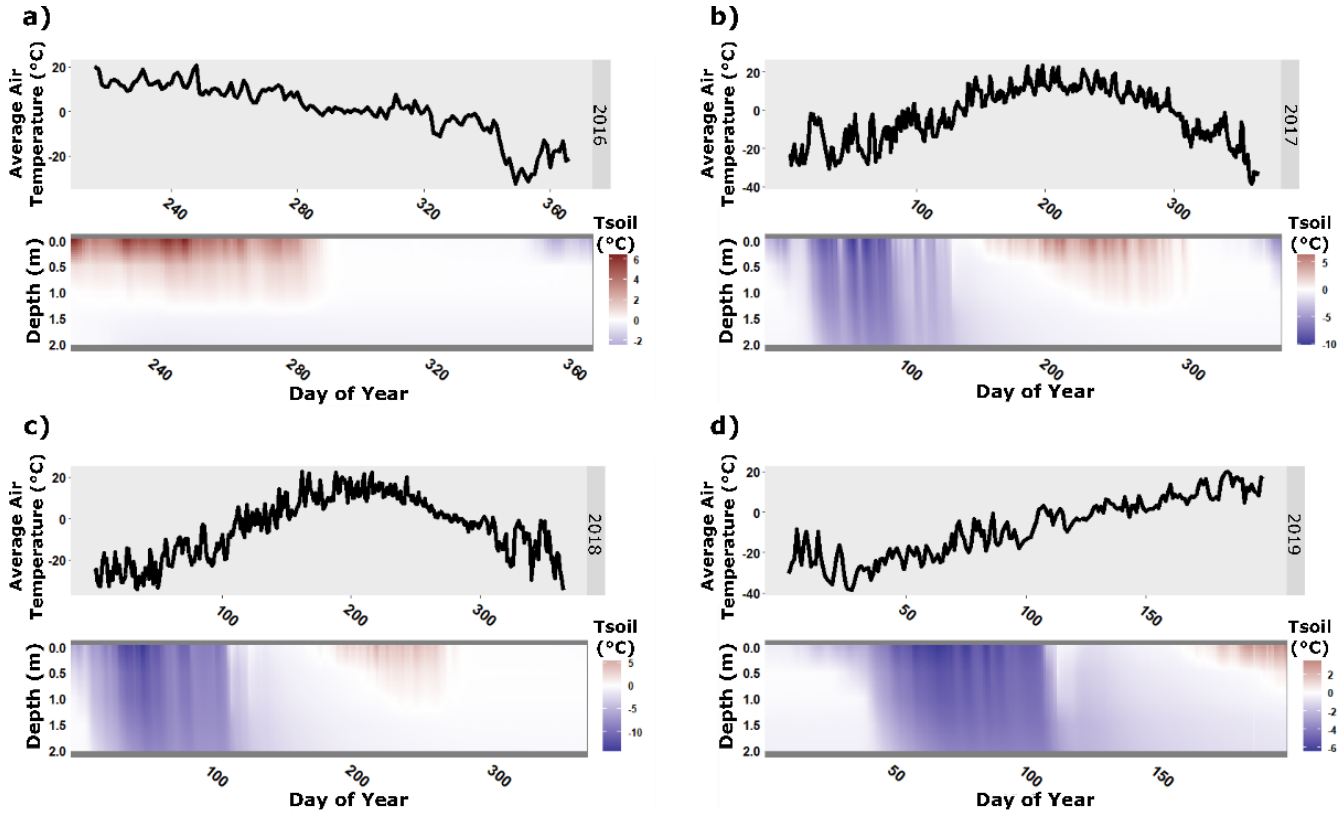

Figure S9. Daily average air temperature and soil temperature profiles across years at Station Palsa 2. Data originates from weather station data.

Appendix J: Palsa 3 Air Temperature and Soil Temperature Profiles

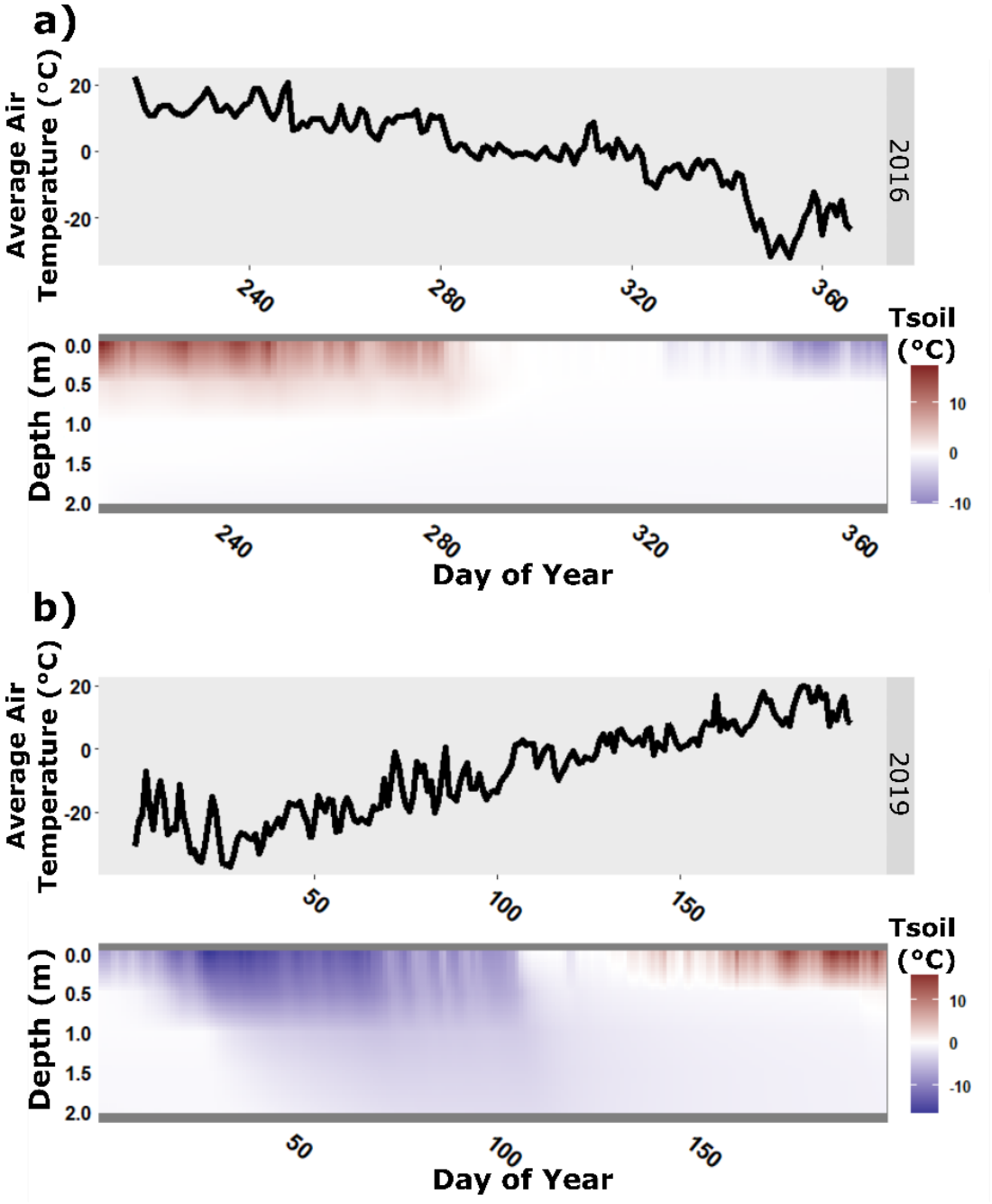

Figure S10. Daily average air temperature and soil temperature profiles across years at Station Palsa 3. Data originates from weather station data.

Appendix K: Palsa 4 Air Temperature and Soil Temperature Profiles

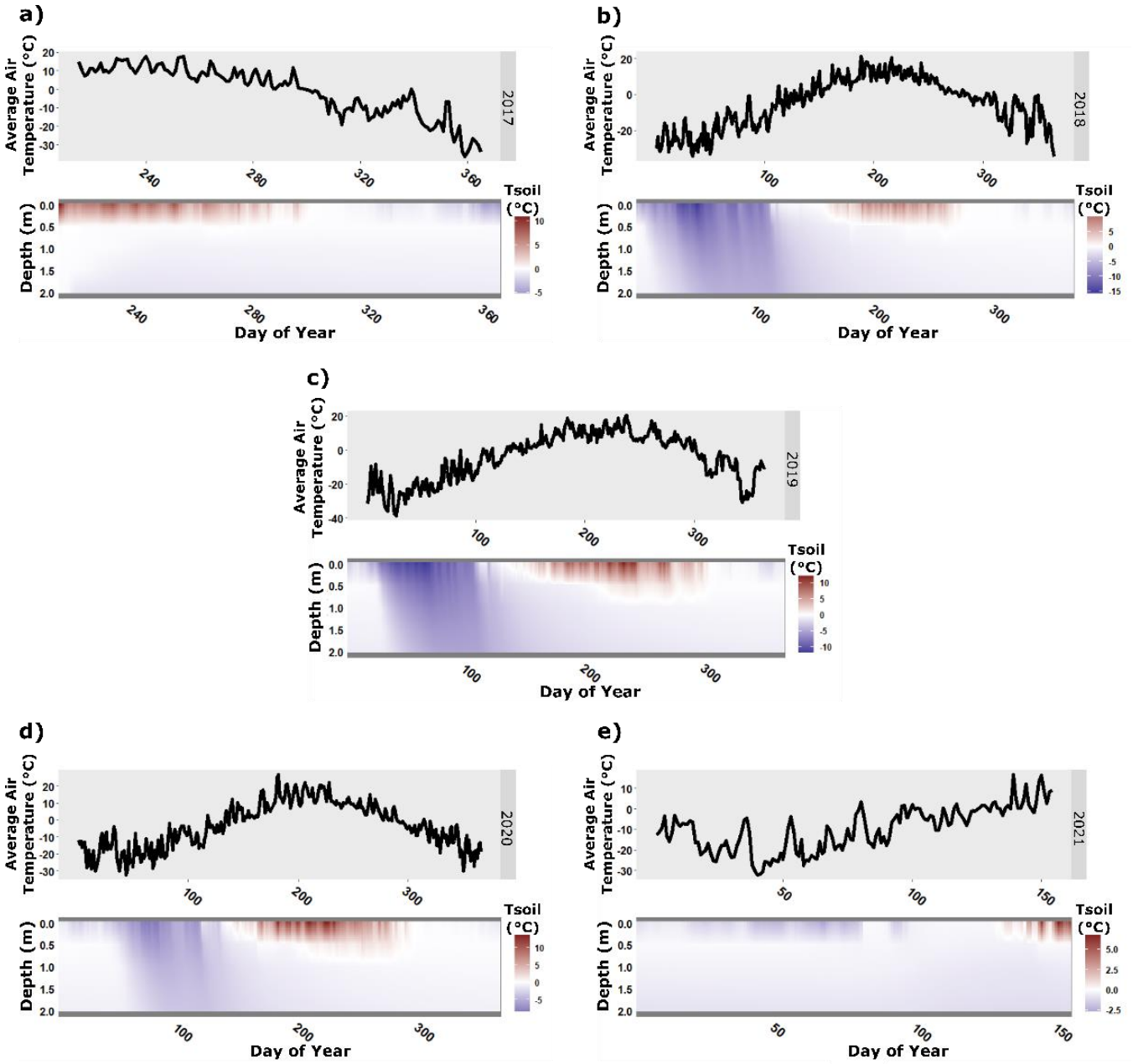

Figure S11. Daily average air temperature and soil temperature profiles across years at Station Palsa 4. Data originates from weather station data.

Appendix L: Results of Unselected GAM Models

Table S1. Results of unselected Generalized Additive Models (GAMs) pooled by response variable. Tundra heath sites are referred to as tundra. Data originates from weather station data.

Model Parameters	Linear Terms				Smoothed Terms				Deviance Explained (%)	AICc
	Estimate	SE	t	P	edf	Ref.df	F	P		
Seasonal Soil Temperature Change									67.4	-135.17
Tundra	0.145	0.008	17.68	**<2E-16**						
Fen	-0.067	0.015	-4.35	**0.00013**						
Palsa	-0.086	0.012	-7.14	**4.4E-08**						
Thaw Days: Tundra					1.21	3	1.40	**0.043**		
Thaw Days: Fen					2.5E-05	3	0	**0.763**		
Thaw Days: Palsa					1.0E-05	3	0	**0.939**		
Seasonal Soil Temperature Change									62.2	-132.55
Tundra	0.147	0.008	17.37	**<2E-16**						
Fen	-0.069	0.016	-4.22	**0.00019**						
Palsa	-0.090	0.013	-6.75	**1.3E-07**						
Last Snow					1	1	0.29	0.594		
Seasonal Soil Temperature Change									61.8	-134.93
Tundra	0.147	0.008	17.78	**<2E-16**						
Fen	-0.069	0.016	-4.26	**0.0002**						
Palsa	-0.088	0.013	-7.02	**4.9E-08**						
Soil Moisture: Tundra					8.9E-06	3	0	0.524		
Soil Moisture : Fen					1.2E-05	3	0	0.469		
Soil Moisture : Palsa					2.7E-05	3	0	0.829		
Seasonal Soil Temperature Change									62.0	132.35

Tundra	0.145	0.010	14.79	**7.4E-16**						
Fen	-0.065	0.021	-3.12	**0.0038**						
Palsa	-0.085	0.015	-5.62	**3.3E-06**						
Soil Moisture					1	1	0.113	0.74		
Seasonal Soil Temperature Change									61.8	-136.22
Tundra	0.147	0.0083	17.78	**<2E-16**						
Fen	-0.069	0.017	-4.26	**0.0002**						
Palsa	-0.088	0.013	-7.02	**4.9E-08**						
Start Thaw Index									87	287.09
Tundra	144.5	2.38	60.65	**<2E-16**						
Fen	17.33	4.76	3.64	**0.00096**						
Palsa	55.73	4.32	12.91	**3.2E-14**						
Tundra: Thaw Days					1.6E-04	3	0	0.619		
Fen: Thaw Days					2.6E-05	3	0	0.378		
Palsa Thaw Days					2.03	3	4.90	**0.001**		
Start Thaw Index									82.8	298.32
Tundra	143.92	2.96	48.66	**<2E-16**						
Fen	17.91	5.58	3.21	**0.003**						
Palsa	52.12	4.55	11.44	**6.7E-13**						
Tundra: Snow					8.6E-01	3	0.567	0.147		
Fen: Snow					6.9E-05	3	0	0.493		
Palsa: Snow					8.5E-01	3	0.438	0.222		
Start Thaw Index									81.3	296.3
Tundra	144.38	2.59	55.58	**<2E-16**						
Fen	14.87	6.09	2.44	**0.019**						
Palsa	49.02	4.02	12.26	**7.5E-15**						
Tundra: Soil Moisture					5.6E-05	3	0	0.969		
Fen: Soil Moisture					6.4E-01	3	0.411	0.157		
Palsa: Soil Moisture					6.3E-06	3	0	0.455		

Start Thaw Index									81.4	295.93
Tundra	147.05	3.30	44.57	**<2E-16**						
Fen	10.86	7.13	1.52	0.14						
Palsa	47.31	5.22	9.07	**1.8E-10**						
Soil Moisture					1	1	2.15	0.152		
Start Thaw Index									80.2	295.58
Tundra	144.5	2.85	50.69	**<2E-16**						
Fen	17.33	5.70	3.04	**0.0045**						
Palsa	51.58	4.40	11.72	**1.7E-13**						
Length Thaw Period									73	317.37
Tundra	159.47	5.05	31.60	**<2E-16**						
Fen	2.53	9.82	0.26	0.799						
Palsa	-63.44	9.40	-6.75	**2.5E-07**						
Tundra: Thaw Days					0.95	3	0.78	0.102		
Fen: Thaw Days					0.0001	3	0.00	0.335		
Palsa: Thaw Days					2.06	3	4.41	**0.0027**		
Length Thaw Period									58.5	323.82
Tundra	159.41	5.99	26.63	**<2E-16**						
Fen	2.59	11.72	0.22	0.827						
Palsa	-58.1	10.23	-5.65	**3.7E-06**						
Tundra: Snow					3.0E-05	3	0	0.909		
Fen: Snow					2.1E-04	3	0	0.113		
Palsa: Snow					9.3E-01	3	0.483	0.219		
Length Thaw Period									69.6	320.02
Tundra	159.41	5.27	30.24	**<2E-16**						
Fen	18.46	12.09	1.53	0.138						
Palsa	-60.53	11.48	-5.27	**1.3E-05**						
Tundra: Soil Moisture					0.0001	3	0	0.521		
Fen: Soil Moisture					1.54	3	2.37	**0.015**		

Palsa: Soil Moisture					1.11	3	1.16	0.06		
Length Thaw Period									66	315.66
Tundra	149.1	6.36	23.43	**<2E-16**						
Fen	29.47	13.72	2.15	**0.039**						
Palsa	-39.3	10.28	-3.82	**0.0006**						
Soil Moisture					1	1	9.58	**0.004**		
Length Thaw Period									55.2	322.32
Tundra	159.4	6.13	26.02	**<2E-16**						
Fen	2.59	11.99	0.216	0.831						
Palsa	-56.5	9.77	-5.78	**2.3E-06**						
Average Soil Temperature									76.4	115.79
Tundra	6.55	0.287	22.80	**<2E-16**						
Fen	-1.37	0.604	-2.26	**0.031**						
Palsa	-4.71	0.486	-9.69	**9.2E-11**						
Thaw Days					1	1	2.69	0.11		
Average Soil Temperature									78.3	117.82
Tundra	6.527	0.287	22.74	**<2E-16**						
Fen	-1.734	0.549	-3.16	**0.0037**						
Palsa	-4.720	0.502	-9.39	**2.5E-10**						
Tundra: Snow					3.2E-01	3	0.136	0.284		
Fen: Snow					8.2E-06	3	0	0.733		
Palsa: Snow					1.48	3	1.1	0.113		
Average Soil Temperature									81.8	113.73
Tundra	6.536	0.239	25.21	**<2E-16**						
Fen	-1.635	0.606	-2.69	**0.012**						
Palsa	-4.439	0.428	-10.38	**3.6E-11**						

Tundra: Soil Moisture					0.0002	3	0	0.227		
Fen: Soil Moisture					2.435	3	2.99	0.025		
Palsa: Soil Moisture					0.207	3	0.11	0.209		
Average Soil Temperature									78.6	116.04
Tundra	6.623	0.331	20.02	**<2E-16**						
Fen	-1.548	0.704	-2.19	**0.036**						
Palsa	-4.848	0.569	-8.51	**2.2E-9**						
Soil Moisture					1.863	2.23	2.06	0.143		
Average Soil Moisture									74.3	115.94
Tundra	6.526	0.264	22.15	**<2E-16**						
Fen	-1.733	0.577	-3.01	**0.0052**						
Palsa	-4.444	0.470	-9.46	**1.2E-10**						
Vertical Thaw Rate									32.2	-21.90
Tundra	0.197	0.036	5.45	**1.2E-05**						
Fen	-0.167	0.076	-2.19	**0.038**						
Palsa	-0.187	0.066	-2.83	**0.0089**						
Thaw Days					1	1	0.265	0.611		
Vertical Thaw Rate									31.9	-21.79
Tundra	0.195	0.037	5.24	**2.0E-05**						
Fen	-0.183	0.069	-2.65	**0.013**						
Palsa	-0.165	0.075	-2.18	**0.039**						
Snow					1	1	0.171	0.683		
Vertical Thaw Rate									32.8	-24.94
Tundra	0.176	0.044	3.67	**0.00052**						
Fen	-0.160	0.071	-2.26	**0.033**						
Palsa	-0.158	0.067	-2.32	**0.028**						
Tundra: Soil Moisture					5.9E-01	3	0.62	**0.082**		
Fen: Soil Moisture					8.2E-06	3	0	1.00		

Palsa: Soil Moisture					8.2E-06	3	0	0.967		
Vertical Thaw Rate										
									36.3	-22.17
Tundra	0.184	0.042	4.40	**0.00018**						
Fen	-0.142	0.090	-1.58	0.127						
Palsa	-0.153	0.079	-2.02	**0.053**						
Soil Moisture					1	1	0.495	0.488		
Vertical Thaw Rate										
									31.4	-24.54
Tundra	0.199	0.035	5.63	**6.4E-06**						
Fen	-0.184	0.068	-2.71	**0.012**						
Palsa	-0.181	0.064	-2.83	**0.0089**						